Set of injury risk curves for different sizes and ages

EUROPEAN COMMISSION
DG RTD

SEVENTH FRAMEWORK PROGRAMME
THEME 7
TRANSPORT - SST
SST.2007.4.1.2: Human physical and behavioral components
GA No. 218516

THORAX
Thoracic injury assessment for improved vehicle safety

Deliverable No.	THORAX D2.3
Deliverable Title	Set of injury risk curves for different sizes and ages
Dissemination level	Public
Written By	Johan Davidsson (Chalmers), Jolyon Carroll and David Hynd (TRL), Erwan Lecuyer, Eric Song and Xavier Trosseille (GIE RE PR) Andre Eggers (BASt) Cecilia Sunnevang (Autoliv) Norbert Praxl (PDB) Paul Lemmen and Bernard Been (HUMANETICS) Luis Martinez (UPM)
Checked by	
Approved by	Paul Lemmen 2013-07-01

Executive summary

When new crash test dummy hardware becomes available it is important to establish how the measurements taken with that tool relate to a risk of injury. THORAX is a collaborative medium-scale project under the EC Seventh Framework. It focuses on the reduction and prevention of thoracic injuries. Within the project an improved understanding of thoracic injury mechanisms has been implemented in an updated design for the thorax-shoulder complex of the THOR dummy. The new dummy hardware, referred to as the THORAX demonstrator, has been evaluated in a number of biomechanical test conditions. The data from these tests has provided the opportunity to compare those data with injury outcome data under equivalent loading conditions. This report describes that comparison and the resulting injury risk curves developed.

When developing injury risk functions for a new dummy it is common practice to repeat tests carried out with post-mortem human subjects (PMHS) with the crash test dummy. Matched dummy data and injury records from the PMHS tests are then used in the development of injury risk functions. Other approaches involve collection of real world accident events that have been recreated with the dummy in the laboratory. Both of these approaches have been adopted in this study.

Injury risk functions are commonly developed for the average male in terms of size and age. However, age, gender and size influence the risk of injury for a given crash condition. Crash test dummies that take these differences into account may be developed in the future. However, as part of the THORAX project advanced scaling methods have been developed that can be used to modify the injury risk functions to account for gender and different sizes. Thereby the measurements obtained in crash tests with the THORAX demonstrator can be used to predict the risk for other occupant categories than those that are close to the average male.

By providing the automotive industry with a superior crash test dummy, the new THORAX demonstrator, associated injury risk functions and scaling techniques it is expected that improved restraint systems will be developed that lead to a reduction of chest injuries.

Contents

1 Introduction

1.1 Motivation

The development of the THOR 50th percentile male dummy was initiated in 1992 by NHTSA with the objective of developing a more biofidelic frontal impact dummy. By now various studies have demonstrated an improved biofidelity of the THOR over the currently used HIII dummy, e.g. Shaw et al. (2000), Kent et al. (2003a) and Vezin et al. (2002). However, studies Kent et al. (2003b) and Forman et al. (2005) also have shown that the THOR dummy, just like the HIII, lacks sensitivity to injury parameters like sternal displacement when belt and airbag loading is imposed on the chest. In particular, it has been shown that the relationship between injury risk and the injury criteria measured by the dummy is sensitive to experimental parameters such as the apportionment of seatbelt and airbag loading. This is a problem both of measurement and of interpretation.

To reduce these limitations, the shoulder-thorax complex of the THOR was improved within the EU FP7 project THORAX. The design changes introduced were mainly softer ribs, additional padding within the suit, new chest compression instrumentation and a new shoulder design. The new dummy version is referred to as the THORAX demonstrator.

1.2 Objective

Following the development of an improved thorax-shoulder complex for the THOR dummy the goals of this study were to derive injury criteria and related risk curves for usage with the EU FP7 THORAX demonstrator.

1.3 Approach

In a first step more robust, restraint independent, injury criterion candidates were identified using a human body FE model. The model was submitted to a wide range of loading types: impactor, static airbag, belt only restraint, airbag only restraint and combined belt and airbag restraint. For each loading type, different loading severities were applied to generate different levels of rib fracture: from the absence of fractures to numerous fractured ribs. From these studies rib bending was identified as being the main loading mode resulting in fracture. Two injury criteria representing this pattern were formulated. The first one, called Combined Deflection (Dc) criterion, uses chest displacements at four locations to compute overall and differential deflections. The second criterion, called Number of Fractured Ribs (NFR), uses locally measured strains at individual ribs to identify those ribs for which the bending strains at any location has exceeded a critical value.

Following the identification of possible candidate criteria an in-depth literature review was conducted to identify all available PMHS datasets relevant for frontal impacts, their test configurations and the quality of the results described. Criteria were developed for inclusion or exclusion of PMHS tests in the development of the injury risk curves related to the proposed chest injury criteria.

Next, those PMHS tests regarded as being relevant were reproduced using demonstrator dummies developed in the THORAX project.

In the final step, the paired test data were used to construct injury risk curves using the guidelines detailed within ISO/TC22/SC12/WG6. These include, among others, the use of survival analysis, means to assess distribution and quality checks.

1.4 Biofidelity of the new EU FP7 THORAX demonstrator

Prerequisites when paired PMHS and crash test dummy data are to be used in the development of injury risk functions are that the test conditions used in the original tests are reproduced well and that the crash test dummy is biofidelic. These two items have been addressed in a separate report established with the EU FP THORAX project.

1.5 Thorax injury mechanisms

The Viscous Criterion was derived as a complementary measure to general spine acceleration and the thorax compression by Lau and Viano [1986]. The concern with compression measurements was that it could become inadequate as an injury predictor when the velocity of deformation exceeds 3 m/s. In modern vehicle restraint systems the typical deformation rate will be less than 3 m/s and probably about 1 m/s. Therefore having a compression measurement alone should be adequate. However, it is recommended that the V*C could still offer useful injury risk information if the occupant was to suffer unexpected forward excursion and be subjected to a hard contact with the steering wheel, for instance. The basis for the THORAX Project was to develop an assessment tool which could be used to drive modern restraint system developments beyond that possible with the existing test tools. To meet this objective, there has been a general assumption made that restraint loading conditions where the system is already performing well will form the basis for further advances. Therefore, whilst it is proposed that V*C should still be considered in assessing frontal impact protection it was considered by the THORAX Project partners that the primary injury risk criterion development should focus on compression-based mechanisms and associated measures.

Several studies have suggested that rib bending is the mechanism responsible for rib fractures. Using a Human Body Model (HBM) (Song et al. 2011 and Song et al. 2012) it was suggested that longitudinal rib strain (along the rib curvilinear axis) is the main component compared to the transverse rib strain (along the rib cross section circumference). The study results imply that measurement of strain along the rib axis is a good descriptor of strain state. Based on these findings, the THORAX demonstrator was fitted with strain gauges on the external side of the ribs to record bending of each rib.

In parallel to installations of strain gauges, additional work using a state-of-the-art HBM, the Humos2 human body model, was carried out as part of the THORAX project to suggest global criterion that correlated to rib fractures but was independent to loading types. As an outcome of this work Song et al. (2011) and Song et al. (2012) suggested a new injury criterion candidate, named Combined Deflection and noted as Dc. It was defined as below:

$$Dc = Ds + Cf \times \left[(dD - Lc) + \left|(dD - Lc)\right|\right]$$

Where:

Ds represents the sternal deflection (the X-component of the mid-sternum displacement relative to the spine in A-P direction). This deflection reflects the amplitude of the symmetric part of the ribcage deflection.

dD, named as differential deflection, is the difference between right and left deflections of lower ribcage measured at the joint between the 7th ribs and the cartilage (the X-components in A-P direction).

Lc, named as characteristic length, serves to amplify the differentiation effect of the term dD – Lc between different types of asymmetric loadings.

Cf, named as contribution factor, is a coefficient to weight the contribution of the differential deflection to the Dc.

Based on simulations of a large number of loading conditions, the following was observed:

- The injury curve, defining the relationship between injury outcome and injury predicator, does not change significantly from one loading type to another.

- Injury risk curves, when developed separately for different restraint types for the HBM used, are closer to each other for the Dc than for sternal deflection (x-direction relative the spine).

1.6 Methods to produce injury risk functions

Petitjean et al. (2011) compared the performance of the commonly used statistical methods to build injury risk curves based on statistical simulations. Further investigations were conducted on behalf of ISO/TC22/SC12/WG6 to determine the guidelines to build injury risk curves for biomechanical samples and to recommend the most relevant injury risk curve depending on the biomechanical sample considered. The survival analysis was recommended over the other methods to build injury risk curves for biomechanical samples. A guide for risk curve development was presented by Petitjean et al. (2012).

2 Methods and Materials

An injury risk curve can be considered to be a statistical model of some biomechanical data. Since 2009, it seems that ISO/TC22/SC12/WG6 has reached a consensus on the definition of guidelines to build injury risk curves, including the selection of data to be included, variables to be used and the use of survival analysis. Other steps are a distribution assessment and quality checks. These guidelines and those presented by Petitjean et al. (2012) were applied to the THORAX demonstrator test results, as obtained in reconstructions of PMHS tests carried out in the past, to provide a set of draft injury risk curves.

2.1 PMHS data review and selection of data

The first step is to collect relevant data, including injury type, severities, and injury values measured. Preferably injury risk curves are to be developed for the entire ribcage and soft organs underneath. The focus of this study is on cortical bone rib fractures since there is a lack of data for other types of chest injuries. Two types of data were identifies as useful and were available; data from experiments using PMHS and accident data suitable for reconstructions in the lab with dummy hardware. Here only PMHS data is considered whereas accident data is reconstructed and reported separately in the Appendix B through D.

2.1.1 Available PMHS data

Frontal and oblique impact tests conducted with PMHS and reported in the literature were reviewed for possible inclusion in the development of injury risk curves for the THORAX demonstrator. Table 1 - Table 4 list the test identified as potentially useful. These tables includes indentor impacts to the chest, out-of-position (OOP) airbag inflation tests inertia tests with harness and diagonal belt, and sled tests in three (3-pt) and four point (4-pt) belt systems have been. Some of these were fitted a system to allow for a pretension of the belt (PTB) whereas others were fitted system to limit the maximum force produced, i.e. a force limited belt (FLB). In some sled tests standard belt (SB) have been used to reduce complexity, often in combination with a knee bar (KB) to reduce pelvis forward motion. In the sled tests both driver and passenger (pass) positions were used. In some of the tests, standard vehicle seats were used while in others seats designed to be easy to reproduce in the laboratory setting (Lab) was developed and used.

Table 1. Original PMHS thorax impactor tests.

Information source	Hub mass (kg)	Hub velocity (m/s)	Test/PMHS ref.	Age	Gender	Body weight (kg)	Stature (m)	Chest depth (mm)	Body mass Index	NRF wo Cartilage fractures	NFR wo Cartilage fractures
Nahum et al. 1970	19,3	5,1	05FM	60	M	86	1,85	257	25	2	2
Nahum et al. 1970	19,3	5,1	06FM	83	M	77	1,82	254	23	11	11
Nahum et al. 1970	19,3	4,0	07FF	86	F	38	1,67	200	13	11	
Nahum et al. 1970	19,3	5,1	09FM	73	M	76	1,85	238	22	0	
Nahum et al. 1970	19,3	4,9	10FF	82	F	43	1,60	168	17	12	
Kroell et al. 1971 and 1974	19,5	6,3	11FF	60	F	59	1,60	208	23	11	11
Kroell et al. 1971 and 1974	22,9	7,2	12FF	67	F	63	1,63	187	24	22	14
Kroell et al. 1971 and 1974	22,9	7,4	13FM	81	M	76	1,68	246	27	21	12
Kroell et al. 1971 and 1974	22,9	7,3	14FF	76	M	58	1,56	216	24	7	6
Kroell et al. 1971 and 1974	23,6	6,9	15FM	80	M	53	1,65	200	19	13	9
Kroell et al. 1971 and 1974	23,6	6,7	18FM	78	M	66	1,77	219	21	14	11
Kroell et al. 1971 and 1974	23,6	6,7	19FM	19	M	71	1,96	203	19	0	0
Kroell et al. 1971 and 1974	23,6	6,7	20FM	29	M	57	1,80	203	17	0	0
Kroell et al. 1971 and 1974	23,6	6,7	22FM	72	M	75	1,74	226	25	17	10
Kroell et al. 1971 and 1974	19,5	7,8	23FF	58	F	61	1,63	226	23	23	11
Kroell et al. 1971 and 1974	22,9	9,7	24FM	65	M	82	1,83	251	24	24	16
Neathery 1974	23,0	10,2	31FM	51	M	75	1,83	238	22	14	11
Neathery 1974	22,9	9,9	32FM	75	M	54	1,71	248	19	20	13
Neathery 1974	19,0	8,3	34FM	64	M	59	1,78	241	19	13	11
Neathery 1974	19,0	7,2	36FM	52	M	75	1,83	226	22	7	7
Neathery 1974	22,9	9,8	37FM	48	M	74	1,79	248	23	9	6
Neathery 1974	22,9	4,9	42FM	61	M	54	1,83	216	16	0	0
Neathery 1974	23,0	5,1	45FM	64	M	64	1,81	254	20	10	10
Neathery 1974	19,3	7,4	46FM	46	M	95	1,78	286	30	0	0
Neathery 1974	23,0	5,2	53FM	75	M	77	1,74	241	25	3	3
Neathery 1974	19,6	6,7	54FF	49	F	37	1,63	205	14	7	7
Neathery 1974	19,6	9,9	55FF	46	F	81	1,77	241	26	8	8
Neathery 1974	23,0	4,3	60FM	66	M	79	1,80	222	25	9	9
Neathery 1974	10,0	6,9	62FM	76	M	50	1,74	245	17	9	9
Neathery 1974	23,0	6,9	64FM	72	M	63	1,63	216	24	6	6
Trosseille et al. 2008	23,7	4,4	MS589	88	M	60	1,69	200	21	14	11
Trosseille et al. 2008	23,7	4,4	MS621	82	M	78	1,71	230	27	9	9
Bouquet et al. 1994	23,4	3,4	MRS01-MRT01	76	M	82	1,73	250	27	*na*	*na*
Bouquet et al. 1994	23,4	3,4	MRS03-MRT02	57	M	76	1,74	230	25	1	1
Bouquet et al. 1994	23,4	5,8	MRS04-MRT02	57	M	76	1,74	230	25	1	1
Bouquet et al. 1994	23,4	3,4	MRS05-MRT03	66	M	69	1,72	230	23	*na*	*na*
Bouquet et al. 1994	23,4	5,9	MRS06-MRT03	66	M	69	1,72	230	23	11	11
Bouquet et al. 1994	23,4	3,4	MRS07-MRT04	69	M	52	1,64	220	19	*na*	*na*
Bouquet et al. 1994	23,4	5,8	MRS08-MRT04	69	M	52	1,64	220	19	11	11
Stalnaker et al. 1973	10,0	5,8	11M	70	M	56	1,67		20		
Stalnaker et al. 1973	10,0	5,8	14M	73	M	55	1,68		19		
Stalnaker et al. 1973	10,0	5,8	15M	65	M	35	1,57		14		
Stalnaker et al. 1973	10,0	5,8	16M	88	M	68	1,73		23		
Stalnaker et al. 1973	10,0	5,8	17M	49	M	70	1,80		22		
Stalnaker et al. 1973	10,0	5,8	18F	65	F	45	1,61		17		
Stalnaker et al. 1973	10,0	5,8	20F	75	F	40	1,42		20		
Stalnaker et al. 1973	10,0	5,8	21M	62	M	51	1,83		15		
Stalnaker et al. 1973	10,0	5,8	22M	63	M	58	1,70		20		
Stalnaker et al. 1973	10,0	5,8	23M	58	M	70	1,78		22		
Yoganandan et al. 1997	23,5	4,3	PC101	72	M	82	1,70	234	28	4	4
Yoganandan et al. 1997	23,5	4,3	PC102	81	M	63	1,75	219	21	4	4
Yoganandan et al. 1997	23,5	4,3	PC103	84	M	68	1,68	233	24	0	0
Yoganandan et al. 1997	23,5	4,3	PC104	86	M	56	1,70	211	19	2	2
Yoganandan et al. 1997	23,5	4,3	PC105	62	M	61	1,74	240	20	3	3
Yoganandan et al. 1997	23,5	4,3	PC106	70	M	91	1,69	312	32	4	4
Yoganandan et al. 1997	23,5	4,3	PC107	68	M	83	1,78	282	26	6	6

Table 2. Original test series of PMHS airbag, out-of-position, harness and belt tests.

Information source	Test condition	Airbag dist. (mm)	Test/PMHS ref.	Age	Gender	Body weight (kg)	Stature (m)	Chest depth (mm)	Body mass Index	NRF wo Cartilage fractures	NFR wo Cartilage fractures	NFR with Cartilage fractures	NFR with Cartilage fractures
Lebarbé et al. 2005	membrane	13	MS554	76	M	77	1,70	235	27	12	12	12	12
Lebarbé et al. 2005	membrane	13	MS555	67	M	65	1,75	220	21	15	15	15	15
Lebarbé et al. 2005	membrane	78	MS559	73	M	67	1,74	205	22	11	11	11	11
Lebarbé et al. 2005	membrane	78	MS561	72	M	83	1,73	235	28	0	0	0	0
Lebarbé et al. 2005	membrane	128	MS560	74	F	73	1,60	195	29	0	0	0	0
Lebarbé et al. 2005	punch out	52	MS557		M	79	1,66	190	29				
Lebarbé et al. 2005	punch out	52	MS558		F	80	1,58	200	32				
Lebarbé et al. 2005	complete	52	MS562		M	80	1,67	200	29				
Lebarbé et al. 2005	complete	52	MS565		M	72	1,70	225	25				
Trosseille et al. 2008	membrane	13	MS607	84	M	56	1,75	190	18				
Trosseille et al. 2008	membrane	78	MS594	78	M	65	1,70	230	22	3	3	8	8
Trosseille et al. 2008	harness		MS599	73	M	72	1,82	230	22	2	2	3	3
Trosseille et al. 2008	harness		MS610	70	M	60	1,70	230	21	3	3	3	3
Trosseille et al. 2008	diagonal belt		MS595	74	M	69	1,74	220	23	0	0	3	2
Trosseille et al. 2008	diagonal belt		MS609	69	M	71	1,70	250	25	0	0	0	0

Table 3. Original test series of PMHS table top test data (Data on NRF and NFR with cartilage fractures was not available).

Information source	Loading device	Hub mass (kg)	Hub velocity (m/s)	Test/PMHS ref.	Age	Gender	Body weight (kg)	Stature (m)	Chest depth (mm)	Body mass Index	NRF wo Cartilage fractures	NFR wo Cartilage fractures
Cesari and Bouquet 1990	D-B	22,4	3,4	K	72	M	53	1,83	180	16	0	0
Cesari and Bouquet 1990	D-B	22,4	3,1	L	71	M	41	1,70	180	14	0	0
Cesari and Bouquet 1990	D-B	22,4	2,8	M	40	M	56	1,83	190	17	0	0
Cesari and Bouquet 1994	D-B	22,4	2,9	Q	64	F	49	1,64	160	18	0	0
Cesari and Bouquet 1994	D-B	22,4	3,1	R	43	M	54	1,86	200	16	0	0
Cesari and Bouquet 1994	D-B	22,4	2,7	S	67	M	67	1,80	229	21	0	0
Cesari and Bouquet 1994	D-B	22,4	3,1	T	63	M	56	1,76	229	18	0	0
Cesari and Bouquet 1990	D-B	22,4	9,3	A	47	F	93	1,70	180	32	8	8
Cesari and Bouquet 1990	D-B	22,4	6,8	B	17	F	59	1,64	175	22	0	0
Cesari and Bouquet 1990	D-B	22,4	4,1	C	86	F	43	1,60	170	17	2	2
Cesari and Bouquet 1990	D-B	22,4	7,1	D	69	M	82	1,73	220	27	17	12
Cesari and Bouquet 1990	D-B	22,4	8,1	E	60	M	69	1,77	200	22	3	3
Cesari and Bouquet 1990	D-B	22,4	7,5	F	59	F	62	1,70	200	21	4	3
Cesari and Bouquet 1990	D-B	22,4	7,8	G	71	M	75	1,77	210	24	7	7
Cesari and Bouquet 1990	D-B	76,1	3,2	H	67	M	47	1,74	200	16	6	6
Cesari and Bouquet 1990	D-B	76,1	2,5	I	83	F	43	1,55	215	18	4	4
Cesari and Bouquet 1990	D-B	76,1	3,1	J	70	M	63	1,60	190	25	18	12
Cesari and Bouquet 1990	D-B	76,1	3,5	K	72	M	53	1,83	180	16	4	4
Cesari and Bouquet 1990	D-B	76,1	2,8	L	71	M	41	1,70	180	14	10	9
Cesari and Bouquet 1990	D-B	76,1	3,0	M	40	M	56	1,83	190	17	0	0
Cesari and Bouquet 1994	D-B	76,1	2,9	P	60	M	45	1,60	200	17	6	6
Cesari and Bouquet 1994	D-B	76,1	2,7	Q	64	F	49	1,64	160	18	6	6
Cesari and Bouquet 1994	D-B	76,1	3,7	R	43	M	54	1,86	200	16	3	3
Cesari and Bouquet 1994	D-B	76,1	2,8	S	67	M	67	1,80	229	21	2	2
Cesari and Bouquet 1994	D-B	76,1	3,1	T	63	M	56	1,76	229	18	10	10
Kent et al. 2004	Various			176	85	F	58	1,57		24		
Kent et al. 2004	Various			182	80	F	65	1,57		26		
Kent et al. 2004	Various			177	79	F	48	1,61		19		
Kent et al. 2004	Various			155a	71	F	54	1,66		20		
Kent et al. 2004	Various			173	67	F	57	1,62		22		
Kent et al. 2004	Various			147	63	F	45	1,61		17		
Kent et al. 2004	Various			186	58	F	61	1,78		19		
Kent et al. 2004	Various			157	55	F	74	1,68		26		
Kent et al. 2004	Various			189	79	M	57	1,59		23		
Kent et al. 2004	Various			190	79	M	73	1,73		24		
Kent et al. 2004	Various			170	75	M	65	1,78		21		
Kent et al. 2004	Various			178	73	M	81	1,82		24		
Kent et al. 2004	Various			188	71	M	85	1,73		28		
Kent et al. 2004	Various			145	54	M	88	1,92		24		
Kent et al. 2004	Various			187	54	M	113	1,78		36		
Shaw et al. 2007	Indentor			343	72	M	66	1,80		20	15	
Shaw et al. 2007	Indentor			342	75	M	73	1,83		22	10	
Shaw et al. 2007	Indentor			320	48	M	68	1,68		24	4	
Shaw et al. 2007	Indentor			319	52	M	77	1,79		24	17	
Shaw et al. 2007	Indentor			203	67	M	77	1,70		27	15	

D-B Diagonal belt

Table 4. Original test series of PMHS sled test data.

Information source	Loading device	Vel. change (km/h)	Test/PMHS ref.	Age	Gender	Body weight (kg)	Stature (m)	Chest depth (mm)	Body mass Index	NRF wo Cartilage fractures	NFR wo Cartilage fractures	NRF wo Cartilage fractures	NFR wo Cartilage fractures
Forman et al. 2006	Pass 4.5 kN 3pt FL + AB	48	111	57	M	70	1,74	185	23	0	0	0	0
Forman et al. 2006	Pass 4.5 kN 3pt FL + AB	48	107	69	F	52	1,55	205	22	4	4	8	8
Forman et al. 2006	Pass 4.5 kN 3pt FL + AB	48	105	57	F	57	1,77	200	18	0	0	0	0
Bolton et al. 2006	Pass Lap belt + AB + KB	49	124	40	M	47	1,50	156	21	4	4	4	4
Bolton et al. 2006	Pass Lap belt + AB + KB	49	121	70	M	57	1,76	177	18	0	0	0	0
Bolton et al. 2006	Pass Lap belt + AB + KB	49	118	46	M	74	1,75	222	24	0	0	0	0
Forman et al. 2006	Pass 3pt SB + AB	48	112	55	M	85	1,76	231	27	3	3	0	0
Forman et al. 2006	Pass 3pt SB + AB	48	115	69	M	84	1,76	192	27	3	3	3	3
Forman et al. 2006	Pass 3pt SB + AB	48	120	59	F	79	1,61	202	30	13	12	13	12
Forman et al. 2006	Pass 3pt SB	29	322	49	M	58	1,78	200	18	0	0	0	0
Forman et al. 2006	Pass 3pt SB	29	323	44	M	77	1,72	180	26	0	0	0	0
Forman et al. 2006	Pass 3pt SB	29	327	39	M	79	1,84	220	23	0	0	0	0
Petitjean et al.2002	Driver 3pt 4kN FLB + AB	64	MS536	78	F	70	1,69	na	25	5	4	6	4
Petitjean et al.2002	Driver 3pt 4kN FLB + AB	64	MS542	76	M	67	1,74	na	22	10	9	17	11
Petitjean et al.2002	Driver 3pt 6kN FLB	64	MS539	81	M	60	1,70	na	21	14	10	21	12
Petitjean et al.2002	Driver 3pt 6kN FLB	64	MS543	75	M	70	1,69	na	25	9	7	17	12
Vezin et al. 2002a+b	Driver 4 kN 3pt FLB + AB	50	FID11	46	M	63	1,83	210	19	11	8	na	na
Vezin et al. 2002a+b	Driver 4 kN 3pt FLB + AB	50	FID12	83	M	69	1,68	265	24	6	5	na	na
Vezin et al. 2002a+b	Driver 4 kN 3pt FLB + AB	50	FID13	74	M	67	1,68	240	24	0	0	na	na
Vezin et al. 2002a+b	Driver 4 kN 3pt FLB	30	FID14	78	M	82	1,80	250	25	2	2	na	na
Vezin et al. 2002a+b	Driver 4 kN 3pt FLB	30	FID15	81	M	58	1,67	175	21	4	3	na	na
Vezin et al. 2002a+b	Driver 4 kN 3pt FLB	30	FID16	90	M	45	1,77	200	14	0	0	na	na
Rouhana et al. 2003	Pass 3pt SB	40	206	75	M	72	1,75	na	24	29	14	29	14
Rouhana et al. 2003	Pass 3pt SB	40	474	72	M	82	1,78	na	26	4	3	16	9
Rouhana et al. 2003	Pass 4pt FL + PTB	40	853	75	M	81	1,80	na	25	7	7	12	11
Rouhana et al. 2003	Pass 4pt FL + PTB	40	247	41	M	82	1,75	na	27	0	0	0	0
Rouhana et al. 2003	Pass 4pt FL + PTB	40	639	60	M	91	1,83	na	27	0	0	3	2
Rouhana et al. 2003	Pass 4pt FL + PTB	40	683	69	F	42	1,52	na	18	9	8	11	10
Rouhana et al. 2003	Pass 4pt FL + PTB	40	657	79	F	59	1,52	na	26	1	1	3	3
Shaw et al. 2009	Lab seat 3pt SB* + KB	40	411	76	M	70	1,78	210	22	2	2	7	6
Shaw et al. 2009	Lab seat 3pt SB* + KB	40	403	47	M	68	1,77	260	22	23	17	27	17
Shaw et al. 2009	Lab seat 3pt SB* + KB	40	425	54	M	79	1,77	na	25	15	10	15	10
Shaw et al. 2009	Lab seat 3pt SB* + KB	40	426	49	M	76	1,84	na	22	7	7	9	8
Shaw et al. 2009	Lab seat 3pt SB* + KB	40	428	57	M	64	1,75	na	21	3	3	5	5
Shaw et al. 2009	Lab seat 3pt SB* + KB	40	443	72	M	81	1,84	na	24	8	7	9	7
Shaw et al. 2009	Lab seat 3pt SB* + KB	40	433	40	M	88	1,79	na	27	9	8	10	8
Shaw et al. 2009	Lab seat 3pt SB* + KB	40	441	37	M	78	1,80	na	24	0	0	2	2

2.1.2 Inclusion and exclusion of PMHS data

Several reasons for excluding a particular test or test series were identified. Some of these reasons were justified on a scientific basis whereas other datasets were excluded based on logical reasoning. Due to the uncertainty created by relying on reasoning only, two datasets were established and used in the development of risk curves. These datasets are named *Core* and *Extended.* The former includes only those test series for which the applied loads are representative of the loads common in a frontal collision when typical restraints are used; the *Core* dataset is limited to sled test and impactor to the thorax data. The *Extended* dataset includes the *Core* data, table top test and sled test data in which 4-point belts have been used (Rouhana et al. 2003). By inclusion of these tests, the sample size increased on the expense of potentially introducing statistical 'noise' to the data used in the risk curve development. For example, some of the PMHSs in the Rouhana et al. (2003) study exhibited negative chest compressions in combination with rib fractures. The mechanism responsible for these injuries is currently unknown and for this reason the data was excluded from the *Core* dataset but included in the *Extended* dataset.

Other reasons for possible exclusion were:

Tests with PMHS 05FM, 06FM, 07FF, 09FM and 10FF are excluded from the *Core* and *Extended* datasets in the analysis. Chest deflections were measured using a rod technique and this may have reduced the integrity of the chest and as such the number of rib fractures may have been influenced by the instrumentation. With the exception of one test, these PMHSs were subjected to static chest compression prior to the impactor test.

Similarly, all impactors tests carried out by Stalnaker et al. (1973) were excluded due to differences in response to those reported by Kroell et al. (1974) and Neathery et al. (1974). This could have been due to malfunction of the equipment used rather than differences in the response due to the lower impactor mass and higher impactor velocity used by Stalnaker et al. (1973).

Stature, body mass index (BMI) and weight were considered important and data outside the 95% confidence limits of the data sample were excluded from both datasets. These were:

- Outside stature range for subjects
  - Frontal impactor, subject 14FF and 19FM.
  - Table top, subject THC19.
- Outside BMI range for subject:
  - Frontal impactor, subject 46FM and 54FF
  - Oblique impactor, subject PC106.
  - Table Top, subject THC11.
  - Sled, subject FID16.
- Outside mass range for subjects:
  - Table Top, subject THC13.
  - Sled, subject 683

Other test-related reasons for exclusions from both datasets:

- Early disruption of the normal impact event occurred:
  - Frontal impactor, subject 24FM, 32 FM, 54FF and 55FF.
- Force deflection curves used to compute effective mass are missing:
  - Frontal impactor, subject MS621.
- Airbag gas generator malfunction:
  - Airbag test AB0_2 with subject MS607.
- Belt pretensioner malfunction:
  - Sled test 222.

Configurations deemed to apply non relevant loads to the ribcage, such as out of position (test P52_1, P52_2, C52_1, C52_2).

Table top tests were not considered to produce loads perfectly equivalent to from those that are common in frontal collisions. For this reason all table top tests were excluded from the *Core* dataset. Selected table top tests were included in the *Extended* dataset. At the time of risk curve development in this project only the Cesari and Bouquet (1990 and 1994) tests were successfully reproduced using the THORAX demonstrator and data made available. For this reason Kent et al. (2004) and Shaw et al. (2007) Table Top tests had to be excluded from the *Extended* dataset also.

Some of the PMHSs were subjected to multiple exposures. The first sled test with PMHS No. 208 produced fractures and the second test with same subject produce additional fractures. Both tests with subject 208 were therefore excluded from the Core and the *Extended* datasets. Also, Cesari and Bouquet carried out two tests per subject. When the first test carried out was considered non-injurious and the following injurious, these subjects (subject K, L, M, Q, R, S and T) were excluded from the two datasets. This is also the case for table top tests carried out by Kent et al. (2004) and Shaw et al. (2007).

In the Rouhana et al. (2003) sled tests a rod technique was used to study chest deformations. For this reason all these tests were excluded from the Core dataset

Clavicle fractures were present in five of the sled tests in D-B Diagonal belt

Table 4. It was anticipated that chest forces were larger in these PMHS tests than in those where no clavicle fractures occurred. However, from the available data it is not possible to judge whether clavicle fractures occurred prior to or after the rib fractures occurred. For this reason, presence of clavicle fracture was not considered a reason for data exclusion.

Sled test data UVA665, UVA666 and UVA667 were excluded both the *Core* and *Extended* datasets due to excessive belt slip in the demonstrator tests.

2.1.3 PMHS datasets used in the development of risk functions

The *Core* dataset includes a total of 59 tests, of which 26 are frontal and oblique impactor tests, 9 are airbag and inertia load tests, and 24 are sled tests. The data set is presented in Table 5.

The *Extended dataset* includes a total of 71 tests, of which 26 are frontal and oblique impactor tests, 9 are airbag and inertia load tests, 8 is table top tests, and 28 are sled tests. The data set is presented in Table 5.

Table 5. The final datasets, Core and Extended, used in the development of risk curves.

Loading device	Information source	Test ref.	PMHS ref.	Core	Extended
Frontal impactor	Kroell et al. 1971 and 1974		11FF	1	1
Frontal impactor	Kroell et al. 1971 and 1974		12FF	1	1
Frontal impactor	Kroell et al. 1971 and 1974		13FM	1	1
Frontal impactor	Kroell et al. 1971 and 1974		15FM	1	1
Frontal impactor	Kroell et al. 1971 and 1974		18FM	1	1
Frontal impactor	Kroell et al. 1971 and 1974		20FM	1	1
Frontal impactor	Kroell et al. 1971 and 1974		22FM	1	1
Frontal impactor	Kroell et al. 1971 and 1974		23FF	1	1
Frontal impactor	Neathery 1974		31FM	1	1
Frontal impactor	Neathery 1974		34FM	1	1
Frontal impactor	Neathery 1974		36FM	1	1
Frontal impactor	Neathery 1974		37FM	1	1
Frontal impactor	Neathery 1974		42FM	1	1
Frontal impactor	Neathery 1974		45FM	1	1
Frontal impactor	Neathery 1974		53FM	1	1
Frontal impactor	Neathery 1974		60FM	1	1
Frontal impactor	Neathery 1974		62FM	1	1
Frontal impactor	Neathery 1974		64FM	1	1
Frontal impactor	Trosseille et al. 2008		MS589	1	1
Frontal impactor	Bouquet et al. 1994	MRS03	MRT02	1	1
Oblique impactor	Yoganandan et al. 1997		PC101	1	1
Oblique impactor	Yoganandan et al. 1997		PC102	1	1
Oblique impactor	Yoganandan et al. 1997		PC103	1	1
Oblique impactor	Yoganandan et al. 1997		PC104	1	1
Oblique impactor	Yoganandan et al. 1997		PC105	1	1
Oblique impactor	Yoganandan et al. 1997		PC107	1	1
Airbag membrane	Lebarbé et al. 2005	M13_1	MS554	1	1
Airbag membrane	Lebarbé et al. 2005	M13_2	MS555	1	1
Airbag membrane	Lebarbé et al. 2005	M78_1	MS559	1	1
Airbag membrane	Lebarbé et al. 2005	M78_2	MS561	1	1
Airbag membrane	Trosseille et al. 2008	AB0_1	MS594	1	1
Inertia harness	Trosseille et al. 2008	HRN_1	MS599	1	1
Inertia harness	Trosseille et al. 2008	HRN_2	MS610	1	1
Inertia diagonal belt	Trosseille et al. 2008	BLT_2	MS595	1	1
Inertia diagonal belt	Trosseille et al. 2008	BLT_2	MS609	1	1
Table top, diagonal belt	Cesari and Bouquet 1994	THC12	B	0	1
Table top, diagonal belt	Cesari and Bouquet 1994	THC14	D	0	1
Table top, diagonal belt	Cesari and Bouquet 1994	THC15	E	0	1
Table top, diagonal belt	Cesari and Bouquet 1994	THC16	F	0	1

Table top, diagonal belt	Cesari and Bouquet 1994	THC17	G	0	1
Table top, diagonal belt	Cesari and Bouquet 1994	THC18	H	0	1
Table top, diagonal belt	Cesari and Bouquet 1994	THC20	J	0	1
Table top, diagonal belt	Cesari and Bouquet 1994	THC75	P	0	1
Sled pass 4.5 kN 3pt FL + AB	Forman et al. 2006	UVA577	111	1	1
Sled pass 4.5 kN 3pt FL + AB	Forman et al. 2006	UVA580	105	1	1
Sled pass Lap belt + AB + KB	Bolton et al. 2006	UVA651	121	1	1
Sled pass Lap belt + AB + KB	Bolton et al. 2006	UVA652	118	1	1
Sled pass 3pt SB	Forman et al. 2006	UVA1094	322	1	1
Sled pass 3pt SB	Forman et al. 2006	UVA1095	323	1	1
Sled pass 3pt SB	Forman et al. 2006	UVA1096	327	1	1
Sled diver 3pt 4kN FLB + AB	Petitjean et al.2002	SL4_1	MS536	1	1
Sled diver 3pt 4kN FLB + AB	Petitjean et al.2002	SL4_2	MS542	1	1
Sled diver 3pt 6kN FLB	Petitjean et al.2002	SL6_1	MS539	1	1
Sled diver 3pt 6kN FLB	Petitjean et al.2002	SL6_2	MS543	1	1
Sled driver 4 kN 3pt FLB + AB	Vezin et al. 2002a+b		FID11	1	1
Sled driver 4 kN 3pt FLB + AB	Vezin et al. 2002a+b		FID12	1	1
Sled driver 4 kN 3pt FLB + AB	Vezin et al. 2002a+b		FID13	1	1
Sled driver 4 kN 3pt FLB	Vezin et al. 2002a+b		FID14	1	1
Sled driver 4 kN 3pt FLB	Vezin et al. 2002a+b		FID15	1	1
Sled pass 3pt SB	Rouhana et al. 2003	209	474	0	1
Sled pass 4pt FL + PT belt	Rouhana et al. 2003	210	853	0	1
Sled pass 4pt FL + PT belt	Rouhana et al. 2003	217	247	0	1
Sled pass 4pt FL + PT belt	Rouhana et al. 2003	218	639	0	1
Sled lab seat 3pt SB* + KB	Shaw et al. 2009	1294	411	1	1
Sled lab seat 3pt SB* + KB	Shaw et al. 2009	1295	403	1	1
Sled lab seat 3pt SB* + KB	Shaw et al. 2009	1358	425	1	1
Sled lab seat 3pt SB* + KB	Shaw et al. 2009	1359	426	1	1
Sled lab seat 3pt SB* + KB	Shaw et al. 2009	1360	428	1	1
Sled lab seat 3pt SB* + KB	Shaw et al. 2009	1378	443	1	1
Sled lab seat 3pt SB* + KB	Shaw et al. 2009	1379	433	1	1
Sled lab seat 3pt SB* + KB	Shaw et al. 2009	1380	441	1	1

2.1.4 Level of injury

AIS coding protocols have changed over time. Hence the AIS codes as reported in original publications cannot be used as a consistent means of comparing injury severities. Therefore the number of rib fractures (NRF) was suggested to be used as a comparative measure instead of AIS. However, it was considered more appropriate to use number of fractured ribs (NFR) for one of the injury criterion candidates and also thresholds for this measure were established. The relation between NRF and NFR for the *Extended* dataset is shown in Figure 1. Based on this plot and AIS coding it was decided that the limits presented in Table 7 will be applied.

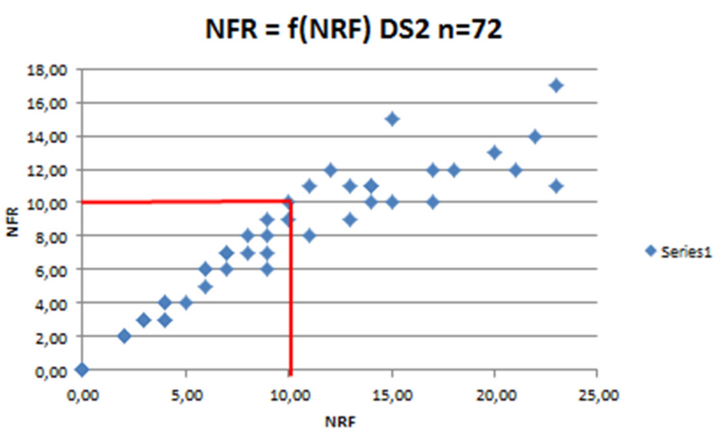

Figure 1. Relation between NRF and NFR.

With the full dataset considered for this study, we have the following numbers regarding subjects and injury coding (Table 6). In this instance the AIS relates to the MAIS for the thorax as reported by the original author. It comes from a variety of AIS codes, certainly not all conforming to the same levels as would be given using AIS 2005.

Table 6. Relationship between AIS, NRF and NFR for the full dataset of PMHS tests.

	Number of subjects injured at that level	Mean NRF	Mean NFR
$AIS = 2$	18	4.1	3.9
$AIS = 3$	42	8.6	7.4

Table 7. NRF and NFR limits used.

	NRF	NFR
$AIS \geq 2$	≥ 5	≥ 5
$AIS \geq 3$	≥ 9	≥ 7

When the proposed NRF limits are used instead of the suggested NFR the PMHS test presented in Table 8 will be coded as injured rather than uninjured, or reverse, in the risk curve development.

Table 8. Specific PMHS tests, out of the *Extended* dataset, for which injury coding change when NRF limits are used instead of NFR.

Author of the study	Test/subject number	NRF	NRF code	NFR	NFR code
Petitjean et al. 2002	MS536	5	Injured	4	Uninjured
Rouhana et al. 2003	210	7	Uninjured	7	Injured
Shaw et al. 2009	1359	7	Uninjured	7	Injured
Shaw et al. 2009	1378	8	Uninjured	7	Injured
Cesari and Bouque et al. 1990	THC17	7	Uninjured	7	Injured
Kroell et al. 1973	11FF	11	Injured	6	Uninjured
Neathery et al. 19	36FM	7	Uninjured	7	Injured
Neathery et al. 19	37FM	9	Injured	6	Uninjured

2.1.5 Assign the censoring status (exact, left, right, interval censored)

In this study only right and left censored data were used. Within the two datasets there is only one subject which was tested twice and therefore could be entered as interval censored data. For simplicity in the data analysis, this option was disregarded. In a few tests, PMHS ribs were instrumented with strain gages which theoretically allow the true time of fracture to be found, and as such, those tests could have been considered as non-censored. However, matching those injury outcomes with the dummy responses at the time of the PMHS fracture would require that there is no phase shift between the ATD and the PMHS responses. Considering this latter condition to be fulfilled is a strong assumption and it was decided to keep those outcomes as censored.

2.2 Crash test dummy data

Injury risk curves are constructed by correlating normalized and non-normalized dummy measures with the PMHS injuries observed in the same test conditions. Table 1 - Table 4 lists the dummy tests carried out within the THORAX project and used in this study. Details on these tests can be found in THORAX report D3.3 (Carroll *et al.* 2013). The final test that were used are presented in Table 5.

A Cox regression (Cox and Oakes 1984) was used to ensure that there were no differences in responses between the two THORAX Demonstrators used in this study which would affect the injury risk estimates. This analysis was based on impactor tests carried out at Humanetics; where equivalent tests were carried out with the two THORAX Demonstrators used in this study. Details of the dummy responses can be found in THORAX report D3.3 (Carroll *et al.* 2013). No significant differences were observed between the two dummies used in this study: the TRL and the Autoliv dummy.

2.2.1 Dummy measurements used for injury risk curve construction

With the multipoint chest deflection measurements from the THOR dummy it has been hoped that an improved injury risk prediction can be generated with respect to a single-point measurement as available with the basic sternal deflection measurement in the Hybrid III. However, the THOR fitted with 3D IR-TRACCS at four different measurement positions is able to generate x, y, z and resultant deflection measurements from each point for any event. This leads to the issue as to how these measurements can be compiled to produce the best potential injury risk prediction.

To provide a baseline for further considerations of how to combine the available measurements, peak values from the IR-TRACCS were generated for each axis at each measurement point for each test. Simple combinations of these were compared with the basic measurements to determine the predictive value of such fundamental measures (most basic x, y, z and resultant output). In this comparisons the underlying factor structure of the maximum resultant and x-axis deflection measurements at each of the four measurement points. The question was to try and help determine how those eight or more predictor variables could be reduced (or summarised) using a smaller set of factors. This analysis is presented in 2.2.1.1.

In addition to the fundamental peak value measures, the combined deflection Dc was revised for use with the THORAX Demonstrators instead of the Humos2 human body model. Please find the revised formulations of this new criterion in 2.2.1.2.

Finally, the THORAX demonstrators were fitted with strain gage instrumentation allowing for investigation of a strain based candidate criteria. A method to transfer the strain measurements to a measure of NFR, that can be used in the development of injury risk curves, is presented in 2.2.1.3

2.2.1.1 Simple combinations of chest deformation data

A principal component analyses was performed using the *Core* dataset without normalisation. The results obtained from the component analysis was further analysed using logistic regression; to identify which of the factors from the principal component analysis was most useful in predicting injury at the NFR ≥ 5 or NFR ≥ 7 level.

A thorough presentation of these analyses can be found in the Appendix A. Below the main findings are presented:

- The largest correlations were found when using factor ‘F1’ to predict both the likelihood of receiving a NFR ≥ 5 and ≥ 7.
- F1 contains the maximum x-axis and resultant deflection measurements for all four quadrants (upper left, upper right, lower left, lower right), suggesting that incorporation of all measurement points is beneficial for the prediction of injury.
- The prediction of injury with the maximum deflection at any of the four points, both in the x-axis and the resultant, is not as complete as the prediction with F1 (which incorporates deflection at all measurement points).
- Based on the NFR ≥ 5 results in particular it seems that for the *Core* dataset, the Maximum peak x-axis measurement from any point offers a better injury risk prediction than the equivalent resultant measure.

The recommendations from this investigation are that for the best predictive ability:

- The Dc formulation for the THORAX Demonstrator needs to include both the x-axis and resultant measurements from all four measurement points.
- If a choice needs to be made between inclusion of either the x-axis or resultant measurements, then at least for NFR ≥ 5 the x-axis measurements would be preferred.
- The maximum peak x-axis measurement from any of the four IR-TRACCS seems to be the most useful fundamental measure to compliment the potentially better, but more complicated Dc.
    - Whilst the x-axis injury risk estimates will be the focus of reporting here, throughout the analysis process the resultant injury risk estimates have also been considered to check the validity of this statistical finding.

2.2.1.2 Development and calculation of DcTHOR

In Thorax project Task 2.3 *Injury mechanism*, a new injury criterion candidate, named the Combined Deflection and noted as Dc, was developed by using a human body model. The principle of this criterion is to combine two metrics: one reflecting the general thoracic compression level, and the second reflecting the ribcage twisting level. Concretely, we use the mi-sternal deflection as the first term; and the lower differential deflection as the second term. This differential deflection corresponds to the difference of deflection measured on the lower right and lower left of the thorax.

The THOR dummy is different from the human body model. Therefore, it was considered necessary to adapt the Dc criterion to the THOR dummy. The adapted Dc criterion for the THOR dummy, denoted DcTHOR, is defined as below:

$$DcTHOR = Dm + dDup + dDlw$$

Where:

1) Dm is the mean deflection of the ribcage, calculated based on the four maximum deflections measured by the IRTRACCs in the X-axis (Formula 1).

$$Dm \ = \ (|ULX|max + |ULX|max + |LLX|max + |LRX|\mathrm{max})/4 \qquad (1)$$

2) dDup reflects the upper thoracic twisting level (Formula 2). The twisting effect is null if the upper left-right differential deflection is less than 20 mm, or if the maximum X-deflection on the one side of the upper thorax does not exceeds 5 mm.

$$dDup = |ULX - URX|max - 20 \qquad (2)$$

3) dDlw reflects the lower thoracic twisting level (Formula 3). The twisting effect is null if the lower left-right differential deflection is less than 20 mm, or if the maximum X-deflection on the one side of the lower thorax does not exceeds 5 mm (Formula 3).

$$dDlw = |LLX - LRX|max - 20 \qquad (3)$$

4) ULX, URX, LLX and LRX are the IRTRACC X-component time histories with respect to the local coordinate system.

Following are some additional comments on the DcTHOR:

1) DcTHOR provides a more complete description of the ribcage deformation than Dmax which is the maximum of the four maximum deflections. In fact, a localized loading may

generate high Dmax but only a few fractured ribs. This is the case with the Yoganadan oblique hub impact in the *Core* dataset (

2) Table 1): Dmax measured on the THOR dummy rose up to 53 mm while the corresponding PMHS tests recorded only a few fractured ribs. It seems reasonable to accept that a test recording 53 mm of deflection at all four IRTRACC measurement points sustains a more severe rib cage deformation than the Yoganandan test although Dmax is the same in the two cases.

3) Field data show that a restraint system combining a 3-points belt equipped with a 4 kN shoulder load limiter and an airbag provides a better level of protection in frontal impact crashes than a restraint system using a 3-point belt equipped a 6 kN shoulder load limiter an no airbag. Neither Dmax nor Dm (mean deflection, Formula 1) measured on the THORAX demonstrator dummy reflected the field data: Dmax = 37 mm and Dm = 22 mm for the 6 kN belt only case; Dmax = 43 mm and Dm = 29 mm for the 4 kN + AB case. The Dc criterion, combining the Dm and the differential deflection, allows discrimination between sled-based recreations of these two restraint system options: DcTHOR = 51 mm for the 6 kN belt only case; DcTHOR = 41 mm for the 4 kN + AB case. The effect of the differential deflection was also demonstrated by human body simulations in Task 2.3.

4) The contribution of the differential deflection is null if it is less than 20 mm (Formula 2 and 3). This number was introduced and chosen to moderate the contribution of the upper and lower differential deflections to the DcTHOR criterion. The number was determined in order for the DcTHOR criterion to be as independent of the loading type as possible.

5) In the DcTHOR criterion, the ribcage twisting level is indicated by the left-right differential deflection on the upper and lower part of the thorax. However, a localized loading such as the Yoganandan oblique hub impact may generate high differential deflection without twisting the ribcage. In fact, the Yoganandan oblique hub impact test on the THOR dummy resulted in high thoracic deflection on the impacted side (53 mm) but almost no deflection in this instance on the other side (3 mm), and no ribcage twisting was observed. A threshold of 5 mm was implemented to judge if the loading localized and is associated with the ribcage twisting.

2.2.1.3 Scheme to go from strain values to predicted NFR

Extensive gage instrumentation has been used in the THORAX project allowing for investigation of a strain based candidate criteria. Expected advantages of such a criterion are twofold:

– First, considering local strains as the metric is expected to be intrinsically linked more closely to the rib fracture mechanism than the rib end deflection. Indeed, for a given deflection various stress states can be observed; in that perspective, considering the local peak stress is theoretically more relevant than using deflection. Furthermore, with the gages being glued on the rib surface, no artefact due to rib rigid body motion is observed.

– Secondly, due to the small space required to use those sensors, a total of twelve ribs have been instrumented, providing three times as many information points as the current four-point deflection system. It appears from investigations on deflection based criteria that using a four-point system is an improvement over monitoring only the sternum compression. In the same way, using twelve peak values is expected to allow for a finer computation of the injury criteria as well as for a deeper understanding of the thorax load pattern

One candidate approach to derive a single value metric from the twelve available peak values has been described in D2.4 report.

Figure 2 illustrates a possible approach to use this criterion. The key point is to determine, for a given dummy, a strain threshold. For each rib of the dummy, once its maximal peak strain reaches the threshold, the rib will be considered as fractured. In this way, we can determine the number of fractured ribs for the dummy in question for each test. But what is the best way to determine the strain threshold? To do this, a three-step approach can be used. First, PMHS-dummy matched tests should be gathered, where we know rib fracture outcome of all PMHS tests, and where the strain distribution of each rib is measured. Then, the NFR-PMHS should be plotted versus the NFR-dummy determined by supposing a strain failure threshold. Finally, we should vary this strain failure threshold until the best correlation is found. This strain threshold will be the threshold for this specific dummy.

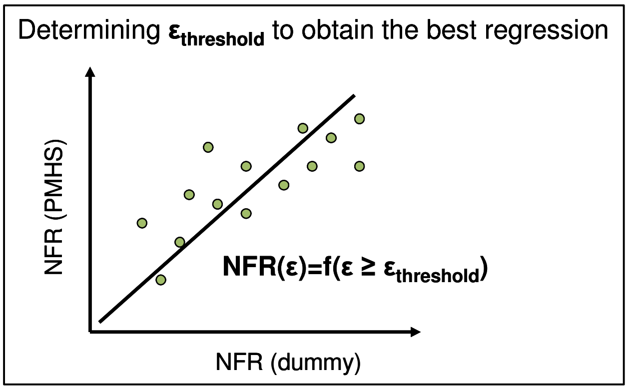

Figure 2. Scheme of a possible approach to apply the NFR as an injury criterion to dummies.

Once the strain threshold has been determined, the NFR can be measured easily and becomes an injury criterion just as sternal deflection. The following sections present the outcomes of applying this approach on the *Core* and *Extended* dataset.

Rib peak strain computing

The first step consists of computing the local peak strain value for each rib. For each rib, the six gage time histories are filtered and any offset is removed.

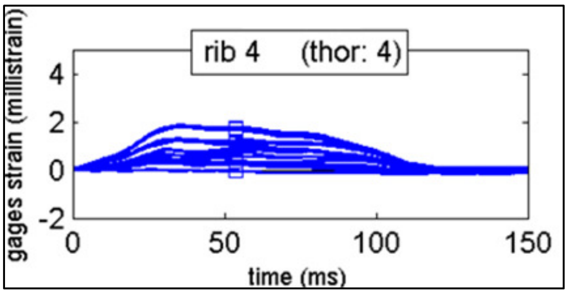

Figure 3. Gages time history for rib level 4.

Each gage time history is then related to the gage location on the rib in order to derive a strain profile (strain value as a function of strain location) for a given time event. Spline interpolation is used so that the computed peak value can be observed in between gage locations.

The following figure shows the strain profile for rib level 4, left and right side, at a given time. Curvilinear gage locations **s** are indicated on the x axis as a percentage of the total rib length.

Gage readings are plotted as blue crosses while blue squares indicate the interpolated peak strain.

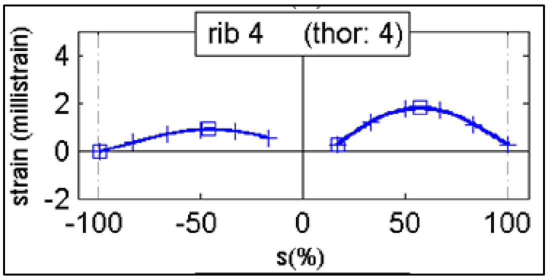

Figure 4. Spline interpolation on rib level 4 for a given time.

Such interpolated peak values are computed for each time step and allow derivation of a peak value time history for both left and right sides of the rib level. The following figure shows the peak strain time history for rib 4 on both the left and right hand sides. The maximum peak values over the test event are indicated with red circles. Note that maximum values can be observed at different times.

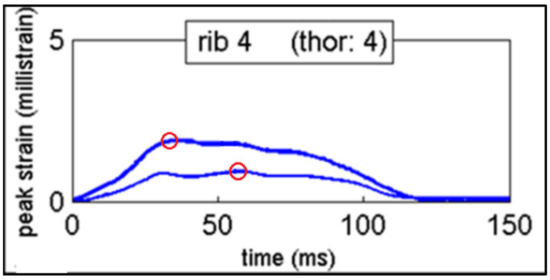

Figure 5. Rib 4 peak strain time history, left and right hand sides.

Those maximum values are computed on each one of the instrumented ribs as shown in the following figure.

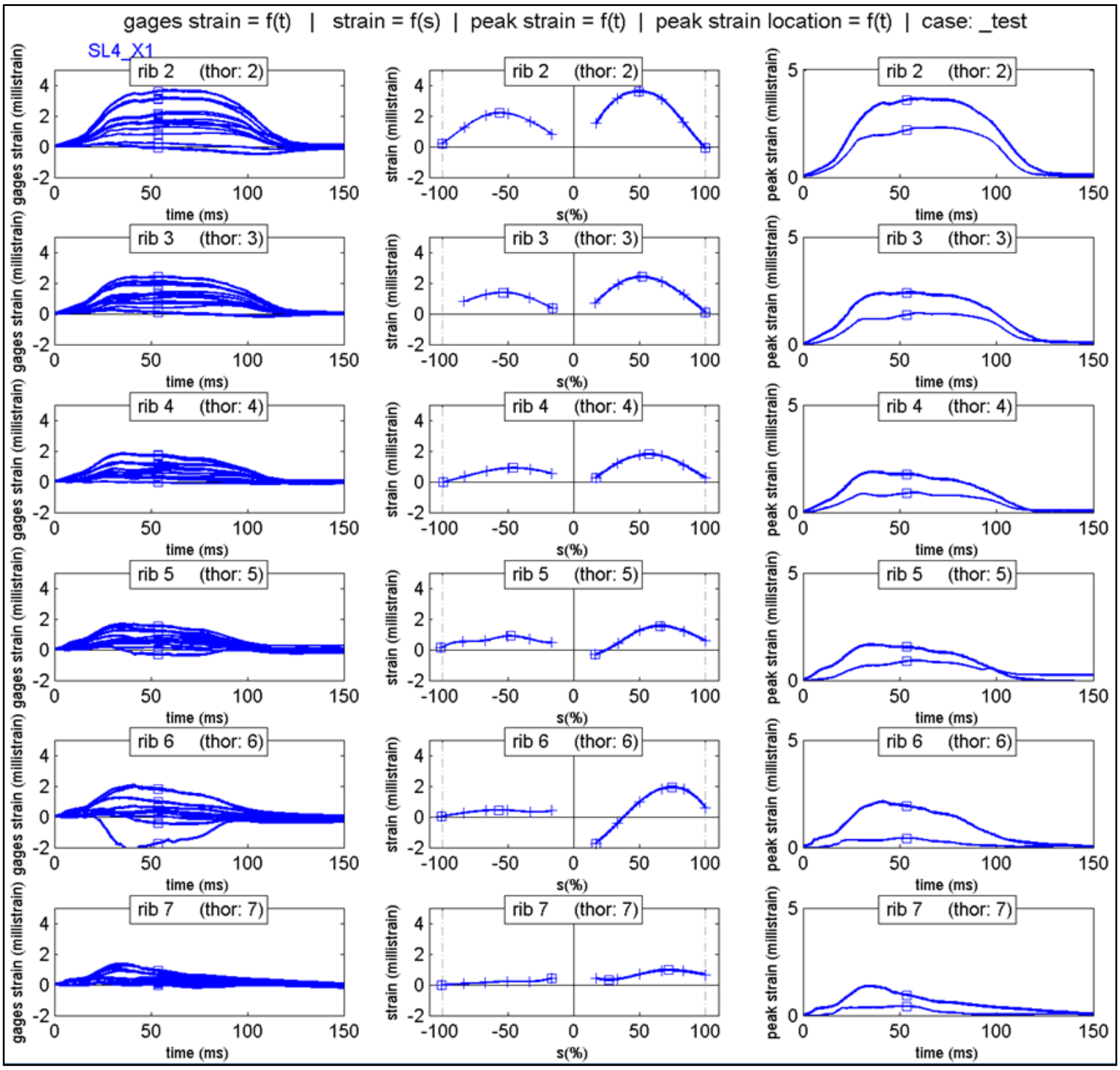

Figure 6. Gage readings, strain profiles and peak value time histories for the 12 ribs.

Thus for each test, twelve peak values are computed and related to the rib level and side. This information is summed up in the following bar graph where the y axis indicates the rib level, rib 1 being the upper most, while the x axis shows the peak strain values up to 6 millistrains.

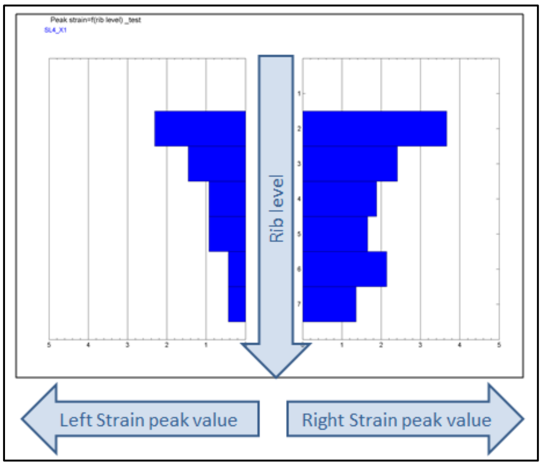

Figure 7. Peak strain values and locations for a given test.

Defining a strain threshold value for the dummy

Then a **D**ummy **F**racture **S**train (**DFS**) value is assumed on the dummy, say for instance DFS=1.2 mStrain. Each dummy rib reading which exceeds this DFS value is considered to be fractured.

This allows computation of a related **N**umber of **F**ractured **R**ibs for the dummy (**NFR_{dum}**). In the following figure, a DFS=1.2 millistrain would lead to NFR_{dum}=8. If the assumed value for DFS were 2 millistrain, the NFR_{dum} would be equal to 4.

Thus the higher the DFS, the smaller the NFR_{dum}.

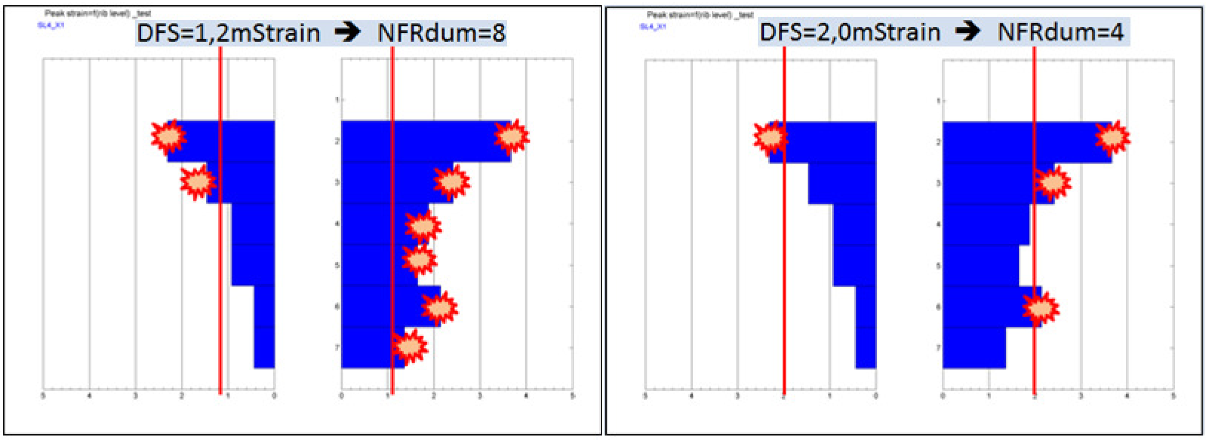

Figure 8. Peak strain values and NFRdum for a given test and DFS.

The DFS value is found out by pairing dummy and PMHS testing in order to relate the NFR_{dum} value to corresponding **N**umber of **F**ractured **R**ibs on the PMHS (**NFR_{pmhs}**). Given that dummy and PMHS does not have the same number of ribs, a rib to rib match is not expected as shown in the following figure.

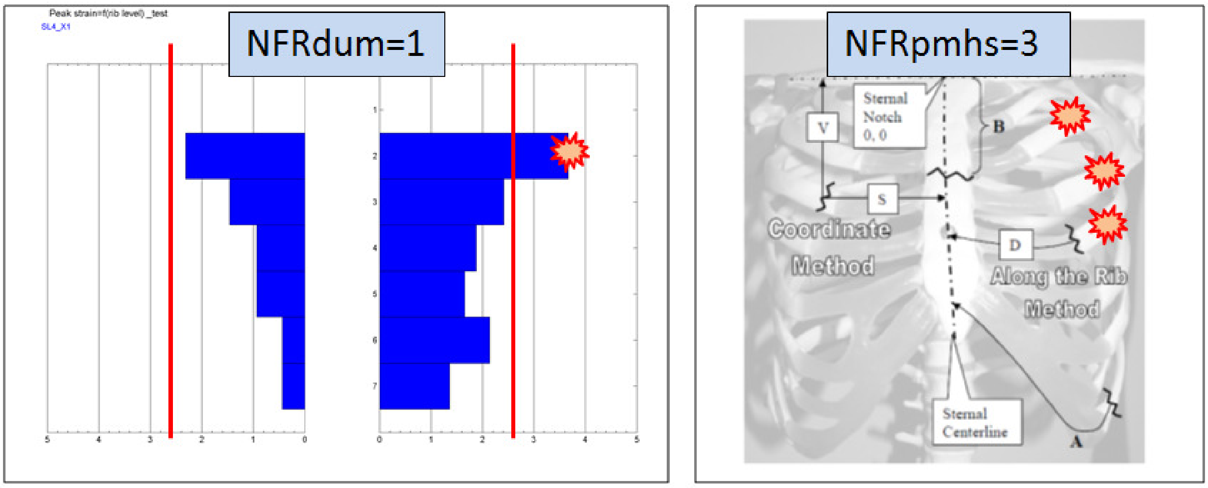

Figure 9. One sample dummy-PMHS comparison with DFS=2.6 millistrain.

A linear relation is assumed between NFR_{dum} and NFR_{pmhs} and the DFS value is varied to get the best R^2 value as shown in the following figure.

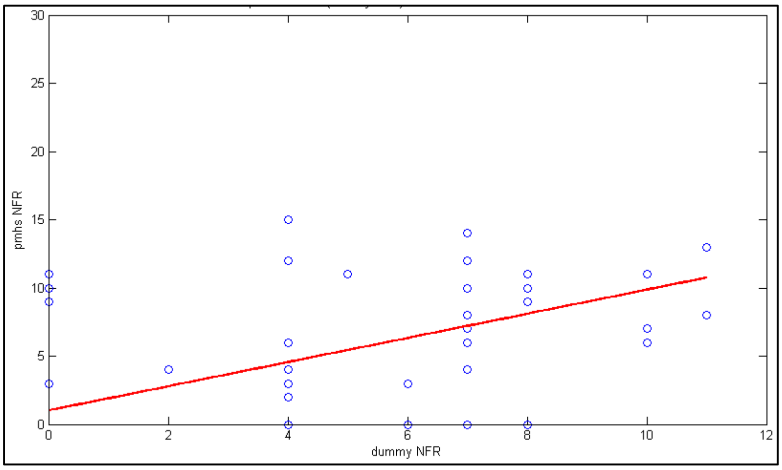

Figure 10. NFR_{pmhs} = f(NFR_{dum}) for a given value of the DFS threshold.

Increasing the DFS value has the effect of decreasing the NFR_{dum} values of each paired test, while keeping constant the related NFR_{pmhs}. In the NFR_{dum}=f(NFR_{pmhs}) plot, each point is then shifted to the left part of the graph, thus altering the R^2 value of the linear relation. The following figures show four sample steps in that process.

The process of varying the DFS values to increase R^2, starts with DFS=0 millistrain and proceeds through to the situation where all of the dummy tests exhibit the maximum number of dummy fractures. In that case all the paired NFR_{pmhs} values, whatever the test, are then related to NFR_{dum}=12.

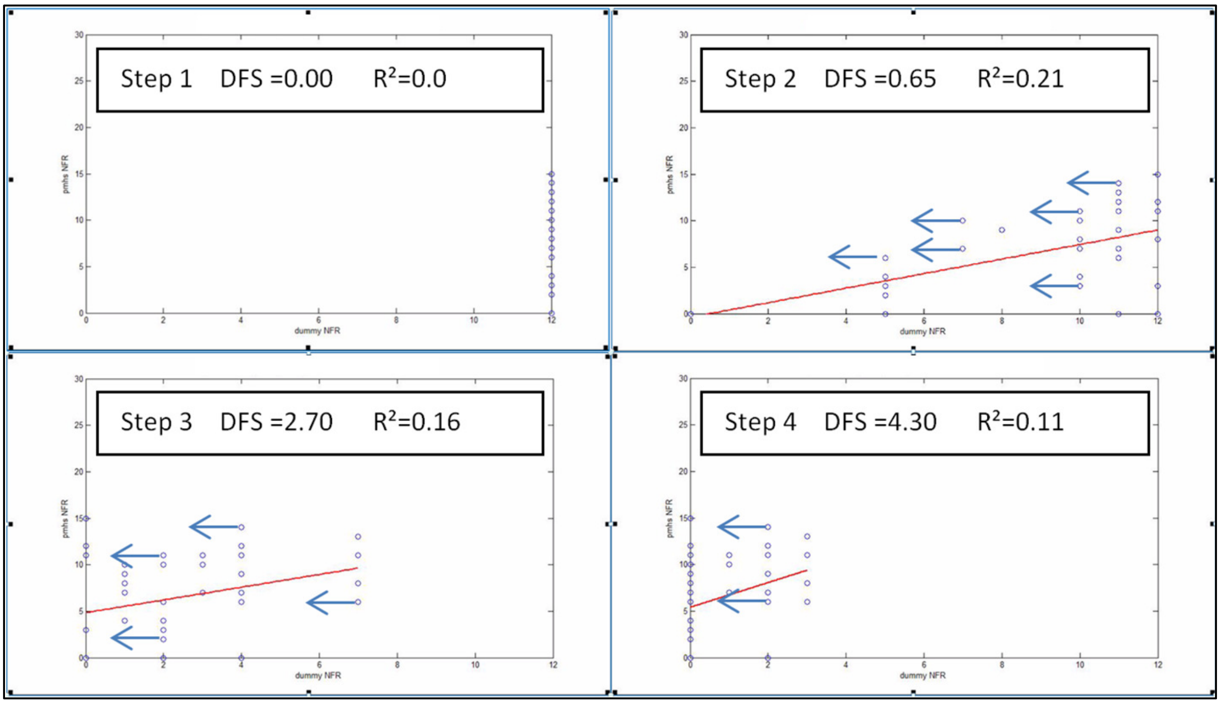

Figure 11. Sample step in the process of DFS optimisation.

For each tested DFS value, the related R^2 value was recorded and the maximum value identified as shown in the following figures.

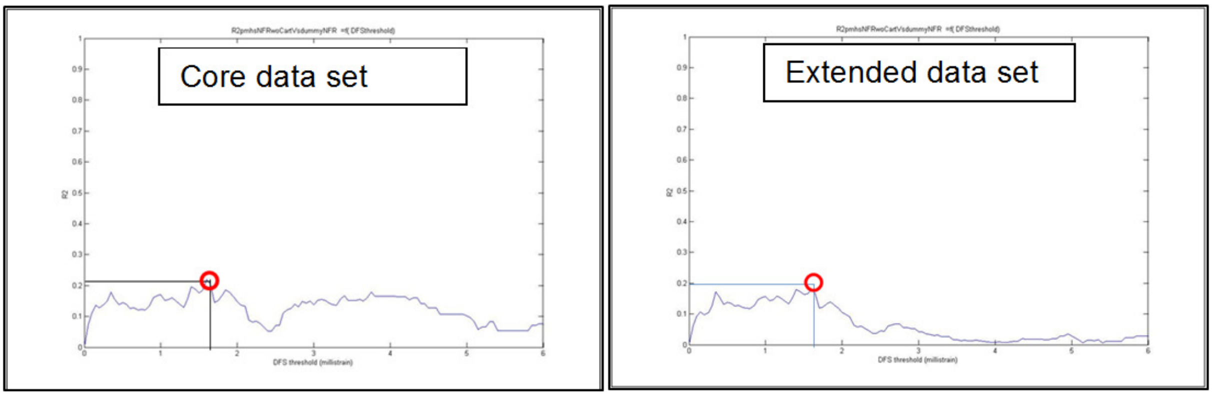

Figure 12. R^2 value as a function of the DFS value for the *Core* and *Extended* datasets.

Although no clear extreme was observed, the maximum R^2 value was 0.22 at DFS=1.6 millistrain for the *Core* dataset and R^2=0.19 at DFS=1.6 millistrain for the *Extended* dataset. The linear regression between NFR_{pmhs} and NFR_{dum} for DFS=1.6 millistrain is plotted in the following figure for the *Core* and *Extended* dataset.

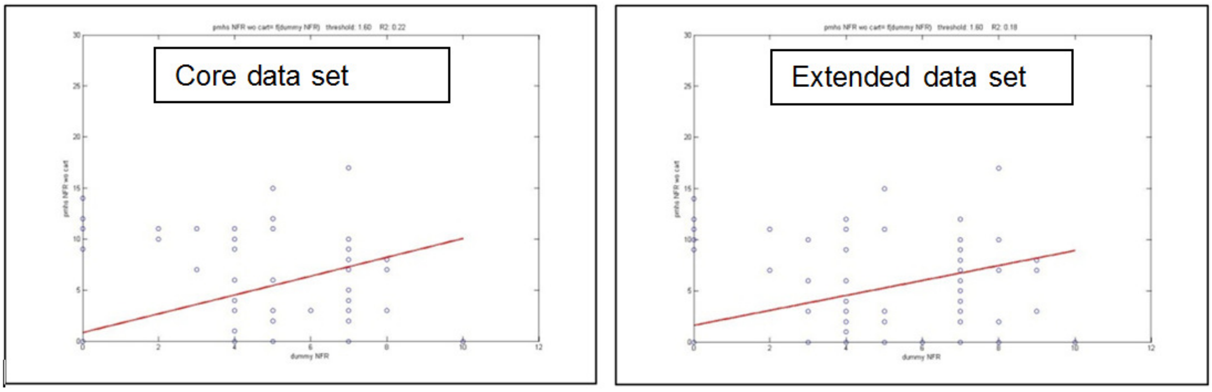

Figure 13 Best R^2 linear regression for *Core* and *Extended* dataset.

The DFS value is therefore set to 1.6 millistrain and the NFR criteria is computed as being the number of dummy ribs exceeding this 1.6 millistrain threshold. One should note that the NFR metric is non-continuous and allowed values are integers ranging from 0 to 12 as shown in the following sample figure.

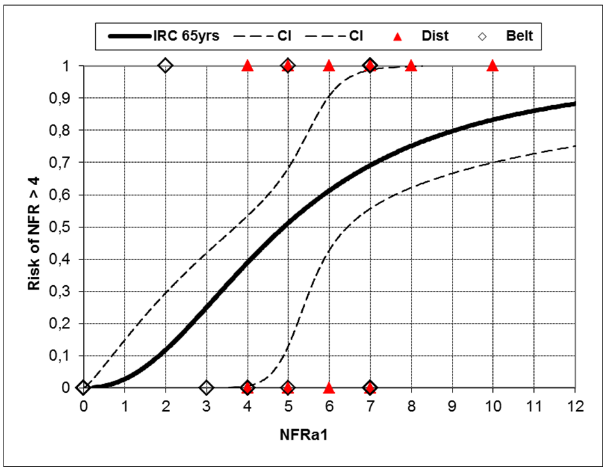

Figure 14. Sample IRC based on NFR.

2.2.2 Normalization of crash test dummy data

The PMHS are generally not mid-size adult males. Therefore, it is considered necessary to scale, in this report referred to as normalize, the dummy response to account for the difference in anthropometry between a dummy and the individual PMHS. In this report injury risk curves were constructed using data normalized for a dummy that represents a mid-size adult male and using non-normalized data. The following scaling methodology was adopted for impactor tests. For the table-top data the same model has been used and an infinite mass has been assumed for the PMHS.

A simple mass spring model is used to represent the Kroell impactor loading condition (Figure 15). In the following sections, subscripts and p relate to the hub and PMHS characteristics respectively.

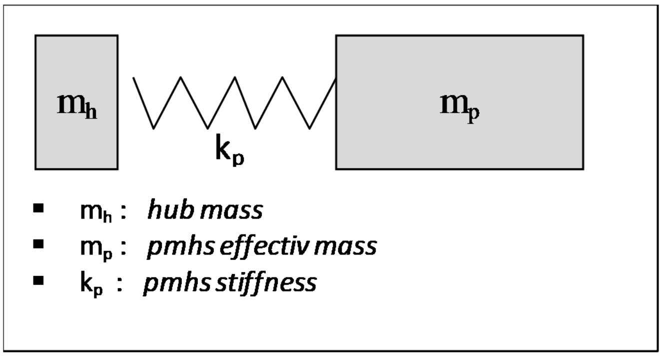

Figure 15. Mass spring model to represent an impactor loading condition.

The governing equation for this system is:

$$x(t) = V_0 \cdot \sqrt{\frac{m_h \cdot m_p}{m_h + m_p} \cdot \frac{1}{k_p}}\, sin\left(\sqrt{\frac{m_h \cdot m_p}{m_h + m_p} \cdot \frac{1}{k_p}} \cdot t\right) \qquad (1)$$

The peak deflection value is derived from the previous equation:

$$x = V_0 \cdot \sqrt{\frac{m_h \cdot m_p}{m_h + m_p} \cdot \frac{1}{k_p}} \qquad (2)$$

Where:

- x is the PMHS deflection
- V_0 is the initial impactor speed
- m_p is the PMHS effective mass

Assuming that peak chest compression (chest deflection normalized to chest depth) is the injury criteria, two different tests lead to the same injury outcome if the following relation holds:

$$\frac{x_1}{L_1} = \frac{x_2}{L_2} \quad \Leftrightarrow \quad \frac{V_{01}}{L_1} \cdot \sqrt{\frac{m_{h1} \cdot m_{p1}}{m_{h1} + m_{p1}} \cdot \frac{1}{k_{p1}}} = \frac{V_{02}}{L_2} \cdot \sqrt{\frac{m_{h2} \cdot m_{p2}}{m_{h2} + m_{p2}} \cdot \frac{1}{k_{p2}}} \qquad (3)$$

Introducing the following lambda coefficients:

$$\lambda_L = \frac{L_1}{L_2} \;;\; \lambda_{m_p} = \frac{m_{p1}}{m_{p2}} \;;\; \lambda_{m_h} = \frac{m_{h1}}{m_{h2}} \;;\; \lambda_k = \frac{k_1}{k_2} \;;\; \lambda_{m_h+m_p} = \frac{m_{h1}+m_{p1}}{m_{h2}+m_{p2}} \qquad (4)$$

The previous equation simplifies into

$$\lambda_{V_0} = \lambda_L \cdot (\lambda_{m_p})^{-1/2} \cdot (\lambda_{m_h})^{-1/2} \cdot (\lambda_{m_p+m_h})^{1/2} \cdot (\lambda_k)^{1/2} \qquad (5)$$

This λ_{V_0} coefficient is used to scale the dummy loading condition in order to compensate the pmhs for not being a 50^{th} subject. For instance, considering a subject exhibiting a 50^{th} stiffness and mass but with a larger chest depth, say L_1=300mm. Then using L_2=229mm as the 50^{th} value, the λ_{V_0} coefficient will be

$$\lambda_{V_0} = \frac{300}{229} \sim 1.31 \qquad (6)$$

To account for this PMHS having a larger chest depth, the dummy should then be tested at a speed increased by 31% with regard to the actual PMHS speed.

Different options can be used in order to relate the λ_k coefficient to the PMHS characteristics. In case the chest depth information is not available, the following assumption can be made

$$\lambda_k = (\lambda_{m_p})^{1/3} \; (Mass\ based\ assumption) \tag{7}$$

In that case, the following is also assumed

$$\lambda_L = (\lambda_{m_p})^{1/3} \tag{8}$$

In case the chest depth is available then one can use

$$\lambda_k = \lambda_L \; (Length\ based\ assumption) \tag{9}$$

WorldSID IRC have been developed using the mass based assumptions, whereas frontal biofidelity targets have used the length based one.

When mass based assumptions are used, the equation simplifies into:

$$\lambda_{V_0} = \; (\lambda_{m_h})^{-1/2} \cdot (\lambda_{m_p+m_h})^{1/2} \tag{10}$$

In case the length based assumptions are used the equation turns into:

$$\lambda_{V_0} = (\lambda_L)^{3/2} \cdot (\lambda_{m_p})^{-1/2} \cdot (\lambda_{m_h})^{-1/2} \cdot (\lambda_{m_p+m_h})^{1/2} \tag{11}$$

For Kroell type impactor tests and Yoganandan impactor tests, the 50th effective mass value has been computed from the *Core* dataset sample in the following way: ratios between effective mass and total mass has been computed. The average value of these ratios have been considered as a 50th value and used in conjunction with the 50th physical mass to derive the 50th effective mass value as being:

$$m_{\,eff.50^{th}} = m_{total\,50^{th}} \cdot \left(\sum_{i=1}^{n} \frac{m_{\,eff.\,i}}{m_{\,total\ \ i}} \right) \cdot \frac{1}{n} \tag{12}$$

For Kroell tests, this value is:

$$m_{\,eff.50^{th}} = 30.69\,kg \tag{13}$$

For Yoganandan tests, this value is:

$$m_{\,eff.50^{th}} = 21.70\,kg \tag{14}$$

When considering the Cesari table top tests, the same model can be used but with the change to assume the PMHS (supported by the table) exhibited an infinite mass. Equations 10 and 11 then simplify in the following form:

$$\lambda_{V_0} = \; (\lambda_{m_h})^{-1/2} \quad (mass\ based) \tag{15}$$

$$\lambda_{V_0} = (\lambda_L)^{3/2} \cdot (\lambda_{m_h})^{-1/2} \quad (length\ based) \tag{16}$$

Lambda coefficients were calculated and used for frontal and oblique test as well as for Cesari and Bouquet 1990-94 table top test.

2.3 Statistical analysis

Survival analysis was developed in medical research to analyse times between two well defined events. A common feature of survival data is its ability to cope with censored data. Censored data requires special techniques and Survival Analysis groups these techniques into parametric, semi parametric or non-parametric.

With a reasonably large sample size ($n > 30$) it is likely that estimated parameters will be normally distributed, which justifies the use of parametric methods.

Because of its ability to deal with censored data, Survival Analysis, and particularly parametric Survival Analysis, has been suggested and have been used to analyse biomechanical data.

2.3.1 Check for effect of subject characteristics

The effect of subject characteristics on Cox regression survival curves was investigated. As the outcome measures, the risk of receiving either NFR ≥ 5 or ≥ 7 were used as a proxy for AIS ≥ 2 and 3. The input measures were either the resultant chest deflection measurements from the four IR-TRACCS or the x-axis measurements. From these the following measurements were included in the analysis: the peak taken from any of the measurement points at any time and the peak of the mean of the top two measurement points.

A Cox regression was used as the statistical test, looking for a 'p-value' less than 0.05 to infer statistical significance.

The subject characteristics assessed were the subject's age, gender, mass, stature and chest depth.

2.3.2 Estimate the distribution parameters

When using the parametric survival analysis, several distributions should be evaluated in order to recommend the one that best predicts the true injury risk function. The distributions Weibull, log-normal and log-logistic were considered within these analyses, as they ensure zero risk of injury for zero stimuli.

2.3.3 Identify overly influential observations

Within the survival analysis 'r' script used for these analyses, there is an implicit check for the number of overly influential data points. A couple of measures exist which can be used to describe the degree to which an observation affects a parameter estimate. The check used here calculates the DFBETA value for each point and compares it with a fixed limit of 0.3. The higher the DFBETA number, the more the point is considered to influence the estimate. The number of points with DFBETAs exceeding 0.3 is reported by the script.

The threshold against which the DFBETA value is compared is set arbitrarily. It is generally considered to be sensible in the range between 1 where a very small dataset is being used and $2/\sqrt{n}$ for larger datasets. In the case of the *Core* dataset used in these analyses, the value of 0.3 is close to the latter limit for large datasets which would be 0.26 for the 59 cases included in the *Core* dataset.

Where a number of overly influential results were observed, then consideration was given as to whether there was a valid physical reason for them to be removed. In these analyses and with the conservative *Core* dataset no justification could be found for further removal of data.

2.3.4 Check the distribution assumption

The distribution assumption was checked. One way is to check graphically using a quantile to quantile plot. The percentiles of the distribution are plotted against the corresponding percentiles of the biomechanical sample. If the plot follows a line through the origin with slope equal to one, then the chosen distribution is appropriate. Another way is to graphically plot the cumulative risk calculated with the survival analysis with a given distribution against the cumulative risk calculated with the CTE method. If the cumulative risks lie close one to the other, then the chosen distribution is appropriate.

In this instance, the estimated risk curve for each of the three distributions was compared with a spline function fitted to the PMHS-THORAX demonstrator data. If the curves from the three assumed distributions had been substantially different from the spline, then there may have been cause to reject them and consider another distribution. However, this was not the case for these analyses and instead the choice of the best distribution to be used was based on an objective evaluation of the best fit to the data.

2.3.5 Choose the distribution

The distribution with the best fit is chosen, based on the Akaike information criterion (AIC). This criterion assesses the likelihood of the model and takes into account the number of variables used in the model. A low AIC indicates the best fit of the model with the test data and large AIC the reverse.

Of the three available distributions considered, the one with the lowest AIC was chosen to be the best estimate.

2.3.6 Calculate the 95% confidence interval

The 95% confidence interval of an injury risk curve was calculated via boot-strapping. The relative size of the confidence interval is defined as the width of the 95% confidence interval at a given injury risk relative to the value of the stimulus at this same injury risk. These were calculated of at 5%, 25% and 50% risks of injury.

2.3.7 Assess the quality index of the injury risk curves

Based on the relative size of the 95% confidence interval four categories of a quality index were defined (Table 9).

Table 9. Quality index categories based on the relative size of the 95% confidence interval.

Quality index	Relative size of the 95% confidence interval
Good	from 0 to 0.5
Fair	from 0.5 to 1
Marginal	from 1 to 1.5
Unacceptable	over 1.5

2.3.8 Study restraint dependency

A Cox regression was used to investigate whether the type of test would influence the risk predictions for the fundamental chest deflection measurements from the THORAX Demonstrators. The peak resultant or x axis deflection measurements from the four IR-TRACCs were used as the injury predictors together with the peak value from any of the four points and the peak of the mean from the top two measurement points. For this analysis the tests were divided into three categories:

1) Sled test;
2) Pendulum test;
3) Out-of-position or deploying restraint system test

Logistic regression was used to evaluate restraint dependency of the DcTHOR criterion. To do this, the restraints (or the loading types) in the *Core* datasets were classified into three configurations:

1) Distributed loading (ConfDist) includes all hub tests and airbag only tests;
2) Belt loading (ConfBelt) includes all tests using only belt to load the thorax;
3) Combined loading (ConfComb) includes all tests using combined belt and airbag to load the thorax.

For both the fundamental chest deflection measurements and the DcTHOR the injury status is the variable to be predicted. Two levels of injuries were examined:

1) At AIS3+ level; uninjured if NFR<7 and injured if NFR≥7;
2) At AIS2+ level; uninjured if NFR<5 and injured at this level if NFR≥5.

For the DcTHOR criterion, the explicative variables were the ($crit), the age($age) and the three restraint configurations (ConfBelt, ConfComb and ConfDist).

The logistic regression was conducted with the R Software, using “binomial” as the family option. Belt restraint was chosen as the reference configuration.

2.4 Age adjustment

Throughout this study, age was used as covariant in the survival analysis. This means that the analyses set the probability of injury to be dependent on both the parameter being measured by the dummy and also the age of the occupant. This feature allows a risk curve to be drawn for any age of occupant. To demonstrate the results the primary age of occupant considered for the study was set to 45 years. In that way, it should be considered that these injury risk curves were constructed for a dummy representing a 45-year-old male.

The age of 45 years was chosen to coincide with previously used injury risk curves. For instance, the recently produced risk curves for the WorldSID were specified for a 45-year-old.

However, as occupant age is known to be a key factor in the risk of thoracic injury (Carroll, 2009) an alternative age was chosen to show how age affects the risk curves. For this reason alternative plots are shown for a 65-year-old occupant as well as the 45-year-old. The 65-years age matches well with the average age of the PMHS test sample used in the analysis and provides a convenient separation from the 45-year-old over which differences in biomechanical tolerance would be expected.

2.5 Check the validity of the predictions against existing results

Real life accident data were available and have been used to check the validity of a subset of the predicted injury risk curves. A detail description of the accident reconstructions and injury risk functions developed is presented in the Appendix B trough D.

3 Results

This section first presents the selected PMHS-dummy measurement data used in the analyses. Thereafter follows a presentation of the statistical analysis conducted prior to the construction of the final injury risk curves. Finally the developed rib fracture injury risk curves for NFR 5 or greater and NFR 7 or greater to be used with the THORAX dummy are presented:

- Curves are presented for occupants 65 and 45 years of age that were constructed using the *Core* dataset and when the data were normalized and non-normalized.
- Curves that were constructed using a more inclusive and larger PMHS-dummy dataset, the *Extended* dataset.

3.1 Selection of PMHS-THORAX data for construction of injury risk curves

In total, ten sled test configurations, two chest impactor conditions, inertia and airbag OOP tests and three series of table top tests were reconstructed. From these tests two datasets were defined and used in the development of risk curves:

The *Core* dataset includes a total of 59 tests, of which 26 is frontal and oblique impactor tests, 9 is airbag and inertia load tests, and 24 are sled tests.

The *Extended dataset* includes a total of 71 tests, of which 26 is frontal and oblique impactor tests, 9 is airbag and inertia load tests, 8 is table top tests, and 28 are sled tests.

3.2 Statistical analysis

3.2.1 Identify overly influential observations

As described in the section 2.3.3, a script is used the check the points with DFBETAs exceeding 0.3. Where a number of overly influential results were observed, then consideration was to be given as to whether there was a valid physical reason for them to be removed.

In these analyses and with the conservative *Core* dataset no justification could be found for further removal of data.

3.2.2 Check for effect of subject characteristics

In an initial analysis, the effect of subject characteristics on the developed injury risk curves was investigated. In brief, the subject characteristics assessed were the subject's age, gender, mass, stature and chest depth. A Cox regression was used as the statistical test, looking for a 'p-value' less than 0.05 to infer statistical significance.

The results reveal that there were no significant effects of any of the covariates on survival function for any of the injury predictor variables.

- The risk of reaching a NFR of 5 or greater (as predicted by each of the 6 maximum resultant deflection measurements – the four x-axis peak values, peak from any one of the four and peak of the mean of the top two) is not dependent on the subject's age, gender, mass, stature or chest depth.
- The risk of reaching a NFR of 7 or greater (as predicted by each of the 6 maximum resultant deflection measurements) is not dependent on the subject's age, gender, mass, stature or chest depth.
- The risk of reaching a NFR of 5 or greater (as predicted by each of the 6 maximum x-axis deflection measurements) is not dependent on the subject's age, gender, mass, stature or chest depth.

- The risk of reaching a NFR of 7 or greater (as predicted by each of the 6 maximum x-axis deflection measurements) is not dependent on the subject's age, gender, mass, stature or chest depth.

The implication of these findings is that the risk functions derived for the fundamental deflection measurements will not be significantly influenced by the subject characteristics. This is important in that it means that additional efforts to control for these variables in the risk function development work are probably not necessary.

The negative aspect of these regression results is that age is not a significant influence on the injury prediction given by the fundamental deflection measurements. It was intended that age specific risk curves would be produced to aid occupant diversity considerations in future frontal impact protection developments. However, it seems that based on this dataset, such age-specific curves would not be significantly different from one another. Furthermore, when deriving the injury risk functions it was noted that the risk estimate gave a better (lower AIC) estimate if age was excluded as a covariant.

Despite the insignificant effect of age, the direction of the age effect was as expected, with a reduction in tolerance being associated with an increase in age. Therefore, whilst the age effect reduced the quality of the prediction and was not of a size to be statistically significant, age was still included as a covariant in order to produce risk estimates for both a 45 and 65 year old occupant.

3.2.3 Study restraint dependency

3.2.3.1 Restraint dependency for simple combinations of chest deformation data

A Cox regression was used to investigate whether the type of test would influence the risk predictions for the fundamental chest deflection measurements from the THORAX Demonstrators. The peak resultant or x axis deflection measurements from the four IR-TRACCs were used as the injury predictors together with the peak value from any of the four points and the peak of the mean from the top two measurement points. For this analysis the tests were divided into being either a sled test, pendulum test or an out-of-position or deploying restraint system test.

1. When maximum resultant deflection measurement at any point was used to predict injury risk:

- The risk of receiving a NFR ≥ 5 is 0.078 times lower with an impactor test compared with a sled test ($p < 0.001$). An example of this effect on the risk predictions is given by the cumulative survival function plot provided in Figure 16.
- The risk of receiving a NFR ≥ 7 is 0.108 times lower with an impactor test compared with a sled test ($p = 0.001$).

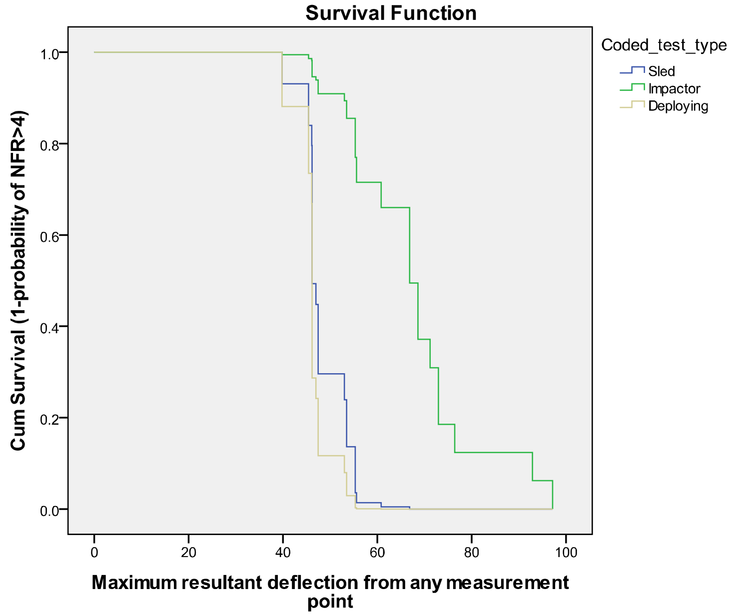

Figure 16. Example of restraint system sensitivity effect on maximum resultant deflection risk prediction of NFR ≥ 5.

2. When maximum x-axis deflection measurement at any point was used to predict injury risk:

- The risk of receiving a NFR ≥ 5 is 0.135 times lower with an impactor test compared with a sled test (p = 0.001).
- The risk of receiving a NFR ≥ 5 is 4.545 times greater with an deploying test compared with a sled test (p = 0.028).
- The risk of receiving a NFR ≥ 7 is 0.194 times lower with an impactor test compared with a sled test (p = 0.008).
- The risk of receiving a NFR ≥ 7 is 4.913 times greater with an deploying test compared with a sled test (p = 0.023). The cumulative survival plat demonstrating this feature of the dataset is shown in Figure 17

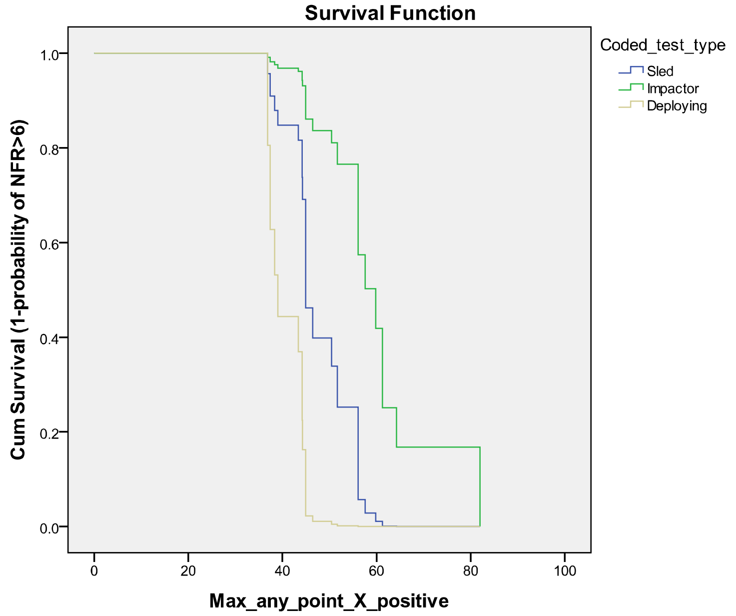

Figure 17. Example of restraint system sensitivity effect on maximum x-axis deflection risk prediction of NFR ≥ 7.

These results demonstrated that both the resultant and x-axis peak measurement injury predictions were dependent on the loading type. The risk curves derived specifically for each type of loading were significantly different from one another (as shown in **Error! Reference source not found.** and **Error! Reference source not found.**). Therefore one could infer from this that the peak deflection measurements are unlikely to be restraint system independent. It implies that for a given chest deflection measurement from the dummy the predicted risk of injury would be different depending on whether the loading had come from a sled, impactor or deploying restraint system test. The risk of injury prediction for a given deflection was slightly lower from impactor tests than from sled tests. This may support the hypothesis that localised belt loading is more injurious than distributed loading. However, it seems to demonstrate a difference between the different types of test that have been reconstructed. In these varied test types we might expect the inertia of the body in the sled, impactor or deploying restraint tests to influence the potential for injuries to occur. Ideally, the dummy measurement would offer equivalent risk assessments in all types of loading to which it is likely to be exposed during future testing. Unfortunately, these results, for these particular dummy measurements, indicate that we may need to know what type of loading caused the deflection before being able to interpret the risk prediction accurately.

Normalisation of the impactor and table-top tests changes these findings, as shown below:

1. When maximum resultant deflection measurement at any point was used to predict injury risk:
- The risk of receiving a NFR ≥ 5 is 0.098 times lower with an impactor test compared with a sled test ($p < 0.001$).
- The risk of receiving a NFR ≥ 7 is 0.076 times lower with an impactor test compared with a sled test ($p = 0.002$).

2. When maximum x-axis deflection measurement at any point was used to predict injury risk:
- The risk of receiving a NFR ≥ 5 is 0.13 times lower with an impactor test compared with a sled test ($p = 0.001$).
- The risk of receiving a NFR ≥ 7 is 0.155 times lower with an impactor test compared with a sled test ($p = 0.006$).
- The risk of receiving a NFR ≥ 7 is 3.919 times greater with an deploying test compared with a sled test ($p = 0.042$).

Therefore, whilst the precise influence of the loading type changed with either the normalised or non-normalised data, the general findings were unchanged. It is not an issue of normalisation causing the loading type dependency.

3.2.3.2 Restraint dependency for DcTHOR

Table 10 and Table 11 presents the results of the restraint dependency analysis based on logistic regression using the R Software (see section 2.3.8):

Table 10. For AIS≥3 level.

Coefficients:	Estimate	Std.	Error z value	Pr(>|z|)
(Intercept)	-7.65	2.497	-3.064	0.0022
data1$crit	0.16	0.045	3.555	0.0004***
data1$age	0.022	0.024	0.900	0.3683
ConfComb	-2.076	1.156	-1.795	0.0726
ConfDist	0.721	0.794	0.908	0.3640

Signif. codes: 0 '***' 0.001 '**' 0.01 '*' 0.05 '.' 0.1 ' ' 1
(Dispersion parameter for binomial family taken to be 1)
Null deviance: 80.9 on 58 degrees of freedom
Residual deviance: 57.1 on 54 degrees of freedom
AIC: 67.1

Table 11. For AIS≥2 level.

Coefficients:	Estimate	Std.	Error z value	Pr(>|z|)
(Intercept)	-9.97	2.997	-3.328	0.0009***
data1$crit	0.22	0.056	3.817	0.0001***
data1$age	0.026	0.027	0.981	0.3266
ConfComb	-1.790	1.158	-1.546	0.1221
ConfDist	1.604	0.933	1.719	0.0856

Signif. codes: 0 '***' 0.001 '**' 0.01 '*' 0.05 '.' 0.1 ' ' 1
(Dispersion parameter for binomial family taken to be 1)
Null deviance: 81.8 on 58 degrees of freedom
Residual deviance: 48.9 on 54 degrees of freedom
AIC: 58.9

The above results show that: 1) the DcTHOR criterion is a significant predictor of the injury status; and 2) the influence of the restraint types is not significant. Nevertheless, it is important to stress that these conclusions should be taken with prudence since it may be conditioned by the database limitations.

3.3 Injury risk curves

3.3.1 Recommended injury risk curves for average age and sample age

Injury risk curves recommended for use with the EU FP7 THORAX demonstrator were developed using the *Core* dataset and using non-normalized demonstrator chest deformation. Curves for a person that is 65 years old are provided in Figure 18.

In this study risk curve were drawn for persons both 45 years and 65 years old. However, as noted in Section 3.2, when analysing the *Core* dataset, it was found that age did not have a significant effect on the survival functions for the fundamental deflection measurements. Furthermore, when deriving the injury risk functions it was noted that the risk estimate gave a better (lower AIC) estimate if age was excluded as a covariant. However, the direction of the age effect was as expected, with a reduction in tolerance being associated with an increase in age. Therefore, whilst the age effect reduced the quality of the prediction and was not of a size to be statistically significant, age was still included as a covariant in order to produce risk curves for a 45 year old occupant (Figure 19).

Table 12 provides the injury measures that correspond to 5%, 25% and 50% risks of injury from the recommended injury risk curves at 65 year old. Confidence limits and the quality index of the injury risk curves are also provided in the Table.

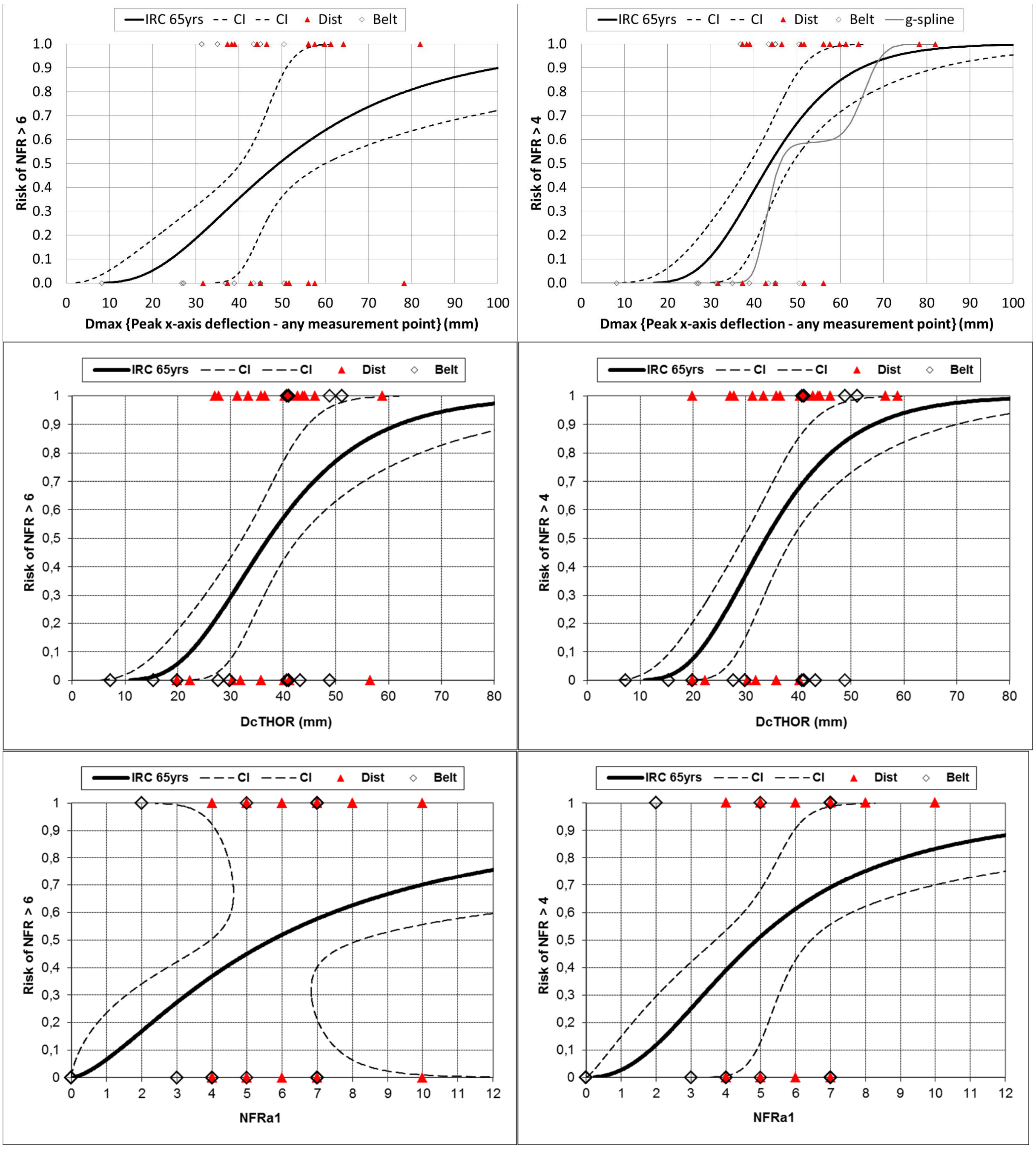

Figure 18. Thoracic skeletal injury risk curve NFR7+ (left) and NFR5+ (right) as a function of the maximum x-axis thoracic rib deflection (measured by any of the IR-TRACC), DcTHORAX and NFR criteria adjusted to 65 year old person for the THORAX demonstrator. *Core* dataset. Non-normalized data.

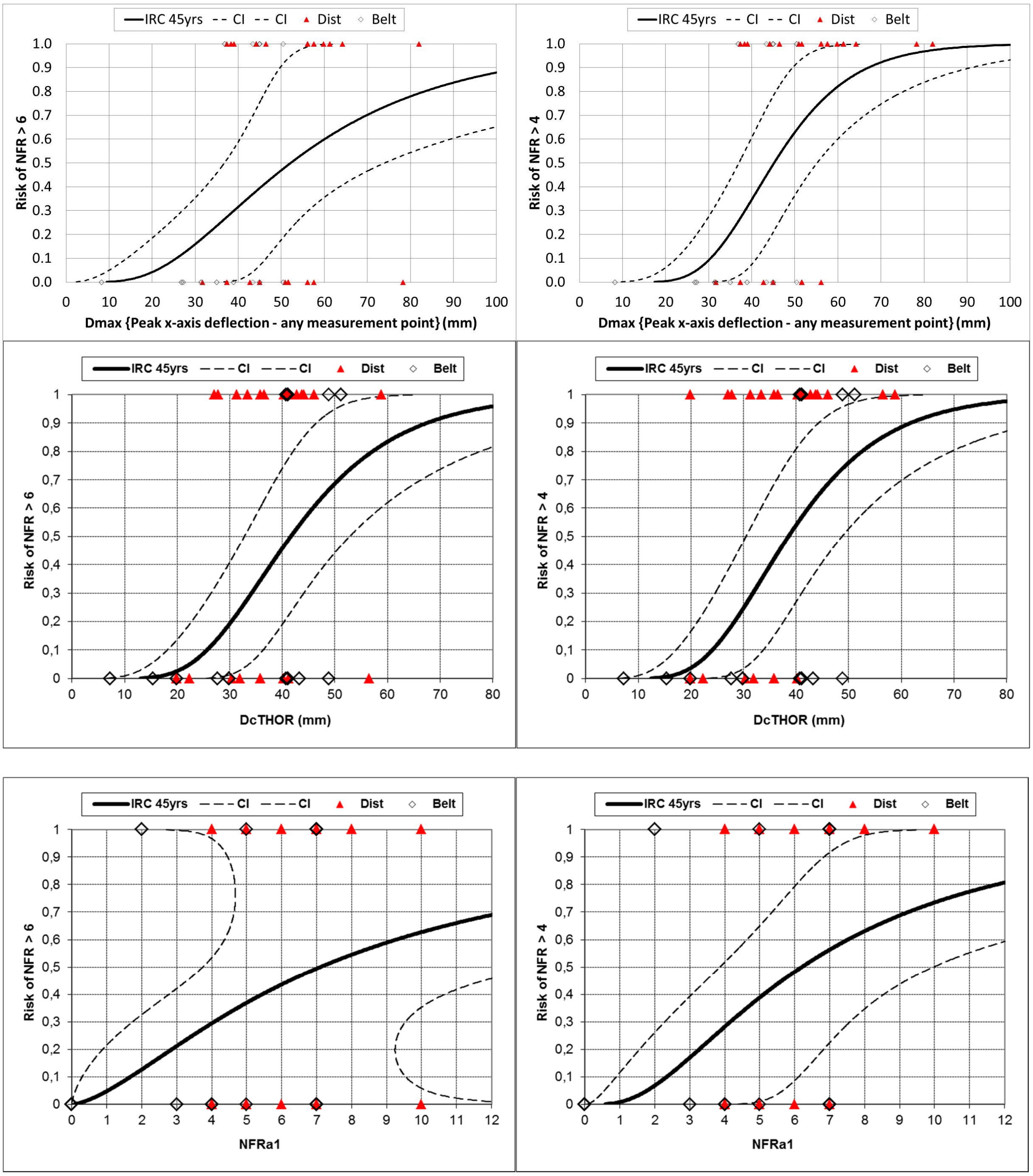

Figure 19. Thoracic skeletal injury risk curve NFR7+ (left) and 5+ (right) as a function of the maximum x-axis thoracic rib deflection (measured by any of the IR-TRACC), DcTHOR and NFR criteria adjusted to 45 year old person for the THORAX demonstrator. *Core* dataset. Non-normalized data.

Table 12. Injury risks and quality index of the injury risk curves for risk curves for 65 year old.

Risk function	Risk (%)	Mean parameter value	Confidence limit, lower	Confidence limit, upper	Confidence error	Grade
Dmax NFR>6	5	19.8	9.7	40.4	1.5	Marginal
	25	33.9	24.9	46.1	0.6	Fair
	50	49.3	40.4	60.1	0.4	Good
Dmax NFR>4	5	26.3	19.0	36.4	0.7	Fair
	25	35.5	29.8	42.2	0.4	Good
	50	43.7	39.1	48.9	0.2	Good
DcTHOR NFR>6	5	19,4	13,0	28,9	0,8	Fair
	25	28,5	23,1	35,1	0,4	Good
	50	37,2	32,3	43,0	0,3	Good
DcTHOR NFR>4	5	18,5	12,9	26,5	0,7	Fair
	25	26,4	21,6	32,4	0,4	Good
	50	33,9	29,5	38,9	0,3	Good
NFR criteria NFR>6	5	0,8	0,1	8,2	9,88	Unacceptable
	25	2,8	1,1	6,9	2,09	Unacceptable
	50	5,7	4,0	8,2	0,75	Fair
NFR criteria NFR>4	5	1,3	0,4	4,6	3,22	Unacceptable
	25	3,0	1,7	5,4	1,23	Marginal
	50	4,9	3,7	6,4	0,56	Fair

3.3.2 Risk curves for the *Core* dataset and normalized dataset

Injury risk curves developed for use with the EU FP7 THORAX demonstrator developed using the *Core* dataset and using normalized demonstrator chest deformation are presented in Figure 20 for 65 and in Figure 21 for 45 year old persons.

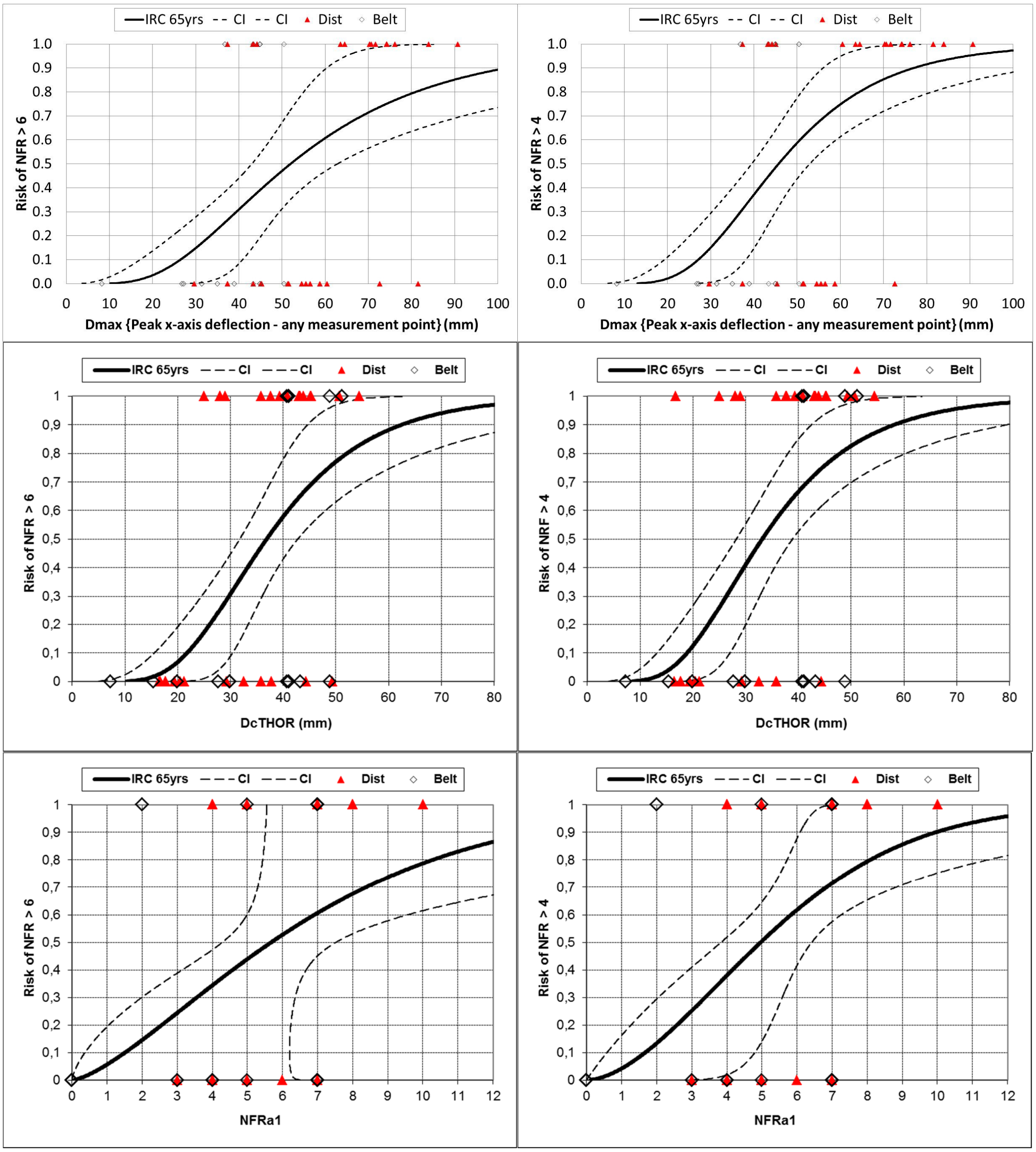

Figure 20. Thoracic skeletal injury risk curve NFR7+ (left) and 5+ (right) as a function of the maximum x-axis thoracic rib deflection (measured by any of the IR-TRACC), DcTHOR and NFR criteria adjusted to 65 year old person for the THORAX demonstrator. *Core* dataset. Normalized data.

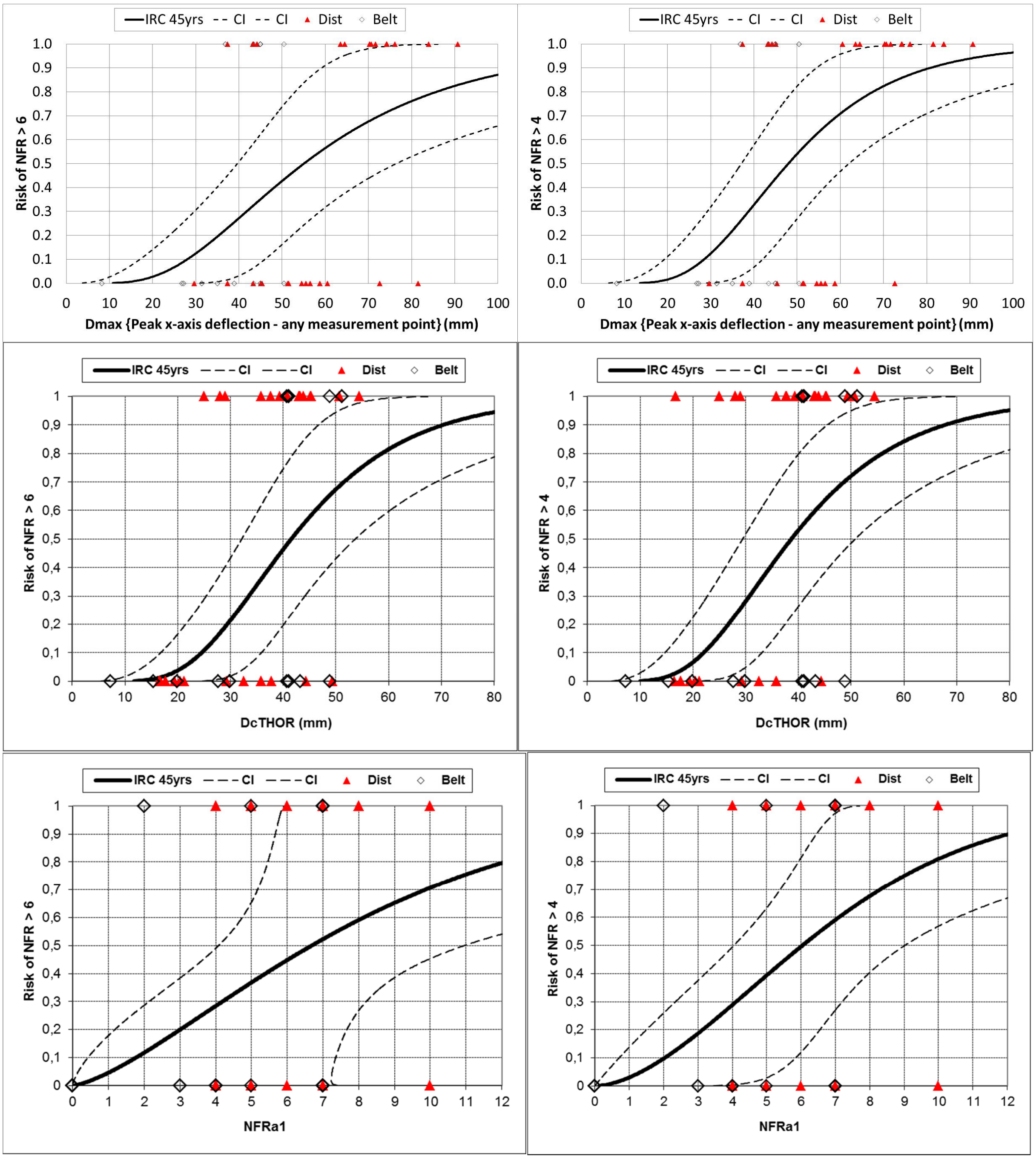

Figure 21. Thoracic skeletal injury risk curve NFR7+ (left) and 5+ (right) as a function of the maximum x-axis thoracic rib deflection (measured by any of the IR-TRACC), DcTHOR and NFR criteria adjusted to 45 year old person for the THORAX demonstrator. *Core* dataset. Normalized data.

Table 13 provides the injury measures that correspond to 5%, 25% and 50% risks of injury from the injury risk curves based on normalized dummy data for 45 year old persons. Confidence limits and the quality index of the injury risk curves are also provided.

Table 13. Injury risks and quality index of the injury risk curves for risk curves for 65 year old.

Risk function	Risk (%)	Mean parameter value	Confidence limit, lower	Confidence limit, upper	Confidence error	Grade
Dmax NFR>6	5	21.9	12.6	37.9	1.1	Marginal
	25	36.4	28.1	47.2	0.5	Fair
	50	52.0	43.0	62.8	0.4	Good
Dmax NFR>4	5	23.4	15.4	35.6	0.8	Fair
	25	34.7	27.8	43.4	0.4	Good
	50	45.7	39.5	52.9	0.3	Good
DcTHOR NFR>6	5	18.8	12.4	28.3	0.8	Fair
	25	27.9	22.5	34.7	0.4	Good
	50	36.9	31.8	42.8	0.3	Good
DcTHOR NFR>4	5	16.1	10.4	24.9	0.9	Fair
	25	24.7	19.4	31.4	0.5	Good
	50	33.1	28.2	38.9	0.3	Good
NFR criteria NFR>6	5	0.9	0.1	6.2	6.70	Unacceptable
	25	3.1	1.5	6.3	1.57	Unacceptable
	50	5.7	4.3	7.5	0.57	Fair
NFR criteria NFR>4	5	1.1	0.3	4.4	3.78	Unacceptable
	25	3.0	1.6	5.4	1.26	Marginal
	50	5.0	3.8	6.4	0.52	Fair

3.3.3 Risk curves for the *Extended* dataset and non-normalized dummy data

Figure 22 show the Dmax and DcTHORAX injury risk curves for the two NFR levels using the Extended dataset. Table 14 provides the injury measures that correspond to 5%, 25% and 50% risks of injury from the injury risk curves. Confidence limits and the quality index of the injury risk curves are also provided. We can observe that for both Dmax and DcTHOR, the confidence limits are wider for the Extended dataset while the threshold for 50% risk remains close.

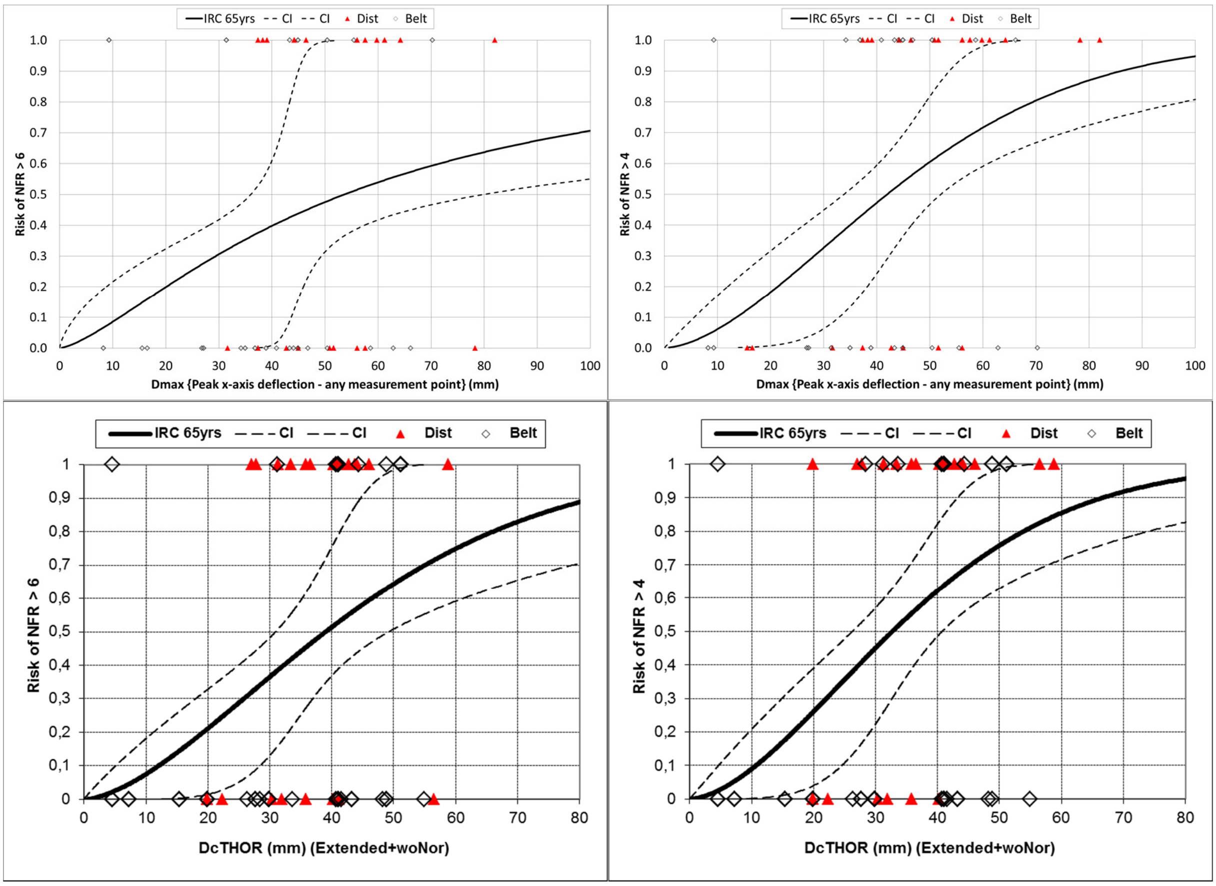

Figure 22. Thoracic skeletal injury risk curve NFR7+ (left) and 5+ (right) as a function of the maximum x-axis thoracic rib deflection (measured by any of the IR-TRACC) and DcTHOR, adjusted to 65 year old person for the THORAX demonstrator. *Extended* dataset and non-normalized data.

Table 14. Injury risks and quality index of the injury risk curves for risk curves for 65 year old. Extended dataset and non-normalized dummy data.

Risk function	Risk (%)	Mean parameter value	Confidence limit, lower	Confidence limit, upper	Confidence error	Grade
Dmax NFR>6	5	6.6	1.0	42.3	3.8	Unacceptable
	25	24.6	12.8	47.3	1.3	Marginal
	50	53.6	36.0	79.9	0.8	Fair
Dmax NFR>4	5	8.8	2.7	28.7	2.4	Unacceptable
	25	24.8	15.2	40.3	1.0	Fair
	50	41.9	33.8	52.0	0.4	Good
DcTHOR NFR>6	5	7.7	2.4	24.9	2.93	Unacceptable
	25	22.5	14.5	34.9	0.90	Fair
	50	39.0	30.9	49.2	0.47	Good
DcTHOR NFR>4	5	7.0	2.3	21.0	2.67	Unacceptable
	25	19.4	12.2	30.9	0.97	Fair
	50	32.7	26.3	40.7	0.44	Good

4 Discussion

4.1 Selection of matched PMHS-THORAX demonstrator tests

The number of matched PMHS-THORAX demonstrator tests that were selected for injury risk curve construction was considered fair to good in comparison to other studies that used a similar approach. In total 59 tests were included, of which 26 were frontal and oblique impactor tests, 9 were airbag and inertia load tests, and 24 were sled tests. Despite this a few concerns related to the matched dataset that may influence the results were identified. These are discussed below.

4.1.1 Type of restraints used

Several of the PMHS tests, that were reproduced using the THORAX demonstrator, were carried out several years ago; before state-of-the-art restraints were readily available. The injury risk curves for skeletal thorax injuries are, however, preferably constructed using data from PMHS test series in which combinations of modern restraints from new car models have been used. In addition, tests that allow the dummy to assess the risk of injuries when loading conditions are not typical, e.g when an occupant is out-of-position or makes contact with a hard object, should be included. Unfortunately, PMHS test data that were generated using very modern restraints and test conditions, and that were suitable for reconstruction, were rare. The approach adopted here was to reproduce all PMHS test series for which the loading induced to the thorax was mainly from the frontal direction. The available test series included both hard contacts and out-of-position along with more typical sled tests. Despite the shortcomings of PMHS test data, we believe that the dataset we have chosen also reflects modern restraints since several tests were carried out with some of the systems commonly installed in modern cars; some of the test series included in the Core dataset included either a traditional diagonal belt, a force limited diagonal belt only, a force limited diagonal belt in combination with an airbag, an airbag only, or a harness.

For 44% of the 59 matched tests included in the *Core* dataset, of the chest was impacted by either a rigid or a padded impactor. These tests loaded the chest symmetrically and the loads were concentrated to a restricted area; these tests were not fully representative of the loads produced by typical modern car restraints. This large proportion may have influenced the analyses carried out here; the development of a risk function that takes asymmetric loading into account would most likely have benefited from additional sled tests with diagonal belts. However, these tests are to some degree representative of airbag loads. In addition, in severe accidents hard contact between the chest and the steering wheel or intruding vehicle components into the survival space is expected to occur and will as such lead to very high risk of skeletal thoracic injuries. In addition, using an impactor is a well-controlled means of loading the chest to non-injurious and injurious subjecting and as such can be considered to be very useful in injury risk curve construction. These reasons justify the inclusion of the impactor tests, although for the future we encourage that additional sled tests with instrumented PMHSs are carried out and data made available for thoracic injury risk curves.

4.1.2 Effect of additional matched tests in injury risk curves

The number of matched PMHS-THORAX demonstrator test included in the *Core* date set and used to produce the injury risk curves appeared to be sufficient. The analysis provided risk curves for DcTHOR and for Dmax with fair to good confidence limits for 50% and 25% risk of AIS 2+ and AIS 3+ thoracic skeletal injuries. For DcTHOR the confidence limits were also fair for 5% injury risks.

An attempt to include additional matched PMHS-dummy tests was introduced; this dataset was denominated *Extended* and included eight table top tests and four sled tests in addition to those included in the *Core* dataset. Unfortunately, the risk curves based on the *Extended* dataset had wider confidence limits than those based on the *Core* dataset. We speculate that the ribcage loading in the included table top test were rather different from those that occur in sled tests and as such inflated the confidence limits; some PMHSs had no injury while the thorax of the THORAX demonstrator exhibited large chest deformations that were expected to produce sever injuries. Other reasons for larger confidence limits could be the inclusion of four additional sled tests. In these tests the PMHS upper body kinematics and chest compressions were very different from those observed in the THORAX demonstrator tests. Additional analysis will be useful to assess this in greater detail.

4.1.3 Reproduction of the original PMHS tests

The quality of the developed injury risk curves is to a large degree a function of how well the actual PMHS tests were reproduced. Not all tests that were carried out with the intension to be used for injury risk curve construction could be included; some were excluded due to excessive belt slippage along the clavicle and some were excluded due to upper body kinematics most likely dissimilar those of the original PMHSs. To assess how well the actual PMHS tests were reproduce, additional tests with the Hybrid III dummy were carried out and the responses compared to Hybrid III tests that were carried out in conjunction with the PMHS tests. These tests are reported in the THORAX report D.3.3 compiled by Carroll et al. (2013). The analyses indicate that the loading modality was well reproduced for most test conditions included in the Core dataset. For a few test conditions there was a lack of Hybrid III data, for these the biofidelity assessments comparisons was used to judge how well the original test conditions was reproduced (Carroll et al. 2013).

4.1.4 Exclusion of demonstrator tests

A few matched PMHS-THORAX demonstrator tests had to be excluded due to excessive belt slip; these tests could not be redone due to limited availability of the dummies. In the future improved injury risk curves could be drawn if these tests are redone and included.

4.2 Normalization of data

For normalization of table top and impactor data we adopted a *Length* based assumption as length measurements were available for the all subjects included in the dataset used here. In addition, we preferred consistency with the frontal impact biofidelity work by Lebarbé (2011). Further, if the mass based normalization method was adopted there would be no effect in the table top cases where an infinite masse was assumed for the PMHSs. In contrast, using length based assumptions allowed scaling of those tests based on PMHs anthropometry.

4.3 Dependency on restraint used

The THORAX demonstrators were fitted IR-Traccs for measurement of chest front wall relative to spine displacements and strain gauges along the ribs to measure rib curvature changes. These measurements were used to calculate criteria Dmax, DcTHOR and NFR. The Dmax takes the maximum x-deformation in any of the four measurement points and as such was expected to differentiate between types of restraints. The DcTHOR also used the chest deformations but includes terms for relative right and left chest compression. Due to the inclusion of differential deformation, the DcTHOR is expected to be more sensitive to restraint type than Dmax. NFR is a measure of the number of ribs for which strain in the ribs reached a predefined limit; roughly it is a measure of the number of ribs that were exposed to a specified curve change. As such the NFR was expected to predict injuries for belted occupants even better, than the deflection measurements, when the chest was exposed to local and asymmetric loads. However, about half of the tests included in the *Core* dataset, mainly load the chest symmetrically; a single diagonal belt, sometimes in combination with an airbag, was used in two inertia load tests and 22 sled tests and 6 tests were carried out with an oblique impactor. The large proportion of tests with symmetric chest loading may be the reason why the confidence limits for the Dmax was rather similar to those obtained for the DcTHOR.

However, one of the features of the Dmax criteria and the fundamental chest deflection measurements from each of the IR-Traccs is that the prediction of injury for a given deflection depends on the type of loading applied to the subject. The implication of this is that one needs to understand the type of loading being applied to the dummy before assessing the injury risk and potentially different risk curves will be needed for sled and other types of tests, for instance. The DcTHOR was specifically tuned so as to try and remove such test type dependence, therefore it is expected that the DcTHOR offers a benefit over the more basic deflection measurements in this respect.

4.4 Check for dual injury mechanism

The complexity of the human ribcage is such that the PMHS injuries may have been due to different injury modes. Different injury modes could lead to injury risk curves with changes of slope and discontinuities. This was addressed in previous THORAX work devoted to establishing an improved understanding of the key injury mechanism (Song et al. 2012). The study supported past research that suggest that the bending of the rib in the plane of the rib was the most important mechanism that led to rib fractures. Based on this finding the authors considered that the thorax injuries in the sample studied are due to a single injury mode and can be assessed by simple measure of thorax compression (Dmax) and the more advanced criteria DcTHOR and strain along the ribs (NFR-criterion).

One key limitation with this study was that the influence of rib rotation on injury risk was not fully addressed and represents an area of potential further work. However, including vertical (z-displacements) or horizontal (y-displacements) did not improve the injury predictability (Appendix A).

4.5 Level of injury

In this study we could not use the AIS coding as supplied in the original work. The AIS code for thoracic skeletal injuries has been changed; different AIS coding schemes were used in the PMHS studies included here. Therefore the number of fractured ribs was used in this study as these were reported in the original documentation of the PMHS tests. To suggest limits to be used, the relationship between the original AIS code assigned each PMHS following the tests and the number of reported rib fractures were established for AIS 2 and AIS 3 (Table 6). The results attained indicated that an AIS 2+ injury was equivalent to 5 or more fractured ribs while AIS3+ was equivalent to 7 or more fractured ribs. Compared to the AIS 2005 scale, these limits appear to be rather high, meaning that a rather high number of rib fractures are needed to be classified as an AIS 2+ or AIS 3+ injury. However, the AIS scale is intended to be used to classify injuries in healthy persons that have been subjected to crashes and that are alive at the time of impact. It is not intended to be used to code injuries produced in PMHS tests and it is expected that AIS coding in PMHSs is quite different to those for traffic victims.

Risks functions for the thoracic skeletal injuries were considered to be a first priority. We also aimed at developing risk curves for costal cartilage injuries, clavicle and sternum fractures. Unfortunately records of costal cartilage fractures were not included in all original PMHS studies and the subset of matched PMHS-THORAX demonstrator tests were considered too few for costal cartilage injury risk curve developments. Similarly for clavicle fractures, the number of PMHS tests in which load was transferred through the clavicle was limited. Sternal fractures occurred in a number of the original PMHS tests; the data may be useful for development of sternal injury risk curves; this was not considered as a high priority as part of this project.

One feature observed with the injury risk curves for the 45 year old occupant, based on Dmax and also for NFR at very low levels is that the estimates for NFR ≥ 5 and NFR ≥ 7 intersect. At very low levels, the risk prediction estimates derived on the basis of the *Core* dataset indicate a higher risk of NFR ≥ 7 than 5 for a given value of the criterion. This seems to indicate that the more severe injury would occur before the less severe injury which is a nonsensical result. It is impossible for seven fractures to occur before 5. This is shown in the comparison of the Dmax risk estimates provided in Figure 23.

On closer inspection of the curves provided in Figure 23 it can be seen that below 60 mm the two curves fall within the confidence limits of one another. This suggests that the curves for the two different injury levels will not be significantly different from each other at low deflection levels. The assertion that an NFR ≥ 7 injury can occur at a deflection level below that for an NFR ≥ 5 injury is not statistically robust. This situation has arisen because of the poorer balance of injured and uninjured data at the NFR ≥ 7 level compared with NFR ≥ 5 with the NFR ≥ 7 curve having wider confidence intervals throughout the range shown.

The estimates shown in Figure 23 are the best available from the dataset and derivation method employed within the study. The intersection of the curves seems to be a valid part of these estimates and as such appear to be inescapable. Therefore, care must be taken when interpreting differences between low risks of injury at the NFR ≥ 5 and 7 levels.

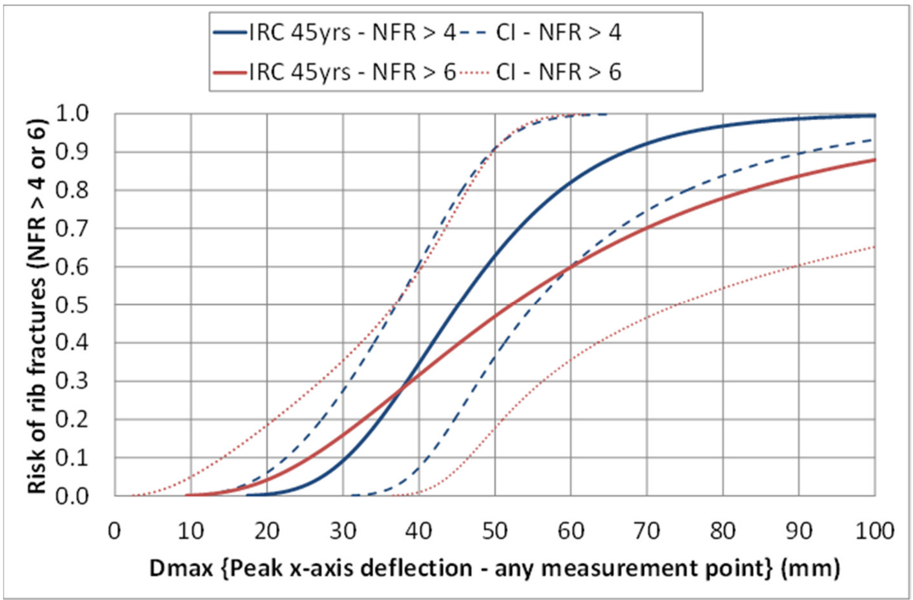

Figure 23. Comparison of thoracic skeletal injury risk curves for NFR7+ and 5+ as a function of the maximum x-axis thoracic rib deflection (measured by any of the IR-TRACC)

4.6 Injury risk curves for other sizes, ages and gender

Risk curves were drawn for persons both 45 years and 65 years old. However, when analysing the *Core* dataset, it was found that age did not have a significant effect on the survival functions for the Dmax. Furthermore, when deriving the injury risk functions it was noted that the risk estimate gave a lower AIC estimate if age was excluded as a covariant and as such a better representation of the original PMHS data (Section 3.2). One reason for this could be that PMHS age distribution; the standard deviation for the *Core* dataset was just 14 years. In addition, the bulk of the PMHSs were above 65 years of age while there were a few PMHSs that were very young at the time of death. It may well be that the three PMHSs that were below 40 years of age were more fragile than the average of their age group. These three subjects may have vastly, due to their low age, influenced the survival functions for Dmax and the AIC values. Additional analysis in which the youngest subjects are excluded from the analysis may clarify this.

4.7 Check the validity of the predictions against existing results

Real life accident data were reproduced to check the validity of the injury risk curves developed using matched PMHS-THORAX demonstrator data. A detail description of the accident reconstructions and injury risk functions developed is presented in Appendix B through to Appendix D.

The results obtained in the reconstruction study support the results obtained here; the injury risk curves for Dmax developed for the THORAX demonstrator mainly fall within the confidence limits of the risk curve developed in the reconstruction study. One difference worth pointing out is the difference in risk for lower Dmax values; here the accident reconstructions suggest that the risk of skeletal thoracic injury at AIS3+ level is miniature for Dmax values below 30 mm (Figure B18) while the curve developed using matched PMHS-THORAX demonstrator data suggests a risk of 20% at 30 mm deformation (Figure 18).

5 Conclusions

The results include injury risk functions for a number of parameters and a criterion developed for the THORAX demonstrator. Two displacement based criteria including the maximum peak deflection measurement (Dmax) and a differential deflection criterion (Dc) were found to have a good injury risk quality index. Furthermore, the Dc was found to be consistent with an established field data observation: a 4kN shoulder belt force limiter associated with an airbag offers better protection than a 6kN shoulder belt. In addition to these global displacement criteria, a local strain based concept was introduced using strains measured in six positions around each of the lower six ribs. Strain values were converted into a prediction of the number of fractured ribs. Although the quality index for the related risk curves was not as good compared to the displacement based criteria, the strain based criterion appears to be a potential injury criterion candidate as by nature it is less sensitive to restraint conditions. The sled and body-in-white results demonstrate that the dummy and these draft injury risk functions are suitable to be used in tests in which various types of vehicle restraints are used.

In conclusion, this report presents draft injury risk curves dedicated to the THORAX demonstrator for thoracic rib deflection when subjected to frontal and oblique loading and their application to a range of sled tests using different restraint systems. These curves are provided for peak deflection measurements, for a new combined thorax deflection criterion and a new rib strain based criterion.

6 References

Bolton J, Kent R and Crandall J (2006) Passenger Air Bag Impact and Injury Response using a Hybrid III Test Dummy and Human Surrogates, NHTSA Biomechanics Test Database, Tests 8377-8379, 2006.

Bouquet R., Ramet M., Bermond F. and Cesari D. (1994). Thoracic and pelvis human response to impact. Enhanced Safety of Vehicles (ESV), Paper number 94-S1-O-03, pp.100-109.

Carroll JA (2009). Matrix of serious thorax injuries by occupant characteristics, impact conditions and restraint type and identification of the important injury mechanisms to be considered in THORAX and THOMO. COVER Project deliverable D5, available from the COVER internet site: http://www.biomechanics-coordination.eu/site/en/documenten.php.

Carroll J, Hynd D, Davidsson J, Vezin P, Been B, Eggers A, Martinez L (2013) Dummy validation report, THORAX project GA No. 218516, D3.3.

Cesari D, Bouquet R (1990) Behaviour of human surrogates thorax under belt loading", Proceedings of Stapp Car Crash Conference, Paper number 902310, pp 73-81.

Cesari D and Bouquet R (1994). Comparison of Hybrid III and human cadaver thorax deformations. Proceedings of Stapp Car Crash Conference, Paper number 942209, pp.65-76.

Cox D and Oakes D (1984). Analysis of survival data. London: Chapman and Hall, First edition.

Forman J., Kent R., Ali T., Crandall J., Boström O., et al., (2005) Biomechanical Considerations for the Optimization of an Advanced Restraint System: Assessing the Benefit of a Second Shoulder Belt, Proceedings of IRCOBI Conference, Prague, Czech Republic, pp 337-353.

Forman J, Lessley D, Kent R, Bostrom O, Pipkorn B (2006) Whole-body kinematic and dynamic response of restrained PMHS in frontal sled tests", Proceedings of Stapp Car Crash Conference, Paper number 2006-22-0013.

Foret-Bruno, J. Y., Hartemann, F., Thomas, C., Fayon, A., Tarrière, C., Got, C. and Patel, A. (1978). *Correlation between thoracic lesions and force values measured at the shoulder of 92 belted occupants involved in real accidents.* Proceedings of Stapp Car Crash Conference, SAE technical paper 780892, Society of Automotive Engineers, Warrendale, PA, USA.

Foret-Bruno, J. Y., Brun-Cassan, R., Brigout, C. and Tarrière, C. (1989). *Thoracic deflection of Hybrid III: dummy response for simulations of real accidents.* Experimental Safety Vehicles (ESV), pp.650-660.

Kent, R., Patrie, J., Poteau, F., Matsuoka, F., Mullen, C., (2003a) Development Of An Age-Dependent Thoracic Injury Criterion For Frontal Impact Restraint Loading, Proceedings of 18th International Conference on Experimental Safety Vehicles (ESV), Nagoya, Japan, Paper No. 72.

Kent R., Patrie J., Benson N., (2003b) The Hybrid III dummy as a discriminator of injurious and non-injurious restraint loading, Annual Proceedings of the Association for the Advancement of Automotive Medicine (AAAM)", volume 47, pp 51-75, 2003.

Kent, R., Lessley, D., Sherwood, C. (2004) Thoracic response to dynamic, non-impact loading from a hub, distributed belt, diagonal belt, and double diagonal belts, Proceedings of Stapp Car Crash Conference, Paper number 2004-22-0022, pp 495-519.

Kroell, C., Schneider, D. and Nahum, A. (1971). Impact tolerance and response of the human thorax. Proceedings of Stapp Car Crash Conference, Paper number 710851.

Kroell, C., Schneider, D. and Nahum, A. (1974). Impact tolerance and response of the human thorax II. Proceedings of Stapp Car Crash Conference, Paper number 741187.

Lebarbé M, Potier P, Baudrit P, Petit P, Trosseille X and Vallancien G (2005). Thoracic injury investigation using PMHS in frontal airbag out-of-position situations. Proceedings of Stapp Car Crash Conference, pp.323-42.

Lebarbé M. (2011) Road Vehicles □ Anthropometric Frontal Impact Dummy □ Frontal Impact Response Requirements to Assess the Biofidelity of the dummy: Part 1: Thorax and Part 2: Abdomen. ISO/TC22 N 3088.

Mertz H, Horsch J, Horn G. and Lowne R (1991). *Hybrid III sternal deflection associated with thoracic injury severities of occupants restrained with force-limiting shoulder belts (910812)*. In PT44 - Hybrid III: The First Human-Like Crash Test Dummy. Society of Automotive Engineers, Warrendale, PA, USA.

Nahum A, Gadd C, Schneider D and Kroell C (1970) Deflection of the human thorax under sternal impact. 700400, Society of Automotive Engineers, Inc., Warrendale, PA, USA.

Neathery R (1974) Analysis of chest impact response data and scaled performance recommendations. Proceedings of Stapp Car Crash Conference, pp.459-493.

Petitjean A, Lebarbé M, Potier P, Trosseille X and Lassau J-P (2002). Laboratory reconstructions of real world frontal crash configurations using the Hybrid III and THOR dummies and PMHS. Proceedings of Stapp Car Crash Conference, Paper number 2002-22-0002.

Petitjean A and Trosseille X (2011) Statistical simulations to evaluate the methods of the construction of injury risk curves, Proceedings of Stapp Car Crash Conference, 2011-55, pp. 411-440.

Petitjean A, Trosseille X, Praxl N, Hynd D, Irwin A (2012) Injury Risk Curves for the WorldSID 50th Male Dummy. Proceedings of Stapp Car Crash Conference, Paper number 2012-08, pp. 323-343.

Rouhana S, Bedewi P, Kankanala S, Prasad P, Zwolinski J, Meduvsky A, Rupp J, Jeffreys T and Schneider L (2003) Biomechanics of 4-point seat belt systems in frontal impacts. Proceedings of Stapp Car Crash Conference, Paper number 2003-22-0017, pp.367-399.

Shaw G., Crandall J. and Butcher J. (2000), “Biofidelity evaluation of the THOR advanced frontal crash test dummy”, Proceedings of the IRCOBI Conference, Montpellier, France, pp 11-29, 2000.

Shaw G, Lessley D, Evans J, Crandall J, Shin J, Portier P and Paoloni G (2007). Quasi-static and dynamic thoracic loading tests, cadaveric torsos. Proceedings of International IRCOBI Conference, pp. 325-348.

Shaw G, Parent D, Purtsezov S, Lessley D, Crandall J, Kent R, Guillemot H, Ridella S, Takhounts E and Martin P (2009). Impact response of restrained PMHS in frontal sled tests: skeletal deformation patterns under seat belt loading. Proceedings of Stapp Car Crash Conference. Paper number 2009-22-0001.

Song E, Lecuyer E, Trosseille X (2011) Development of Injury Criteria for Frontal Impact Using a Human Body FE Model. Enhanced Safety of Vehicles (ESV), Paper number 11-0330-O.

Song E, Troisseille X, Mendoza-Vazquez M, Davidsson J, Vezin P (2012) Definition of injury mechanism and related physical parameters based on datasets from PMHS tests and advanced HBM simulation", THORAX project GA No. 218516, Deliverable D2.4.

Stalnaker R, McElhaney J, Roberts V and Trollope M (1973) Human torso response to blunt trauma. Human Impact Response - Measurement and Simulation. Proceedings of the Symposium on Human Impact Response, Warren, MI, USA. New York: Plenum Press, pp.181–198.

Trosseille X, Baudrit P, Leport T and Vallancien G (2008) Rib cage strain pattern as a function of chest loading configuration. Proceedings of Stapp Car Crash Conference, Paper number 2008-22-0009.

Vezin P., Bruyere-Garnier K., Bermond F., Verriest J.P. (2002) Comparison of HIII THOR-alpha and PMHS response in Frontal Sled Tests", Proceedings of 46th Stapp Car Crash Conference, paper 2002-22-0001.

Vezin P (2002a). Human Thorax/Shoulder Behaviour during Frontal Impact with Airbag. FID Project, Work Package 2, D5 Part 1.

Vezin P (2002b). Human Thorax/Shoulder Behaviour during Frontal Impact without Airbag. FID Project, Work Package 2, D5 Part 2.

Yoganandan N, Pintar F, Kumaresan S, Haffner M, Kuppa S (1997) Impact biomechanics of the human thorax-abdomen complex", IJCrash 2(2), pp 219-228.

Appendix A. Analysis of chest parameter combinations that predicts chest injury

With the multipoint chest deflection measurements from the THOR dummy it has been hoped that an improved injury risk prediction can be generated with respect to a single-point measurement as available with the basic sternal deflection measurement in the Hybrid III. However, the THOR fitted with 3D IR-TRACCS at four different measurement positions is able to generate x, y, z and resultant deflection measurements from each point for any event. This leads to the issue as to how these measurements can be compiled to produce the best potential injury risk prediction.

To provide a baseline for further considerations of how to combine the available measurements, peak values from the IR-TRACCS were generated for each axis at each measurement point for each test. Simple combinations of these were compared with the basic measurements to determine the predictive value of such fundamental measures.

In addition to the fundamental peak value measures, the combined deflection Dc was revised for use with the THORAX Demonstrators instead of the Humos2 human body model. Please find the revised formulations of this new criterion below.

To support the efforts and justifications for use of the new Dc criterion, it was considered important to investigate the underlying factor structure of the maximum resultant and x-axis deflection measurements at each of the four measurement points. The question was to try and help determine how those eight or more predictor variables could be reduced (or summarised) using a smaller set of factors. The following analyses were performed using the *Core* dataset without normalisation (unless otherwise stated). The original data was used; meaning that e.g. data was not mirrored so that all diagonal belts in the 3-pt sled tests were supporting the right shoulder.

When looking at just the peak resultant or x-axis deflections from the four measurement points, principal component analysis showed that:

- The pattern of relationships between the eight variables may be explained by two factors
- The upper measurements and the lower right measurements are highly correlated and the pattern of relationships between them may be explained by a single factor – i.e. all the upper measurements and the lower right measurements contribute comparable bits of information.
    - It may be important to note here that for the prediction of rib fractures to the upper right quadrant of the rib cage (either ribs 1 to 4 or 1 to 5), the peak x-axis upper right measurement point showed the strongest correlation of the upper right or left x-axis or resultant peak values. However, the upper right x-axis peak value also showed the strongest correlation with rib fracture prediction for the upper left quadrant as well. Therefore with the THORAX Demonstrators it is not clear that the peak value from the measurement point in one quadrant will always be the best point for predicting rib fractures in that same quadrant.
- The lower left measurements may be explained by different factors than the upper measurements and lower right measurements – i.e. the lower left measurements contribute comparable bits of information.
    - The findings regarding the reduction of the deflection measurements to two factors needs to be considered with regard to the test conditions forming the dataset from which the results were generated. In the *Core* dataset 26 of the 59 tests recreated were sled tests. In the sled tests 15 of them had the seat belt passing over the right shoulder of the occupant and for the other 11 the belt passed over the left shoulder. With this balance of left and right shoulder belt

paths, it is not possible to explain the different factor consisting of the lower left measurement point results as being due to the belt lie. However, the remaining 33 tests were impactor or deploying restraint (or OOP) tests. These include the Yoganandan oblique tests which were directed to the lower left of the thorax. It could be that these results together with the responses from the sled tests with the shoulder belt over the left shoulder account for the difference between the information from the lower left measurement point and the other three points.

- The x-axis measurements and the resultant measurements (in each specific location) are explained by the same factors – i.e. the x-axis and resultant measurements at each location contribute comparable bits of information.

These results were similar when comparing the x-axis or resultant measurements in isolation.

Previously, the peak value from the mean of the top two measurement points in the THOR has been used as a measure that is similar to the Hybrid III sternal deflection measurement. When this peak value for both the x-axis and resultant deflections was added to the basic eight peak values the principal component analysis showed that:

- The pattern of relationships between the ten variables may still be explained by two factors
- The upper measurements, the lower right measurements and the peak mean of the top two quadrants are highly correlated and the pattern of relationships between them may be explained by a single factor – i.e. all the upper measurements and the lower right measurements contribute comparable bits of information.

When considering the x, y and z-axis measurements for the four IR-TRACCS, the principal component analysis showed that:

- The pattern of relationships between the twelve variables may be explained by three factors
- The upper x-axis and z-axis measurements and the lower z-axis measurements are highly correlated and the pattern of relationships between them may be explained by a single factor – i.e. they contribute comparable bits of information.
- The lower y-axis and the upper y-axis measurements are contained in separate factors – suggesting the information which they contribute is not comparable.

Logistic regression was then used to try and identify which of the factors from the principal component analysis was most useful in predicting injury at the NFR ≥ 5 or NFR ≥ 7 level. The results indicated that:

- Using x-axis and resultant measurements from the upper left, upper right and lower right quadrants offers the best prediction of NFR ≥ 5 (Exp(B) = 1.014, $p = 0.001$; Cox & Snell $R^2 = 0.255$, Nagelkerke $R^2 = 0.343$) and NFR ≥ 7 (Exp(B) = 1.011, $p = 0.001$; Cox & Snell $R^2 = 0.206$, Nagelkerke $R^2 = 0.275$).
- Including x-axis and resultant measurements from the lower left quadrant adds no value to the prediction. However, this may be a peculiarity of the dataset used and it is therefore not suggested for the lower left measurements to be excluded from further considerations.
- Including either the x-axis or the resultant measurements from any quadrant does not offer as good a prediction as including both sets of measurements.
- Including the measurement of peak of mean from the top two quadrants does not improve the prediction.

Compared with the x-axis and y-axis measurements, including lower y-axis measurements and upper y-axis measurements adds no value to the prediction.

In fact, of all the possible deflection measures, using x-axis and resultant measurements from the upper left, upper right and lower right quadrants offers the best prediction of NFR ≥ 5 or NFR ≥ 7. Including any of the other deflection measures does not add value to the prediction.

Finally a check was made to see what predictive power would be lost by using either the maximum x-axis peak value from any of the four measurement points or the maximum resultant peak versus taking both x-axis and resultant information from all four points. Logistic regression was used to determine this and the exponents, p-values and R^2 values are shown in the following tables; Table A1 and A2 for NFR ≥ 5 and ≥ 7, respectively.

Table A1. Prediction of NFR ≥ 5

	Exp(B)	p-value	Cox & Snell R^2	Nagelkerke R^2
F1 = all x-axis and resultant peak values	1.014	0.001	0.264	0.354
Max of any point – x-axis	0.925	0.002	0.230	0.309
Max of any point – resultant	1.069	0.003	0.223	0.300

Table A2. Prediction of NFR ≥ 7

	Exp(B)	p-value	Cox & Snell R^2	Nagelkerke R^2
F1 = all x-axis and resultant peak values	1.011	0.001	0.209	0.279
Max of any point – x-axis	0.949	0.006	0.148	0.198
Max of any point – resultant	1.047	0.006	0.149	0.199

The conclusions based on this table are that:

- The largest R^2 values were found when using F1 to predict both the likelihood of receiving a NFR ≥ 5 and ≥ 7.
- F1 contains the maximum x-axis and resultant deflection measurements for all four quadrants (upper left, upper right, lower left, lower right), suggesting that incorporation of all measurement points is beneficial for the prediction of injury.
- The prediction of injury with the maximum deflection at any of the four points, both in the x-axis and the resultant, is not as complete as the prediction with F1 (which incorporates deflection at all measurement points).
- Based on the NFR ≥ 5 results in particular it seems that for the *Core* dataset, the Maximum peak x-axis measurement from any point offers a better injury risk prediction than the equivalent resultant measure.

The recommendations from this investigation are that for the best predictive ability:

- The Dc formulation for the THORAX Demonstrator needs to include both the x-axis and resultant measurements from all four measurement points.
- If a choice needs to be made between inclusion of either the x-axis or resultant measurements, then at least for NFR ≥ the x-axis measurements would be preferred.
- The maximum peak x-axis measurement from any of the four IR-TRACCS seems to be the most useful fundamental measure to compliment the potentially better, but more complicated Dc.

- Whilst the x-axis injury risk estimates will be the focus of reporting here, throughout the analysis process the resultant injury risk estimates have also been considered to check the validity of this statistical finding.

Appendix B. Injury risk curves: reconstruction of accidents

Executive summary

When developing injury risk functions for a new dummy it has become best and common practice to repeat PMHS tests with the dummy. This is the approach being adopted within Task 2.6 of the THORAX Project, the development of injury risk curves for the dummy demonstrator delivered by the Project.

The process used to develop the injury risk function for the Hybrid III sternal chest deflection measurement differs from the process described above. With the Hybrid III dummy, real world accident events were simplified and recreated in the laboratory. The dummy measurements from these sled tests were related to the human injury incidence from the original accidents. To extend the work of Task 2.6, the Hybrid III approach is being duplicated with the THORAX Demonstrator so as to provide a direct comparison with the injury risk function currently used with the Hybrid III in European regulatory and consumer information testing. This report documents the testing to replicate the Hybrid III approach.

The test set-up used in the development of the Hybrid III sternal deflection risk prediction relationship, which recreated French accident cases on a sled, was reproduced at TRL. Tests with a Hybrid III dummy suggested that the replication of test conditions was appropriate, although some differences between the current and historical shoulder belt force results were observed (in the relationship between peak belt force through the shoulder portion of the three-point belt and chest deflection).

A new AIS ≥ 3 injury risk function was calculated for Hybrid III sternal chest deflection. The original injury risk function for the Hybrid III dummy was developed using the probit method. Recently, ISO WG6 has reviewed the statistical methods for developing injury risk functions and has developed guidelines for a new process that includes the use of survival analysis. The opportunity was therefore also taken to review the potential implications of switching to use survival analysis to derive the risk curve. This emphasised the limitations in using the original data to develop injury risk functions. The risk functions developed using the recommended survival analysis method had wide confidence limits, probably due to the very small proportion of injured occupants in the accident sample. As such, it was evident that the risk curves for the Hybrid III would not meet new requirements on the confidence boundaries of the estimate, as are now being recommended by ISO Working Group 6.

Preliminary risk curves for the THORAX Demonstrator have been derived, also using survival analysis. These risk functions allowed for a comparison of the measurements that are equivalent to the Hybrid III 50 mm sternal deflection limit to be made (i.e. that represent a 50% risk of AIS ≥ 3 thorax injury. The threshold for deflection measurements in the THOR would be expected to be either:

- Lower if based on the mean peak from the top two IR-Traccs
- Similar if based on the peak from either top two IR-Traccs
- Higher if based on the peak from any IR-Tracc

These differences demonstrate the sensitivity of the THORAX Demonstrator chest to this particular loading regime.

Although the THORAX Demonstrator was tested with some additional mass added to the upper arms, this is believed not to have caused a substantial influence on the chest deflection results obtained.

All the injury risk functions developed throughout this study are based on the original injury outcome data used by Mertz *et al.* They all have wide confidence limits associated with only

fair or marginal levels of quality using the metric recommended by ISO WG6. This means that great care should be taken when trying to use them. This fact supports the continuing efforts within the THORAX Project to developed improved injury risk curves for the THORAX Demonstrator based on a wider set of biomechanical data.

1 Introduction

When developing injury risk functions for a new dummy it has become best and common practice to repeat PMHS (post-mortem human subject) tests with the dummy. Ideally, the dummy is subjected to the exact conditions from a variety of PMHS tests. Then for a specific injury criterion, the dummy measurement can be paired to the PMHS injury outcome. A statistical function can then be fitted to the measurement and outcome pairs providing a function which predicts the probability of injury given a particular dummy measurement. This is the approach being adopted within Task 2.6 of the THORAX Project, the development of injury risk curves for the dummy demonstrator delivered by the Project.

The process used to develop the injury risk function for the Hybrid III sternal chest deflection measurement differs from the process described above. With the Hybrid III dummy, real world accident events were simplified and recreated in the laboratory. It was the dummy measurements from these sled tests which were related to the human injury incidence from the original accidents. The advantages of this approach are that the loading condition (if replicated appropriately) should be realistic and that the injury outcome is based on a broad range of living human subjects with muscle tone (instead of PMHS), and soft tissue injuries are therefore more likely to be identified. The disadvantage is that with accident analysis, unlike laboratory-based sled tests, there is always some uncertainty as to the exact loading conditions (for instance the exact pre-impact posture of the occupants).

To extend the work of Task 2.6, the Hybrid III approach is being duplicated with the THORAX Demonstrator so as to provide a direct comparison with the injury risk function currently used with the Hybrid III in European regulatory and consumer information testing.

This report documents the testing to replicate the Hybrid III approach. It describes testing with the Hybrid III to validate the set-up, then the derivation of injury risk functions for both the Hybrid III and THORAX demonstrator.

1.1 Background

The two components of the original Hybrid III sternal deflection work are the French accident analysis reported by Foret-Bruno et al. (1978) and the Hybrid III sled tests reported by Mertz *et al.* (1991).

The background to the Foret-Bruno et al. study is that Peugeot and Renault vehicles sold in France between 1970 and 1977 were equipped with static 3-point seat belts for the front seating positions, with a load limiter located between the shoulder and the upper anchorage point (1989). Several designs of load limiter were used, but all of the load limiter systems were made up of several bands of textiles that tore successively with increasing levels of force exerted by the occupant. Accident investigators from the Laboratoire de Physiologie et de Biomécanique PSA/RNUR studied cases involving these vehicles and recorded the number of bands of textiles that had torn in each case. Based on the load limiter technology, they were able to document, not only the thoracic injury outcome for the occupants, but also the peak level of shoulder belt load associated with the accident. This allowed Foret-Bruno et al. to comment on the relationship between shoulder belt force and thoracic injury outcome.

The work of Mertz et al. (1991) built on the information presented by Foret-Bruno et al. Mertz et al. recreated a typical set-up for a front seat from a 1970s French car on the sled. They used the Hybrid III dummy as the occupant in the seat and performed a series of sled tests. The shoulder belt force was varied by altering the sled impact speed and by using one of the load limiter types from the French cars. Mertz et al. observed that as the shoulder belt force increased the peak sternal deflection measurement from the Hybrid III also increased and that the relationship was approximately linear. This observation gave Mertz et al. a mechanism to relate sternal deflection measurements to thoracic injury outcome and they used probit analysis to establish that relationship and show the resulting injury risk function.

2 Method

The test work described in this report was carried out in the TRL Impact Sled Facility.

2.1 Test seat

The geometry of the test seat used in the previous testing was reported by Mertz et al. (1991) (Figure B1). This geometry was recreated for this test series. The exact measurements prior to testing are provided below.

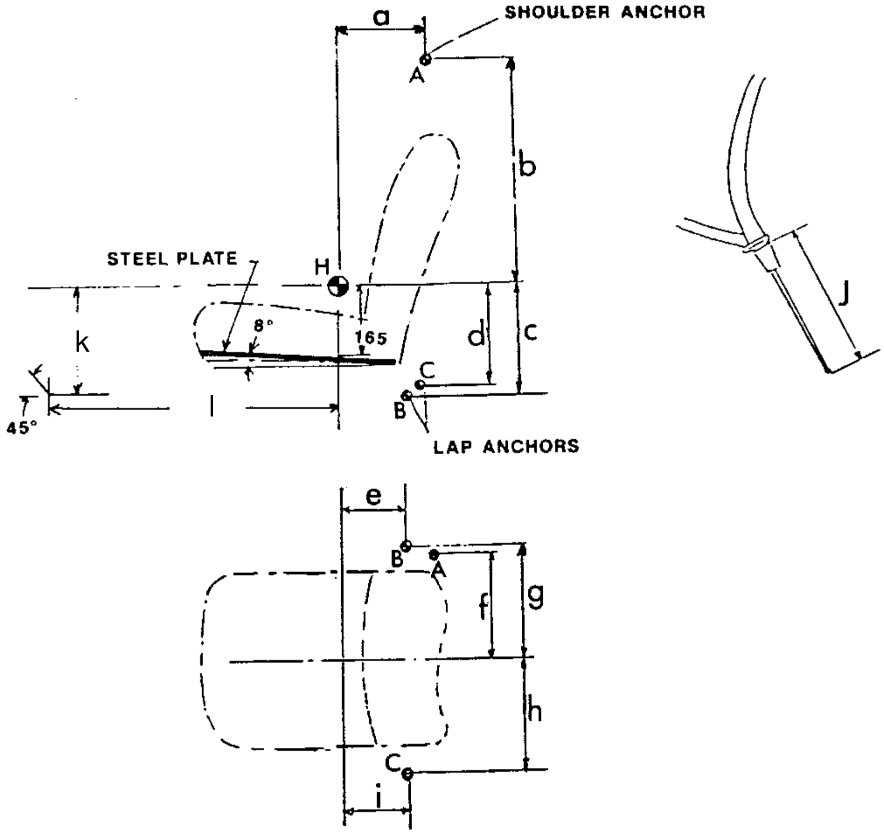

Measurement	a	b	c	d	e	f	g	h	i	j	k	l
Original series	270	600	230	280	170	260	280	300	170	380	320	740
New set-up	279	614	232	275	180	253	282	292	176	380	368	745

Figure B1. Coordinates of belt anchorage points with respect to the H-point of the 50th percentile Hybrid III dummy.

According to Mertz et al., for their reconstructions,
‘The sled fixture consisted of a “hard” seat, toe pan, and belt anchor supports. The “hard” seat contained a rigid metal plate under the cushion, which provides a reusable and repeatable seat resulting in a nominal horizontal pelvic motion… The belt restraint used current automotive webbing, fixed at all three anchors (no retractors), and had a locking latch plate. The force-limiting element was located at the shoulder belt anchor. Adjustment of the belt restraint was “snug” for the lap belt and 25 mm slack in the shoulder belt. Placement of the belt on the shoulder was distal to the neck belt-guard. Dummy positioning included a pelvic angle of 22 degrees and head x-axis horizontal.’ (Mertz et al., 1991)

In the Mertz et al. description they note that a 'hard' seat was used. Presumably this relates to the seat base stiffness available in production vehicles at that time. It is suspected that the vehicles which were involved in the original accidents had very soft seats compared with modern vehicles, though the relationships between original French vehicles, Mertz et al. test seat and modern vehicles is unknown. To try and quantify this variation, simple drop weight trials were carried out on a Renault 4 van to characterise the stiffness of the seat foam. The base of the seat was very soft by current standards. However, the majority of the compliance was produced by the springs under the seat which had only a thin sheet of soft foam over them. Designing a similar seat structure would seem to contradict the description of the test bench used by Mertz et al. (1991). Therefore, it was decided to investigate the effects of a soft seat base by using three different foams of varying stiffness and depth, incorporated into a UN Regulation 44 style test bench seat. The foams were chosen based on vehicle tests and the foam products readily available:

1. NPACS (New Programme for the Assessment of Child restraint Systems) bench foam
    a. Originally selected to be representative of modern vehicles
    b. Substantially stiffer than the Renault 4
2. UN Regulation 44 bench foam
    a. Representative of vehicles around the time of implementation
    b. Also stiffer than the Renault 4
3. FMVSS 213 bench foam
    a. Softer option
    b. Chosen from the U.S. market and known to be softer than the R44 bench.

A seat incorporating a back and base of each foam type was made and used in a trial test with the Hybrid III dummy. Figure B2 shows the curves of belt force from the shoulder portion of the seat belt plotted with the sternal chest deflection measurement from the Hybrid III. Due to the study limitations it was not possible to perform repeats of these tests to determine the intrinsic variability in response. However, even though the difference is small, the Regulation 44 foam produced the largest maximum deflection and the FMVSS foam produced a slightly higher force response with respect to the deflection.

Based on the results published by Mertz et al. (1991) the expected relationship between peak deflection and force was 2 kN for every 10 mm. From this it can be inferred that a peak belt force of around 9 kN would be expected to produce 45 mm of chest deflection.

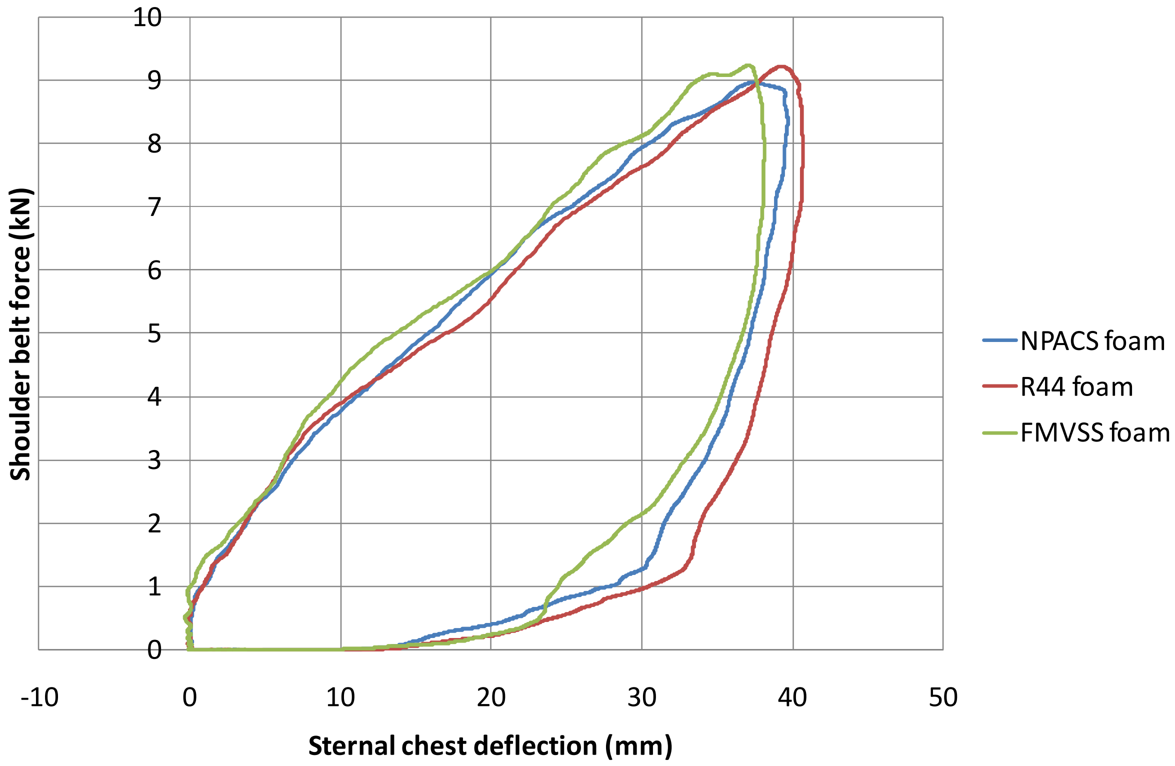

Figure B2. Belt force – chest deflection curves for the three foam types.

The results from this set-up do not yield exactly the same relationship of 2 kN per 10 mm deflection. A smaller peak chest deflection of around 40 mm was seen with a 9 kN shoulder belt force.

Of the three foams tried, the softest, the FMVSS foam test led to the smallest peak chest deflection value despite having a peak belt force of over 9 kN. It was also observed prior to the test that the dummy seemed unstable on the seat. It was prone to lean to one side or the other where the pelvis was sinking into the foam with time. These two features suggested that the FMVSS foam was not suitable for the test programme.

Instead, the UNECE Regulation 44 foam allowed the largest peak deflection and therefore produced results which were closest to the expected force-deflection relationship. The properties of this foam are clearly documented for use in the Regulation. Therefore, although there was only a small difference between the results for the Regulation 44 and NPACS foam, the Reg. 44 foam was selected to be used in the rest of the test series.

2.2 Load limiters

There were three different types of load limiters fitted to the crashed cars analysed by Foret Bruno et al. (1978). Together with the consideration of when the load limiter is fully exhausted and the belt behaves as a simple static belt, this gives four load limiting conditions to replicate.

It should be noted that Mertz et al. (1991) only replicated one type of load limiter (Type B, as shown below, Figure B3) and the static condition in their testing. Similarly, in the TRL replication tests, static belts were used to provide the higher belt force conditions. It is understood that there may be a different chest deflection response comparing a peak belt force from a test where a load limiter has been exhausted to one where there was no load limiting element. This may present a source of inaccuracy when relating dummy measurements to real world injury outcomes where the dummy was tested with a static belt and the vehicle had a load limiter fitted. Cases such as this will need to be reviewed before inclusion in subsequent parts of THORAX Task 2.6. However, it should not adversely affect the THORAX and Hybrid III replications as this approach was used in all phases of dummy testing, including the original Mertz *et al.* tests.

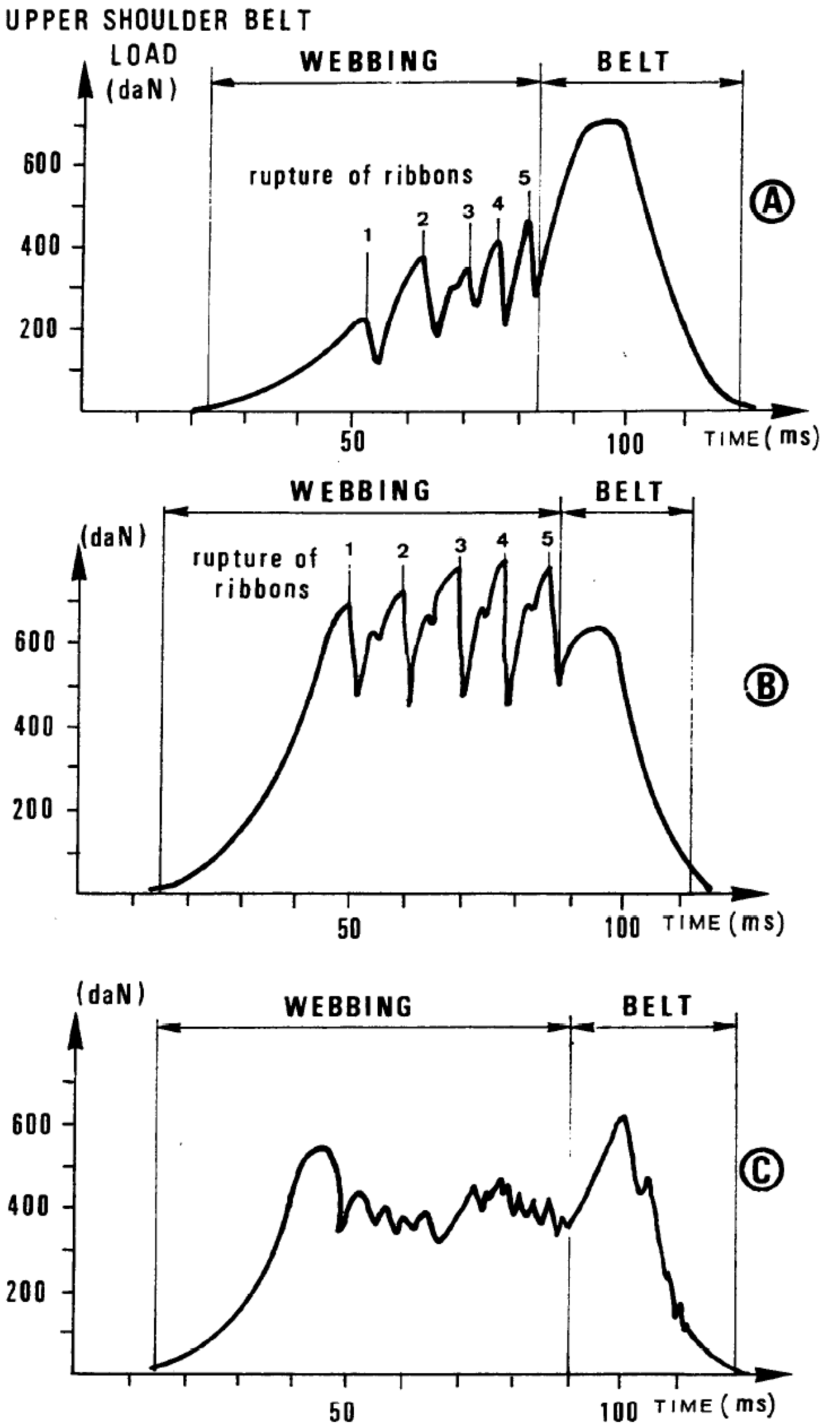

Figure B3. Characteristics of load limiters, Types A, B, and C (reproduced from Foret Bruno et al. 1978).

Equivalent load limiters to those used in the original cars were not still available today. Therefore a small programme of work was undertaken to develop stitched webbing patterns which would tear to give similar force profiles.

The load limiting element was generated by making a fold in the standard webbing and adding bands of stitching to create a small loop of redundant webbing. Up to the critical force, the stitching would hold and the extra loop of webbing would not be used in the restraint. However, beyond a critical force level the stitching would yield allowing the extra webbing to be introduced to the restraint limiting the applied force by allowing further forward excursion. A pre-test photograph of a load limiting element is shown in Figure B4.

Figure B4. Load limiting element – Type A with five transverse bands of stitching.

The Type A load limiter as shown in Figure B4. was the prime option for delivering discrete force peaks in the load limiting, as was described with the original load limiters. This seemed to be effective in component tests; however, in the sled tests some aspect of the loading caused the buckle to open. This happened in a repeatable manner when testing with this kind of load limiter. An example shoulder belt force profile is shown in Figure B5.

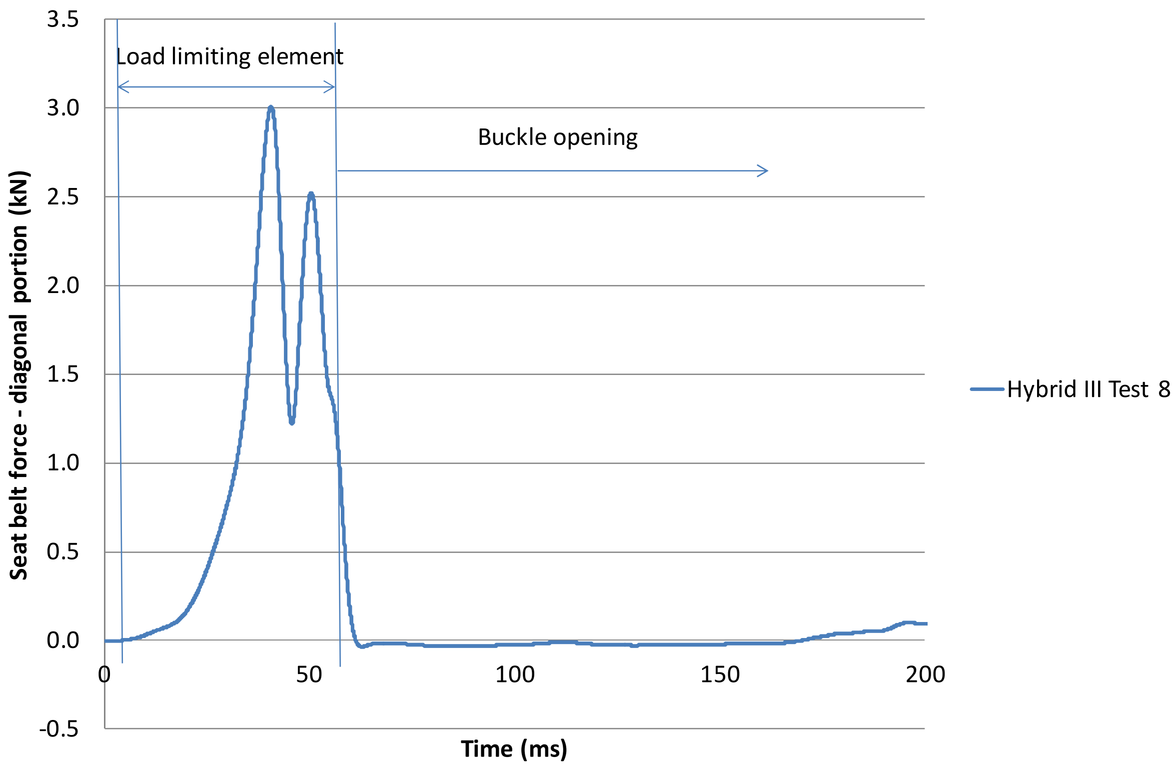

Figure B5. Characteristics of first load limiter type used in the test replications (Type A).

An alternative stitching configuration was also implemented in a second type of load limiter, Type B. In this case, the stitching was along the length of the load limiting fold and not across it. Also two folds of webbing were used in parallel to increase the limited force. This type of load limiter can be seen in Figure B6.

Figure B6. Load limiting element – Type B with stitching along the length of the webbing and two folds of limiting elements to act in parallel.

An example of the force profile obtained with the double fold, longitudinal stitching of the Type B limiters is shown in Figure B7.

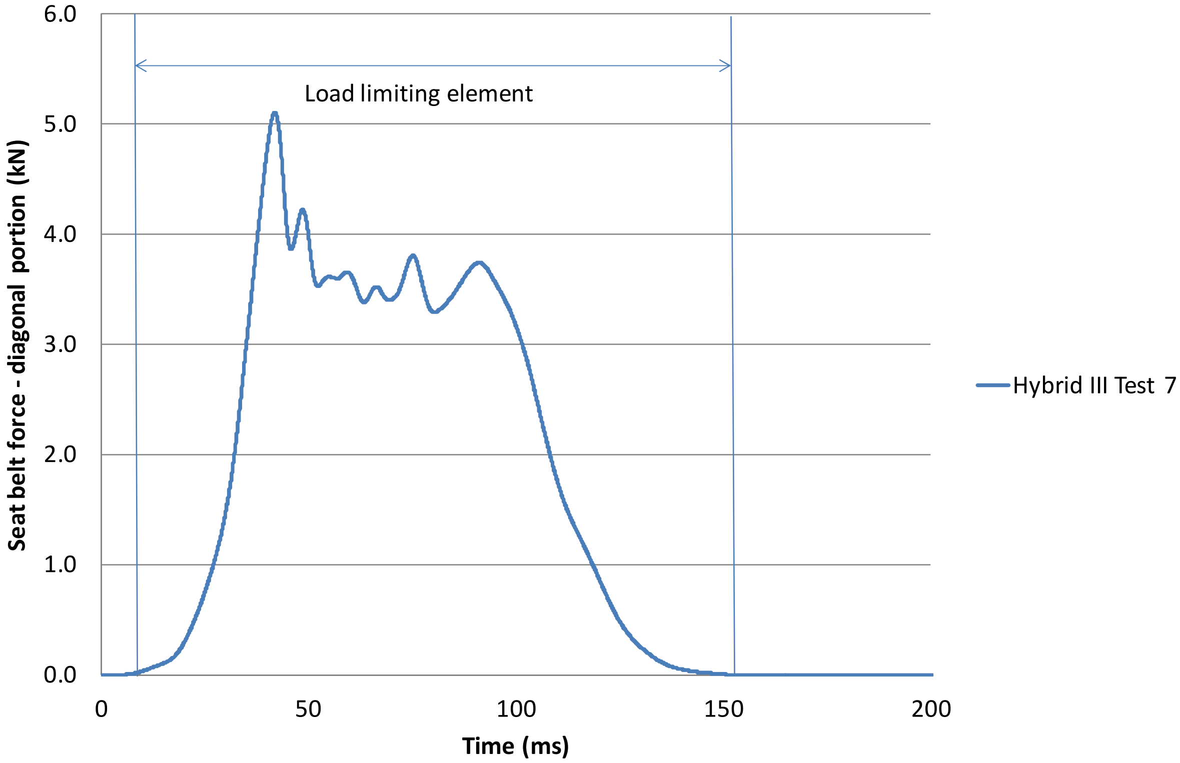

Figure B7. Characteristics of second load limiter type used in the test replications (Type B).

The last of the options taken into the testing (Type C) involved just a single load limiting fold in the webbing again, but with longitudinal stitching, as in the previous case. The peak force observed in the load limiting phase in tests with this load limiter type was 2.37 kN (e.g. as shown in Figure B8 up to about 75 ms), with an average force just under 2 kN.

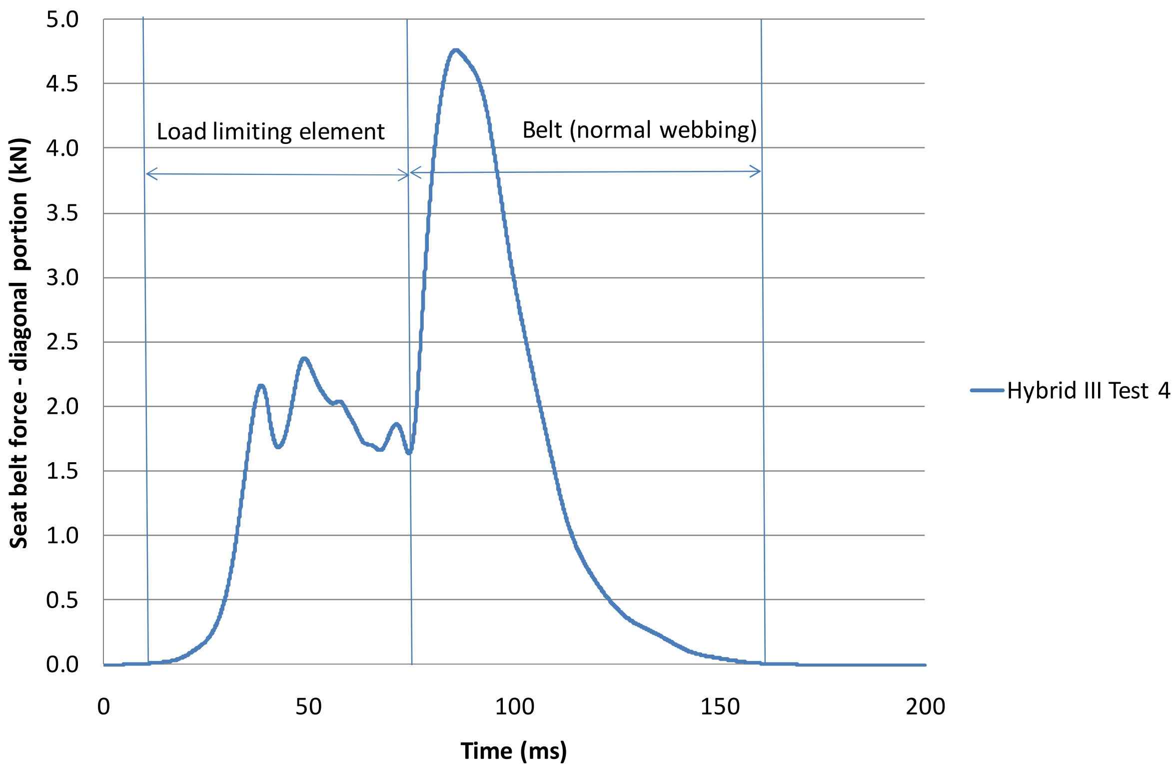

Figure B8. Characteristics of third load limiter type used in the test replications.

2.3 Seat geometry

The geometry of the test seat as used by Mertz et al. (1991) was designed to be representative of the French cars from the 1970s in which the load limiters were originally fitted. Generic vehicle geometry information is reported by Foret-Bruno et al. (1989). However geometry from specific cases is compared with the sled test geometry by Mertz et al. and is reproduced in Figure B9. For the purposes of the THORAX test work, the sled geometry of Mertz et al. was recreated.

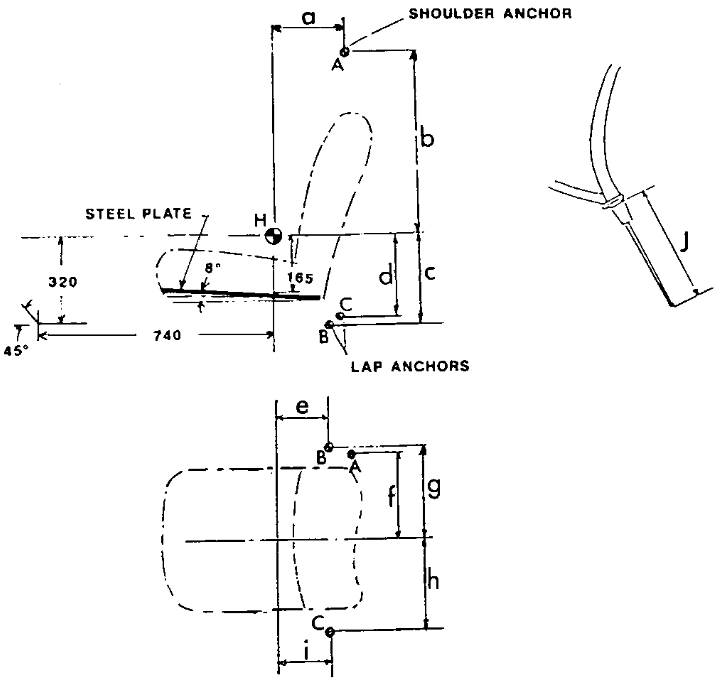

		APR DATA						
	CASES	2091	2165	3168	3805	4061	4549	SLED TESTS
DIMENSIONS	a	220	430	220	125	500	205	270
	b	600	600	600	600	600	600	600
	c	220	220	220	270	220	270	230
	d	270	300	270	310	300	310	280
	e	170	150	170	100	220	180	170
	f	270	250	270	270	250	270	260
	g	350	250	350	280	250	280	280
	h	300	300	300	300	300	300	300
	i	170	150	170	100	220	180	170
	j	310	360	310	340	360	340	380

Dimensions in mm; A, B, C are belt anchor locations.

Figure B9. Dimensions used in the sled test compared with vehicle dimensions provided by APR (Mertz et al., 1991).

The exact dimensions used in the THORAX testing are shown in Table B1.

Table B1. Dimensions used in THORAX sled tests.

Dimension	Target	Measured
a	270	280
b	600	610
c	230	220
d	280	280
e	170	170
f	260	260
g	280	285
h	300	300
i	170	175
j	380	380

A pre-test image of the Hybrid III dummy on the test seat is shown in Figure B10 and the THORAX Demonstrator is shown in Figure B11. Once positioned in the seat and the H-point position confirmed, the dummy's head level and pelvis angle were not adjusted. This deviates slightly from the original sled tests where those extra steps were included. However, the lack of these two actions is not thought to interfere significantly with the chest deflection measurements obtained or the test-to-test repeatability.

Figure B10. Pre-test image of Hybrid III on the test seat.

Figure B11. Pre-test image of THORAX Demonstrator on the test seat.

2.4 Instrumentation

Two dummies were used in this work, the Hybrid III and the THORAX modified THOR dummy. The instrumentation used for the Hybrid III tests is shown in Table B2.

Table B2. Hybrid III test instrumentation.

Area	Channel	Filter	Channel count
Head	Acceleration (triaxial) (*g*)	CFC_1000	3
Chest	Deflection (mm)	CFC_600	1
Chest	Acceleration (triaxial) (*g*)	CFC_180	3
Chest	Acceleration (sternum) (*g*)	CFC_1000	1
Pelvis	Acceleration (triaxial) (*g*)	CFC_1000	3
Seat belt	Belt force (lap and diagonal) (kN)	CFC_60	4
Sled	Acceleration (inc. back-up) (*g*)	CFC_60	2
Total			17

The instrumentation used for the THORAX Demonstrator tests is shown in Table B3. The 96 dummy acceleration, deflection and strain measurements were recorded via an in-dummy data acquisition system.

Table B3. THORAX Demonstrator test instrumentation.

Area	Channel	Filter	Channel count
Head	Acceleration (triaxial) (*g*)	CFC_1000	3
Chest	Deflection (mm)	CFC_600	4 x 3-axes = 12
Chest	Strain (millistrain, s^{-1})	CFC_180	6 x 12 ribs = 72
Chest	Acceleration (triaxial) (*g*)	CFC_180	3
Thoracic spine	Acceleration (T1) (*g*)	CFC_1000	3
Thoracic spine	Acceleration (T12) (*g*)	CFC_1000	3
Seat belt	Belt force (lap and diagonal) (kN)	CFC_60	4
Sled	Acceleration (inc. back-up) (*g*)	CFC_60	2
Total			102

3 Results

3.1 Original Hybrid III Injury Risk Curve

In the work of Mertz et al. (1991) an important observation from their Hybrid III testing was that for every 200 N of shoulder belt force the Hybrid III sternum was deflected 1 mm. This result was used to define predicted Hybrid III sternal chest deflections for groups within the French accident data. Mertz et al. used groupings within the accident data based on the number of bands torn in the accident case and hence the expected shoulder belt load. Then, using the relationship between shoulder belt force and sternal deflection, a mean or middle of group prediction for Hybrid III chest deflection was provided. The tabulated data generated by this process are reproduced in Table B4.

Table B4. Estimated Hybrid III sternal deflections with risks of thoracic injury based on French accident data of Foret-Bruno et al. (1978) and Mertz et al. (1991).

Force limiter type	Stitch bands torn	Load range	Hybrid III sternal deflection		Total occupants	Thoracic injury	
		(kN)	Range (mm)	Mean (mm)		AIS 3+	AIS 4+
A	None	0 to 2.1	0 to 10.5	5.3	123	0	0
A	1	2.1 to 3.85	10.5 to 19.3	14.9	26	0	0
A	2 to 4	3.85 to 4.4	19.3 to 22.0	20.7	91	2	1
C	None	0 to 5.5	0 to 27.5	13.8	21	0	0
C	Partial	5.5	27.5	27.5	3	0	0
B	None	0 to 7.4	0 to 37.0	18.5	72	5	2
B	1 to 4	7.4 to 8	37.0 to 40.0	38.5	6	1	1

The mean Hybrid III sternal deflections and associated thoracic injury risks were subjected to Probit analyses by Mertz et al. This analysis produced the curve shown in Figure 12 and the associated confidence limits. According to Mertz *et al.* the confidence limits shown reflected the spread in the upper and lower bounds or the risk values shown in Table B4. Those authors acknowledge that whilst the curve is 'well-determined' for Hybrid III sternal deflections of 20 mm or less there is greater uncertainty for larger chest deflections.

The curve shown in Figure 12 is the basis for the UN Regulation 94 limit of 50 mm chest deflection as used in the crash test required for the frontal impact protection assessment of cars. The limit was chosen as it corresponds with about a 50 percent risk of AIS ≥ 3 thoracic injury. The curve also forms the basis of the bands in thorax protection (chest deflection as opposed to the Viscous Criterion) used to determine the frontal impact Euro NCAP score.

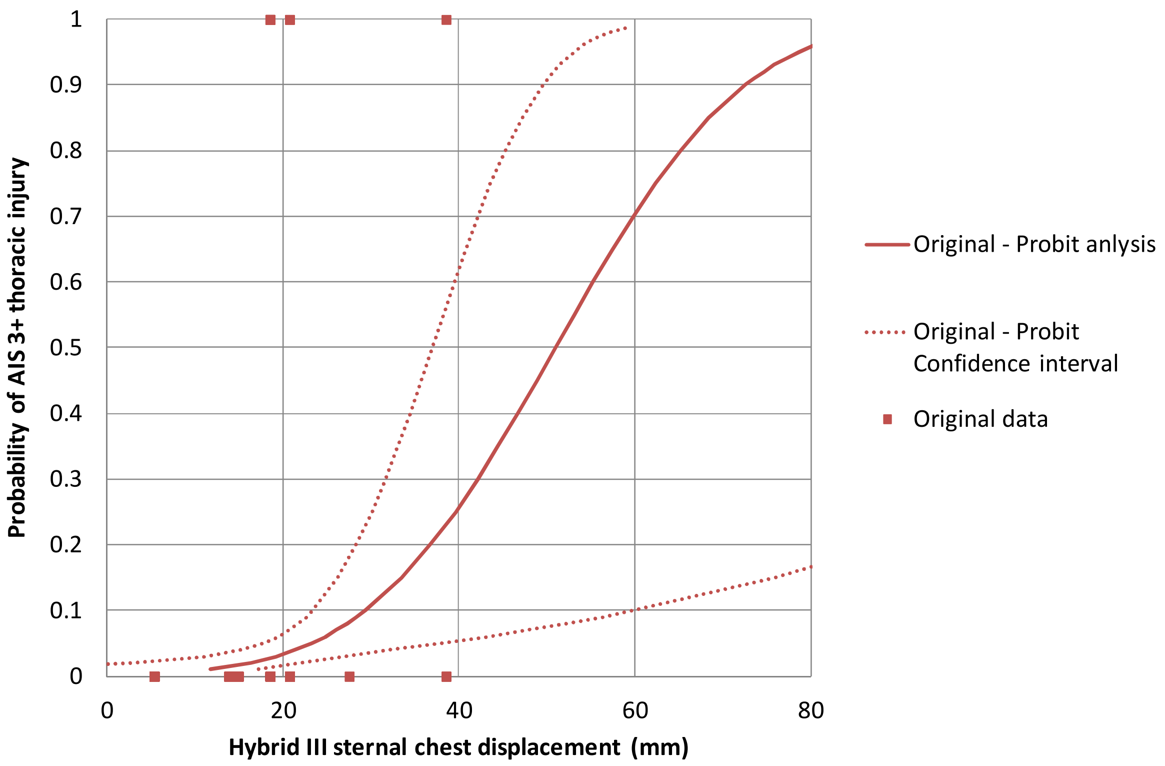

Figure B12. Risk of AIS ≥ 3 thoracic injury as a function of Hybrid III sternal deflection for shoulder belt loading. Risk curve determined by Probit analysis.

3.2 New Hybrid III Injury Risk Curves

Based on the Hybrid III tests carried out for this study a new relationship between peak shoulder belt force and Hybrid III sternal deflection can be produced. This new relationship is shown in Figure B13.

From the lines plotted as a best fit through the test data points, the relationship can be seen. The equations for these lines are also given. Assuming that the relationship must go through the point 0 kN, 0 mm then about 4.4 mm of Hybrid III sternal deflection is expected with each 1 kN of applied shoulder belt force.

If a non-zero intercept is allowed, then a slightly better fit with the data can be achieved (r2 = 0.97 instead of 0.96). This better fit describes more closely the data points; however, the implication that there would be a 2.5 mm deflection at zero force seems unrealistic. Such a result is indicative of the variation in the test data and the confidence one should put in the resulting relationship.

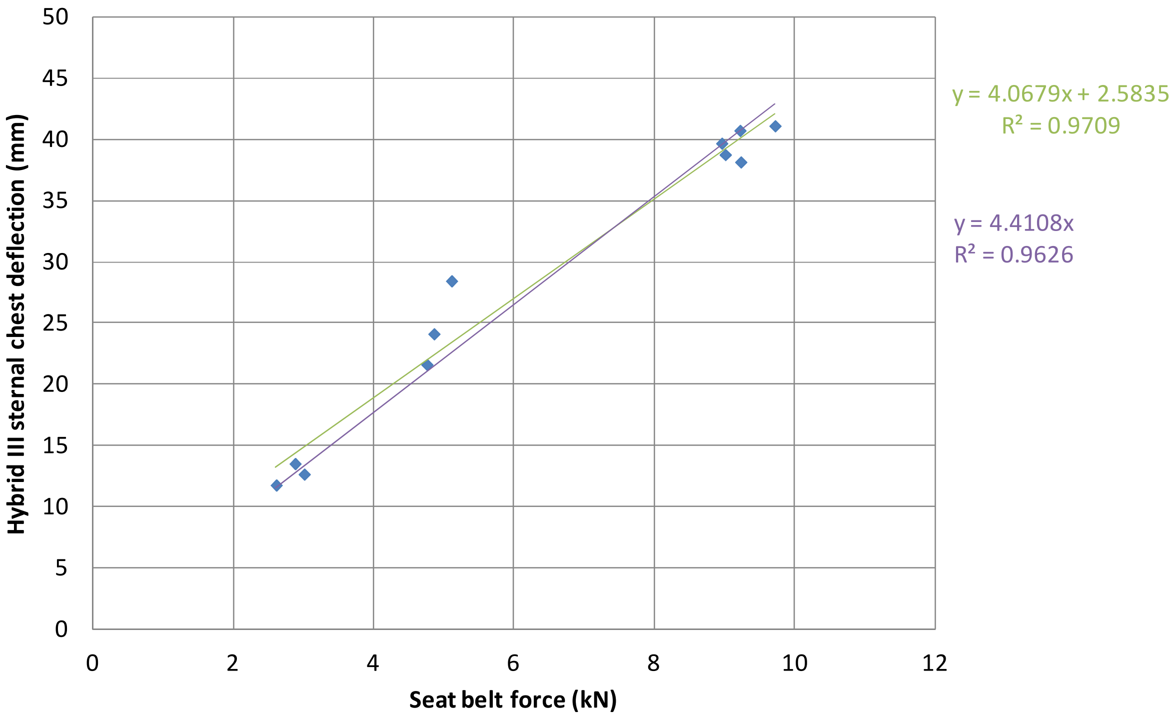

Figure B13. Hybrid III sternal chest deflection versus seat belt (diagonal portion) force.

Using the relationship derived from the Hybrid III tests (as shown in Figure B13) new expected Hybrid III sternal deflection values were generated to accompany the French accident data. In equivalence to Table B4. , these new values are shown with the accident data groups in Table B5..

Table B5. New estimated Hybrid III sternal deflections with risks of thoracic injury based on French accident data of Foret-Bruno et al. (1978).

Force limiter type	Stitch bands torn	Load range (kN)	Hybrid III sternal deflection		Total occupants	Thoracic injury	
			Range (mm)	Mean (mm)		AIS 3+	AIS 4+
A	None	0 to 2.1	0 to 11.1	6.9	123	0	0
A	1	2.1 to 3.85	11.1 to 18.2	14.7	26	0	0
A	2 to 4	3.85 to 4.4	18.2 to 20.5	19.4	91	2	1
C	None	0 to 5.5	0 to 25.0	13.8	21	0	0
C	Partial	5.5	25.0	25.0	3	0	0
B	None	0 to 7.4	0 to 32.7	17.6	72	5	2
B	1 to 4	7.4 to 8	32.7 to 35.1	33.9	6	1	1

The Probit analysis result, when using the updated data from Table B5., is shown in Figure B14. The most obvious difference compared with the original curve is that the two curves diverge with increasing sternal displacement. The new data suggest a higher probability of AIS ≥ 3 thoracic injury for a given chest deflection. For instance the original curve suggests a 50 percent risk of injury is reached at 51 mm of deflection whereas the new curve suggests this risk of injury occurs at the lower deflection value of 44 mm.

This shift in relationship between risk of injury and sternal deflection is well within the limits provided by the confidence interval. Again it is worth noting that the spread of data would be expected to give greater confidence to results at lower chest displacements. Nevertheless, a 7 mm reduction in chest deflection limit may necessitate additional development work for future designs from some car manufacturers.

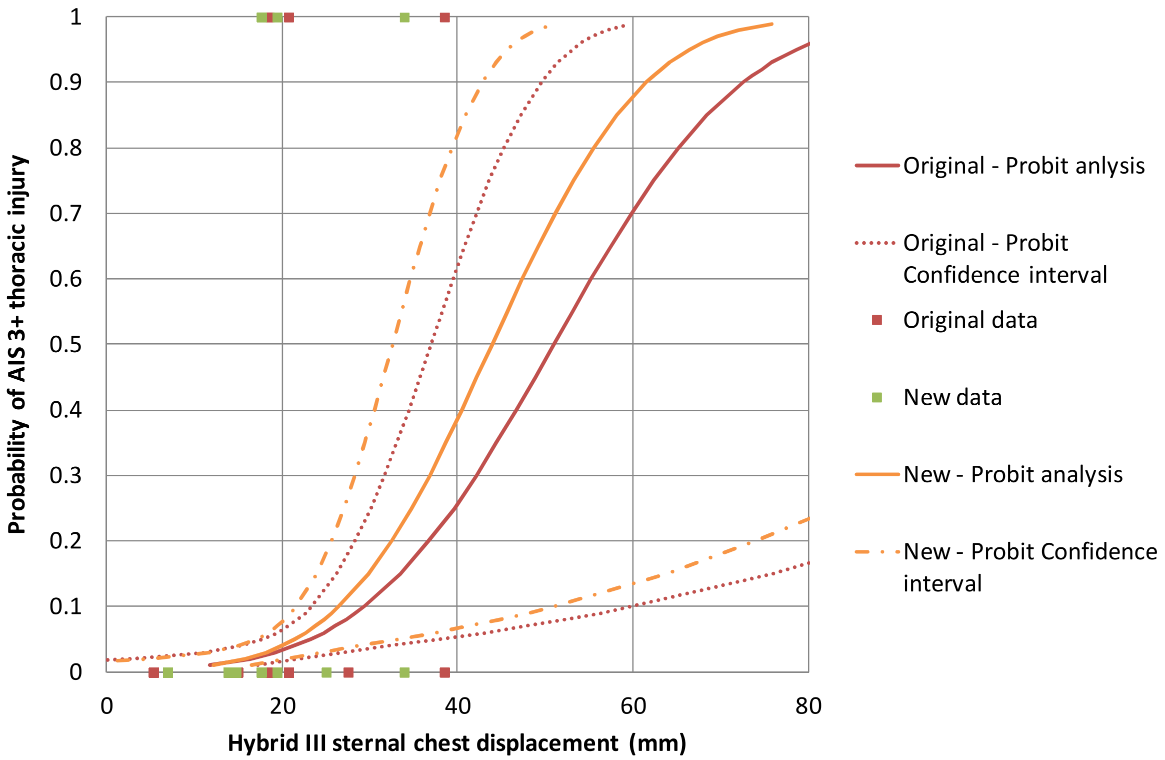

Figure B14. Risk of AIS ≥ 3 thoracic injury as a function of Hybrid III sternal deflection for shoulder belt loading. Risk curve determined by Probit analysis using original and new expected Hybrid III displacement measurements.

Recently an ISO Working Group (WG6) has been reviewing available statistical methods and developing guidelines to build injury risk curves. These guidelines now promote the use of survival analysis in the risk curve building. In accordance with these guidelines, the original data used by Mertz *et al.* were reviewed using survival analysis. The resulting injury risk curve is shown in Figure B15. A log-normal distribution was assumed to describe the data (AIC = 70.7).

Of interest is the agreement in the two curves, Probit and survival, up to about a 10 % risk of AIS ≥ 3 injury (approximately 30 mm of chest deflection). However, beyond that range (where there are fewer data points) the curves diverge with the survival analysis predicting a lower probability of thoracic injury for a given sternal deflection. Based on the data the survival analysis suggests that a 50 percent risk of injury will not have been reached even with 80 mm of deflection in the dummy (which is beyond the available measurement range).

Another thing illustrated by the survival analysis is the lack of confidence in the estimate. The 95th percentile confidence interval extremes are very broad and encompass a huge range of viable solutions. These limits envelope the original Probit curve and almost all of the confidence limit estimates from the Probit analysis. It may be worth noting that the width of the confidence intervals at a 25, 50 and 75 percent risk of injury would be classed as unacceptable using the latest ISO WG guidance (being more than 1.5 when divided by the estimate value at that risk).

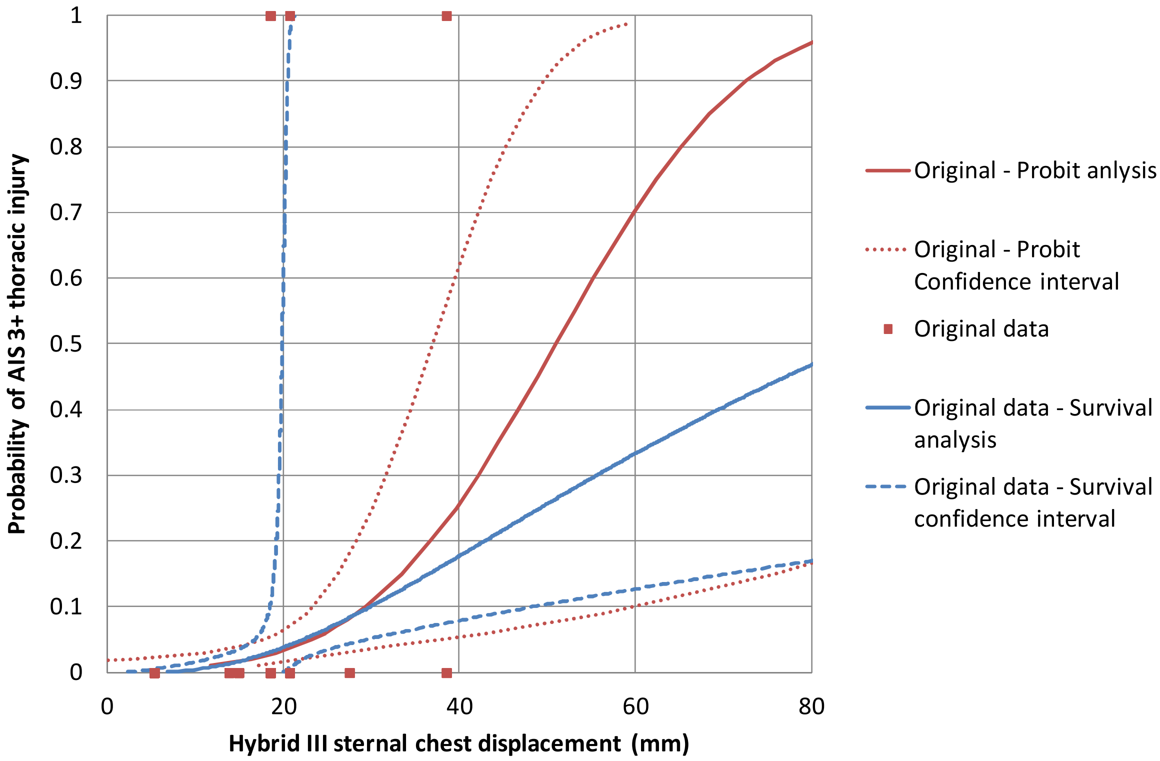

Figure B15. Risk of AIS ≥ 3 thoracic injury as a function of Hybrid III sternal deflection for shoulder belt loading. The alternative risk curve was determined by survival analysis.

Finally, the survival analysis was repeated but using the new values for Hybrid III sternal deflection. The resulting risk curve is shown in Figure B16.

As with the comparison of the original and new Probit curves, the survival estimate based on the new test data with the Hybrid III predicts a slightly higher risk of injury for a given sternal deflection than would be predicted based on the original test data.

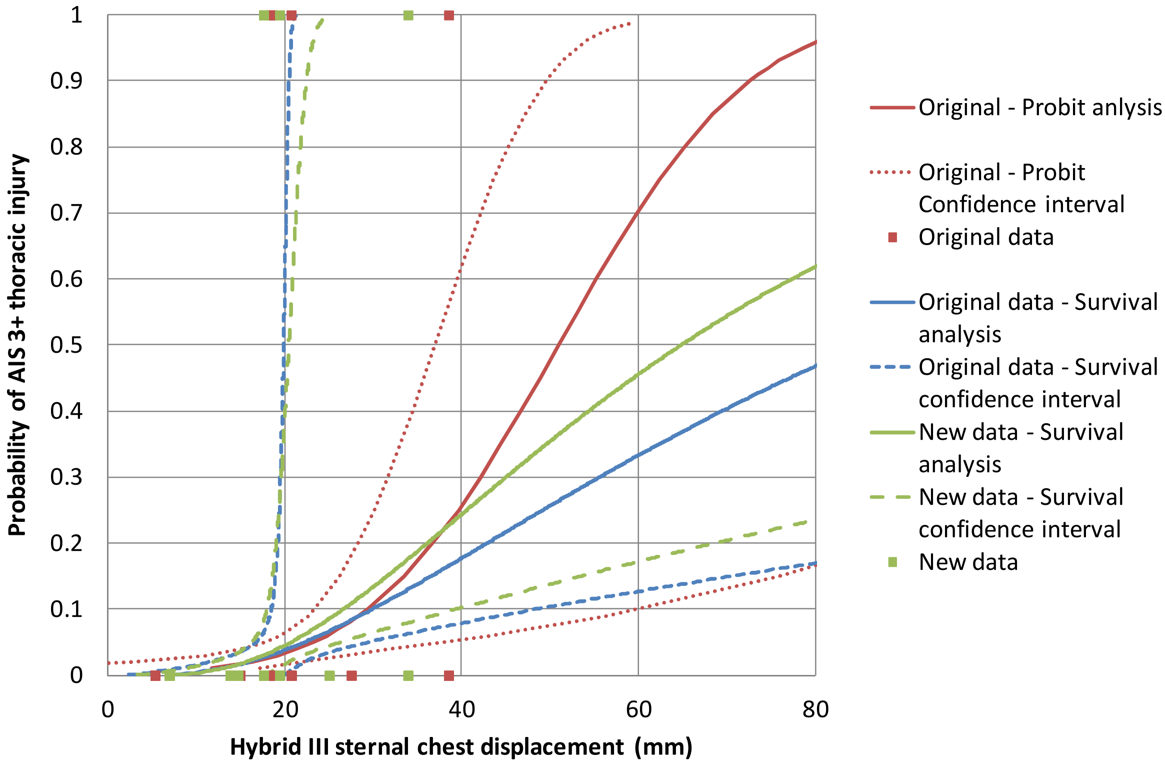

Figure B16. Risk of AIS ≥ 3 thoracic injury as a function of Hybrid III sternal deflection for shoulder belt loading. Risk curves determined by survival analyses using the original and new expected Hybrid III displacement measurements.

3.3 THORAX Demonstrator

In a similar way to the Hybrid III results, linear relationships between the THORAX Demonstrator chest deflection measurements and the shoulder belt forces were sought.
With the THORAX dummy the multipoint chest deflection measurement points give the potential for several parameters to be considered in relation to chest injuries. The 3D outputs from the four IR-Traccs can be combined in a variety of ways to give a criterion or the individual peak values can be considered in isolation. In each case, a relationship to the shoulder belt force needs to be established in order to relate the chest deflection measure to the risk of injury from the French accident data.

As an example, the peak deflection results, from any one of the four 3D IR-Traccs, are plotted with the shoulder belt force in Figure B17. The four series of data represent the three orthogonal measurement axes for the IR-Traccs and the resultant deflection. The formula for each of the lines and its r^2 value are also shown in the figure. From Figure B17 it can be seen that there is a reasonably linear correlation between shoulder belt force and either largest x-axis or resultant deflection peak values as measured by any of the four positions. The negative sign to the x-axis deflection relationship corresponds with the measurement being compression rather than extension of the chest. The relationship between the y-axis measurements and shoulder belt force explains less of the variation in the y-axis measurements than for the x-axis or resultant. However, the correlation with the z-axis measurements is even poorer. The lack of a robust relationship between belt force and z-axis deflection is likely to have been affected by the potential for the measurement points to go either up or down and hence give positive or negative values. It should also be noted that for the z-axis only the intercept had to be forced to pass through the origin to generate the line shown in Figure B17.

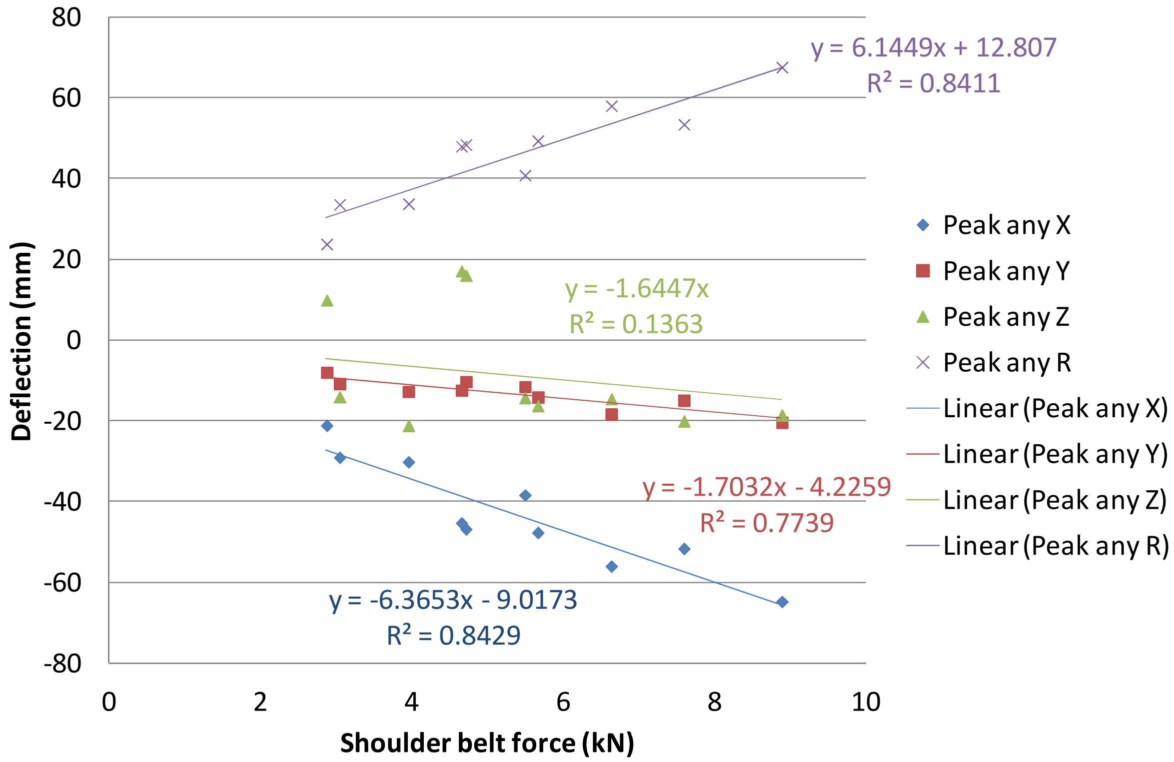

Figure B17. Linear relationships between peak chest deflection measures from any one of the four 3D IR-Traccs and the shoulder belt force measured during the test.

When comparing the THOR outputs with those from the Hybrid III, one very clear result is that the THOR instrumentation is more sensitive to belt force than the Hybrid III (see Figure B13). For instance the results in Figure B17 indicate that the IR-Traccs in the THOR will give a peak measurement of about 60 mm (measured at any one of the four IR-Traccs) with 8 kN of shoulder belt force whereas the Hybrid III would only be expected to have a peak sternum deflection value of about 35 mm.

The basic deflection measurements considered as potential criteria, at this stage were:

- Peak from any of the four measurement points (x, y, z-axis and resultant)
- Peak from either of the top two measurement points (x, y, z-axis and resultant)
- Mean peak value from the top two measurement points (x, y, z-axis and resultant)

The use of these preliminary assessment criteria was not meant to exhaust the full potential for the use of the data from the four IR-Traccs. Instead it is accepted that more advanced combinations of the data may provide a better correlation with injury and offer more accurate injury predictions. Such combinations can be considered in the same way as these measurements, once they have been proposed. For instance, the THORAX Project has already developed the Combined Deflection (Dc) criterion. Based on the initial suggestions for this criterion it has been included in the assessment of these THORAX Demonstrator sled test results.

The linear relationships between these criteria and the shoulder belt force are shown in Appendix C.

Based on the linear relationships established for the THORAX Demonstrator criteria considered, it was possible to derive equivalent data tables as shown for the Hybrid III sternal deflection in Table B5.. For the sake of brevity these are not reproduced in this report though example measurements are shown in Table D1. Table D1. Appendix D.

At this stage it was decided to consider only the x-axis and resultant measurements of peak chest deflection as they gave a better correlation with the shoulder belt force.

Using those data tables described above, injury risk functions were derived and risk curves plotted. The relationship between the probability of an AIS ≥ 3 thorax injury and the peak deflection measured at any of the four IR-Tracc positions (in the x-axis direction or as a resultant) and derived using survival analysis is shown in Figure B18. For the purposes of the survival analysis, and in all cases with the data derived from testing with the THORAX Demonstrator, an assumption was made that the data had a log-normal distribution (this gave a lower AIC value than risk functions derived using log-logistic or Weibull distribution assumptions).

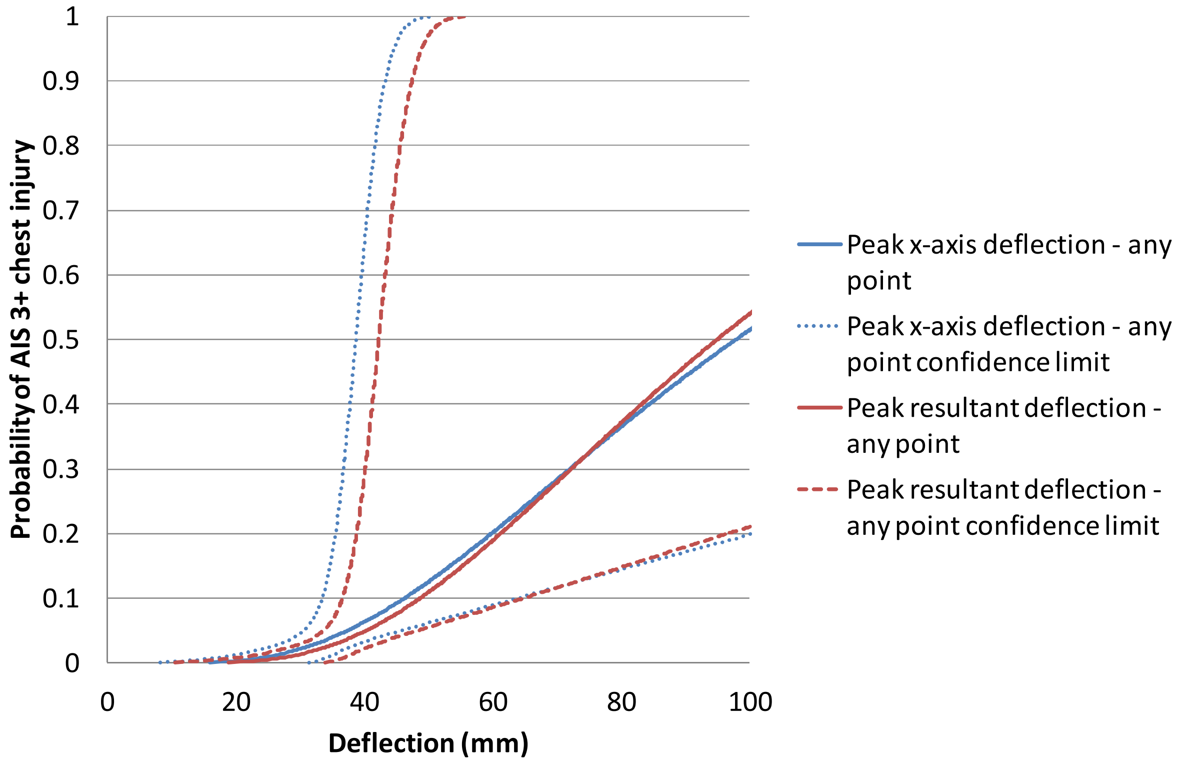

Figure B18. Risk curves showing the probability of an AIS ≥ 3 thorax injury with peak x-axis or resultant chest deflection measured at any of the four IR-Tracc positions in the THORAX Demonstrator, derived using survival analysis.

The curves shown in Figure B18 are typical of the THORAX Demonstrator risk curves produced as a result of this experimental work. The gradient of the estimated curve is not particularly steep and the confidence limits become increasingly wide as the loading severity increases. The other curves can be found in Appendix D.

The quality of a risk curve can be assessed by comparing the width of estimate between the two 95th percentile confidence limits and the value of the central estimate. With this dataset, the survival analysis produces a quality ratio (width of confidence limit divided by central curve value) which is less than 0.5 for all of the candidate criteria (x-axis and resultant deflections and Dc) at the 5 % risk of injury level. The ratio was between 0.42 and 0.88 at the 25 % risk of injury level and between 0.64 and 1.38 at the 50 % risk level.

It should be noted that a quality ratio between 1 and 1.5 is considered to be ‘marginal’ for further use by ISO WG6.

The THORAX Demonstrator risk curve with poorest quality ratio was the Dc criterion. However, the formulation of this criterion will be changed later in the project to make it specific for use with the Demonstrator dummy. Hopefully, this result would then be improved if the curve was recalculated.

The risk curve with the best quality ratio values was the peak resultant deflection from either of the top two IR-Traccs. All of the THORAX Demonstrator risk curves had lower (i.e. better) quality ratios at the 5, 25 and 50 % risk of AIS ≥ 3 thorax injury than the original Hybrid III risk curves derived with either the Probit or survival analyses. Whilst this seems to recommend the THORAX risk curves as being better than the Hybrid III, it must be remembered that the THORAX Demonstrator chest was more sensitive to deflection than the Hybrid III. As the deflection values are higher with the THOR, we should expect better quality ratio values (the denominator is higher). Nonetheless, it is encouraging that the risk functions would be acceptable for use according to the ISO WG6 assessment recommendations.

3.4 Comparison of Hybrid III with THOR results

Based on the original Hybrid III probit injury risk curve developed by Mertz *et al.* it was expected that 50 mm (or 51 mm rounded up) of sternal deflection would be associated with a 50 % risk of sustaining an AIS ≥ 3 thoracic injury (for a human adult under equivalent loading conditions). If the original data used by Mertz *et al.* are analysed using the survival approach instead of the probit analysis then 50 mm of sternal deflection gives a 26 % risk of an AIS ≥ 3 thoracic injury. A 50 % risk is only reached with 85.5 mm of deflection.

The corresponding injury risk at 50 mm and the measurements associated with either a 26 or 50 % risk of an AIS ≥ 3 injury for the THOR criteria are shown in Table B6. All values other than the first column containing the Hybrid III sternal deflection results are based on injury risk functions developed using survival analysis.

It is interesting to note that the peak measurement from either of the top two IR-Traccs provides a similar measurement to the Hybrid III sternal deflection at the 26 % risk of AIS ≥ 3 injury level. When taking the mean of the top two measurement points in the THOR, a lower value is needed to match this risk prediction.

The largest deflections of the THOR chest were at the lower thorax rather than the upper measurement points. This explains why the peak values from any point are greater than the upper points for a predicted risk of injury. Also there were large differences between the top two measurement points with the upper left IR-Tracc giving consistently larger peak x-axis and resultant deflection values. This is why the mean of the top two points gives a much larger risk prediction than the peak of the top two points for a similar deflection measurement.

Again it should be noted that the constants in the Dc formulation are due to be amended after this testing to adjust them specifically for the Demonstrator dummy design.

Table B6. Comparison of injury risk values for Hybrid III and THOR chest deflection measurements.

Measurement	Original HIII sternal deflection - Probit	Original HIII sternal deflection - Survival	New HIII sternal deflection	THOR Peak any point x-axis	THOR Peak any point resultant	THOR Peak top two points x-axis	THOR Peak top two points resultant x-axis	THOR Mean peak top two points x-axis	THOR Mean peak top two points resultant x-axis	Dc
Risk of injury at 50 mm (%)	50	26	35	13	11	27	26	40	48	30
Measurement at 26 % injury risk (mm)	40.1	49.9	41.1	66.7	67.4	49.0	49.7	38.2	37.6	45.5
Equivalent measurement to 50 mm (i.e. assumed to be 50 % risk)		85.5	64.8	97.8	94.9	67.5	65.3	58.5	50.9	75.9

4 Discussion

When the new Hybrid III test results were compared with those from the original sled test work, they indicated a slightly different relationship between peak belt force and Hybrid III sternal deflection. It is not clear from where this difference arises. On the one hand there is uncertainty regarding the recreation of the test conditions. It is known that the geometry of the seat is close to that documented by Mertz *et al.*; however, there is uncertainty as to whether the stiffness of the seat foam is correct. It is certainly stiffer than a Renault 4, but it may not be identical to the 'hard' seat of the previous test bench. Also the load limiters and seat belts can only be an approximation to the original restraint. The load limiters do not behave in exactly the same way as before (peak forces occur at different levels), although the peak force is measured and taken into account. Another feature of the restraint system may be the webbing itself. It is not known whether the elongation characteristics of the modern webbing are the same as used previously. This may result in a different restraint system performance for any given belt force. Finally, the loading through the lap belt was monitored in all tests, but this data is not available from the literature documenting the previous tests. If the lap belt loading is different it could lead to variations in the balance of the interaction between the dummy and the shoulder and lap portions of the seat belt. This could lead to a different thoracic response for a given applied shoulder belt force.

On the other hand there may be real changes and dummy differences being picked up by these results. As an example, in the last few years Euro NCAP has implemented a low severity certification test for the dummy. This was put in place because it was found that some Hybrid III dummies with similar chest deflections at the standard certification test severity had significantly different chest deflections at lower test severities that were more representative of the loading in a Euro NCAP test with a modern five-star vehicle. On the assumption that the applied force and deflection relationship between zero and peak loading may have been non-linear and variable from dummy to dummy prior to this lower severity certification, then one might expect some difference in performance between recent tests and earlier ones.

Comparing both the recently tested Hybrid III and the original results, it seems as though both dummies responded in a linear way to the shoulder belt force applied, though the TRL Hybrid III was slightly stiffer. Another consideration is the stiffness variation allowed by the certification performance requirements. In the high severity chest certification test, the limits of allowable deflection and force are 63.5 to 72.6 mm and 5160 to 5894 N, respectively. This yields an allowable stiffness range from 71.1 to 92.8 N/mm (± ~13 %). The variation in stiffness between the dummies under shoulder belt loading was from 200 N/mm (previous tests) to 227 N/mm (current series). At about a 6 % difference in stiffness response under belt loading this seems to fall within the dummy-to-dummy reproducibility that the certification limits would allow.

The probit and survival analysis risk curves developed using the same original Hybrid III data showed good agreement up to about 30 mm of chest deflection. After this point the curves started diverging as the risk function was extrapolated beyond the last few data points. This observation illustrates the influence of the data assumptions and techniques when deriving risk functions. It may be worth noting that as the curves diverge, both the probit and survival estimates have extremely wide confidence limits and each estimate falls within the confidence boundary of the other. Therefore, whilst the estimates may look very different, the valid interpretation of them may not be too different.

The survival analysis with either the original or new Hybrid III or some of the new THORAX Demonstrator data and French accident injury outcome information showed 'marginal' quality at levels of loading associated with current regulatory chest deflection limits. This highlights a known limitation with the data in that there are few injury cases with which to refine the confidence boundaries at injurious loading levels. This gives weight to the importance of the

THORAX Project initiative under which new injury risk functions for the new dummy demonstrator will be developed.

Due to the time-pressures associated with the development and testing of the THORAX Demonstrator, a mistake was made and the dummy was tested in a configuration with additional mass added to the upper arms. About 320 g was added to each arm by taping strips of lead to the humerus (below the flesh) at another test laboratory. This was not identified until after the sled testing, therefore of the THORAX Demonstrator results presented in this report were obtained with the additional mass in place. This mass will not be present for the final version of the dummy and was removed from the Demonstrator as soon as it had been realised that it was still there for the TRL tests.

The consequence of the additional mass on the results obtained through the work described in this report is not known precisely. In certification-type pendulum tests striking the sternum of the dummy, the additional mass led to a reduction of the peak deflection of 2.6 mm. The measurements obtained from the sled test programme could be similarly sensitive to the extra mass in the upper arms. This causes a problem when interpreting the results presented in this report in a quantitative way. However, the extra mass is likely to have a simple relationship with respect to increasing test severity and hence the qualitative trends identified should still be correct for the THOR without additional mass in the arms.

Sled tests conducted by BASt under a different impact condition, with and without the extra arm mass showed negligible influence from that mass. This also supports the assertion that the qualitative trends observed are likely to be maintained when using the THOR without that extra mass on the arms.

5 Risk Register

Risk No.	What is the risk	Level of risk[1]	Solutions to overcome the risk
WP2.5	Hybrid III injury risk curve developed using survival analysis deviates from original Probit curve	1	Need to consider this change when interpreting Hybrid III results. To be discussed amongst peers to increase awareness of issue
WP2.6	New Hybrid III test data does not fall in line exactly with historic results	1	This may indicate the Hybrid III has changed since the original injury risk function tests were performed. Otherwise, it may indicate inaccuracy of current test replications.
WP2.7	Injury risk curves from this data source have marginal quality, this may prevent future use of this information	2	This was a known problem with this dataset prior to testing. It strengthens the need for further work within THORAX to provide improved injury risk functions for use with the Demonstrator dummies.
WP2.8	THORAX Demonstrator was tested with additional arm ballast. This may alter the exact measurements obtained during the test work	2	Sled tests from BASt suggest that the additional mass has a negligible effect on chest deflection measurements under sled test conditions. However, even if it does, it is considered unlikely to change the qualitative information derived from this testing.
WP2.9	The sled test conditions used a static belt to simulate high belt forces that may have been created after exhausting load limiting elements in the original accident	2	The use of these test data needs to be considered carefully in Task 2.6 and the development of improved injury risk functions for use with the THORAX Demonstrator. It may be that only the low force level tests (with load limiters) can be included in those activities.

[1] Risk level: 1 = high risk, 2 = medium risk, 3 = Low risk

6 Conclusions

The test set-up used by Mertz et al. (1991) to recreate French accident cases on a sled was reproduced at TRL. This included development of webbing-based load limiting elements that use a tearing of stitching failure mode.

Tests with a Hybrid III dummy suggested that the replication of test conditions was appropriate. However, differences in the relationship between peak belt force through the shoulder portion of the three-point belt compared with the historic results were observed. The risk curve based on the new data predicted a higher risk of injury for a given chest deflection measurement than the original test data.

Noting the differences in the belt force to deflection relationship, a new AIS ≥ 3 injury risk function was drawn for Hybrid III sternal chest deflection. The opportunity was also taken to review the potential implications of switching form Probit analysis to derive the risk curve to the alternative approach, supported by ISO, of using survival analysis. The use of survival analysis emphasised the limitations in the original data. It was evident that the risk curves for the Hybrid III would not meet new recommendations on the confidence boundaries of the estimate, as are now being proposed by ISO Working Group 6. Nevertheless, the survival estimate indicated a lower risk of injury for a given chest deflection measurement than was predicted by the Probit analysis.

Preliminary risk curves for the THORAX Demonstrator have been derived using survival analysis. These risk functions allowed for a comparison of the measurements that are equivalent to the Hybrid III 50 mm sternal deflection limit to be made. Expected deflection measurements from the THOR would be expected to be either lower, about the same or higher depending on whether the mean peak from the top two IR-Traccs, peak from either top two IR-Traccs or peak from any IR-Tracc is considered, respectively. These differences demonstrate the sensitivity of the THORAX Demonstrator chest to this particular loading regime.

As all the injury risk functions developed throughout this testing are based on the original data used by Mertz *et al.*, they are all associated with only fair or marginal levels of quality, as defined by ISO WG6. This means that great care should be taken when trying to use them as they have broad confidence limits. Most of the risk functions have a ‘good’ level of quality at the 5 % risk of injury, where most of the injury outcome data are concentrated. The fact that there is less confidence in the risk estimates and higher risk levels supports the continuing efforts within the THORAX Project to developed improved injury risk curves for the THORAX Demonstrator based on a wider set of biomechanical data.

Appendix C. Relationships between THORAX criteria and shoulder belt force

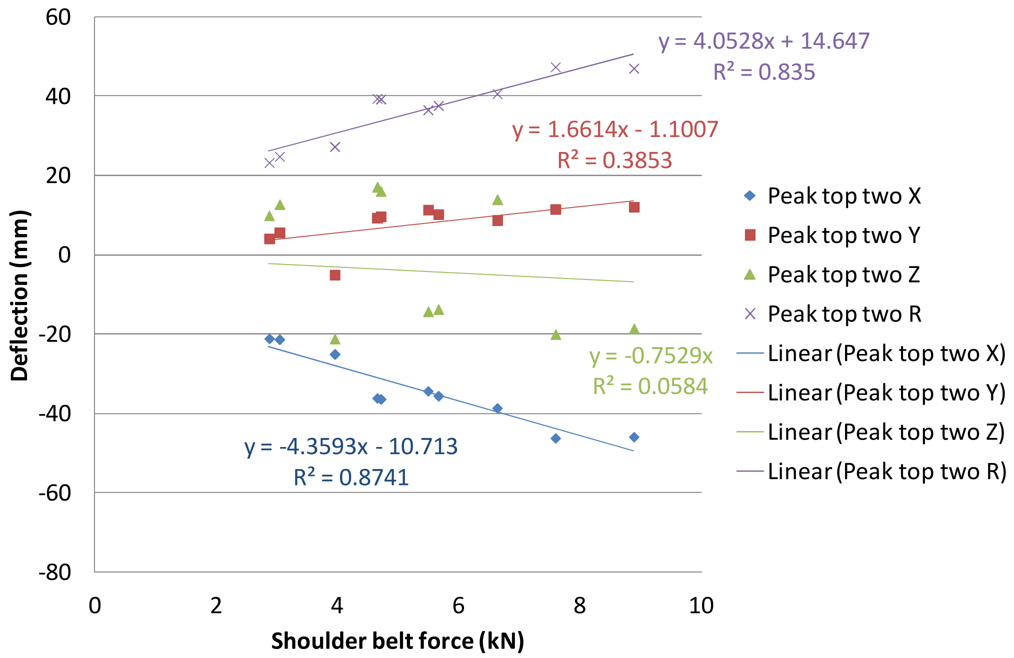

Figure C1. Linear relationships between peak chest deflection measures from any one of the top two 3D IR-Traccs and the shoulder belt force measured during the test.

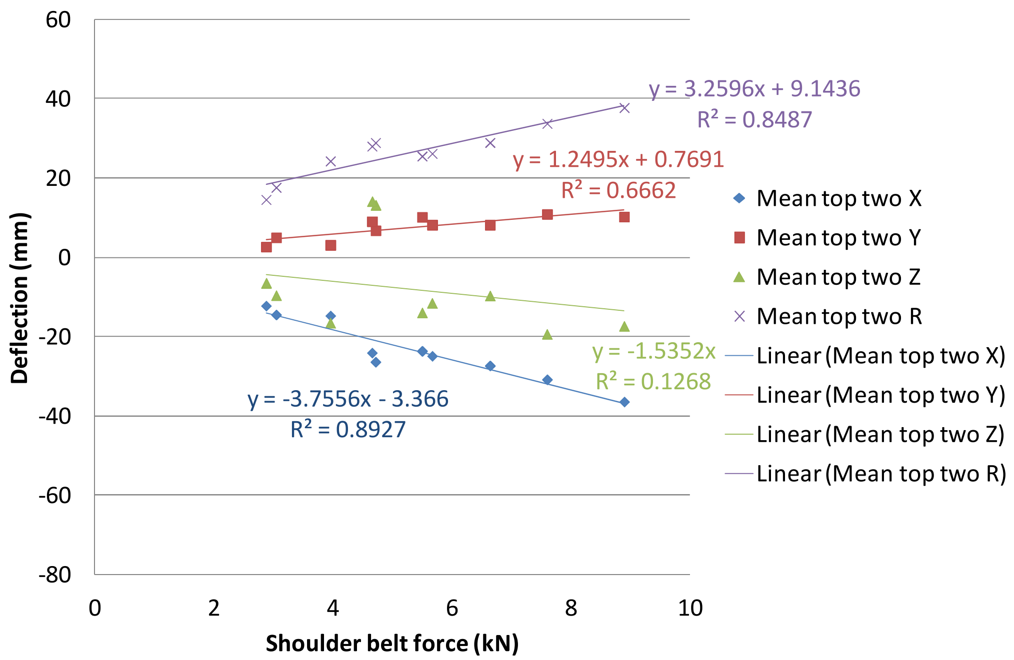

Figure C2. Linear relationships between the mean peak chest deflection measures from the top two 3D IR-Traccs and the shoulder belt force measured during the test.

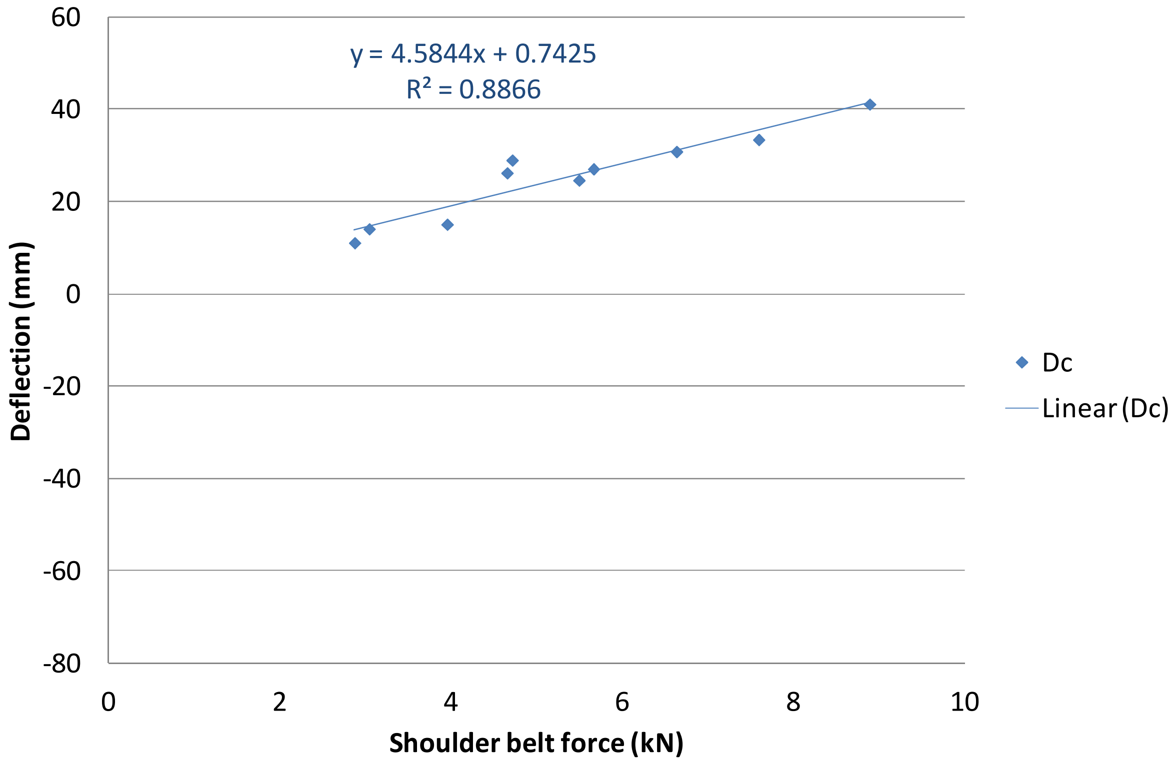

Figure C3. Linear relationship between the Dc (Combined Deflection) chest deflection measure and the shoulder belt force measured during the test.

Appendix D. Examples of equivalent deflection measures for THORAX

Table D1. Example measurements to match Hybrid III sternal deflection in the risk function derivatives.

Load range	Hybrid III sternal deflection		THORAX Demonstrator – peak from top two points		THORAX Demonstrator – mean peak from top two points	
(kN)	Range (mm)	Mean (mm)	x-axis (mm)	Resultant (mm)	x-axis (mm)	Resultant (mm)
0 to 2.1	0 to 11.1	6.9	15.3	18.9	7.3	12.6
2.1 to 3.85	11.1 to 18.2	14.7	23.7	26.7	14.5	18.8
3.85 to 4.4	18.2 to 20.5	19.4	28.7	31.4	18.9	22.6
0 to 5.5	0 to 25.0	13.8	22.7	25.8	13.7	18.1
5.5	25.0	25.0	34.7	36.9	24.0	27.1
0 to 7.4	0 to 32.7	17.6	26.8	29.6	17.3	21.2
7.4 to 8	32.7 to 35.1	33.9	44.3	45.9	32.3	34.2

Appendix E. Injury risk curves for the THORAX based on recreation of accidents

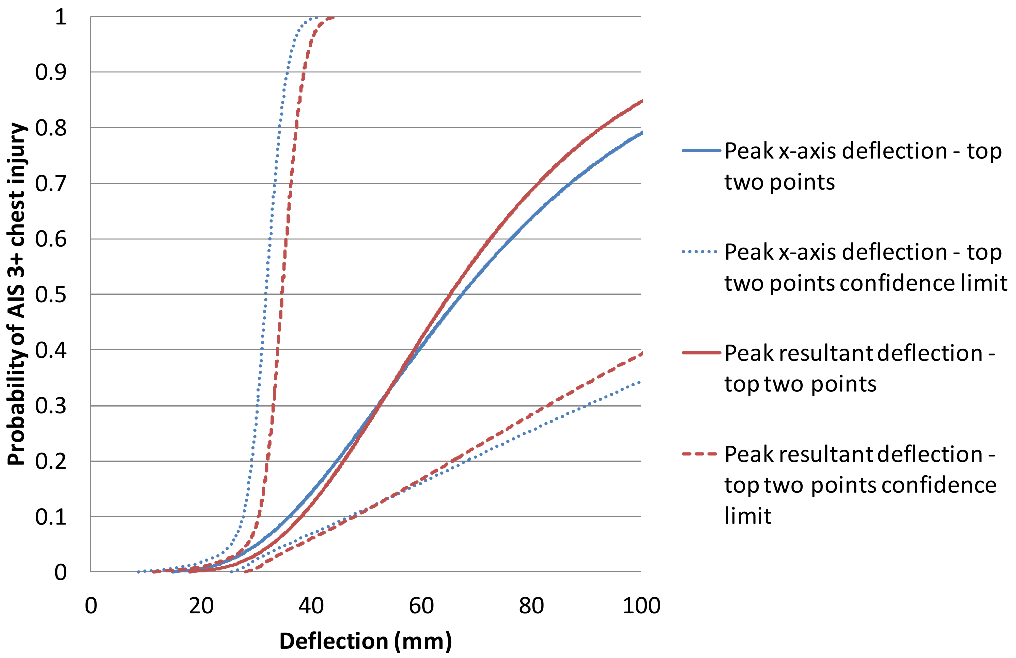

Figure D1. Risk curves showing the probability of an AIS ≥ 3 thorax injury with peak x-axis or resultant chest deflection measured at either of the top two IR-Tracc positions in the THORAX Demonstrator, derived using survival analysis.

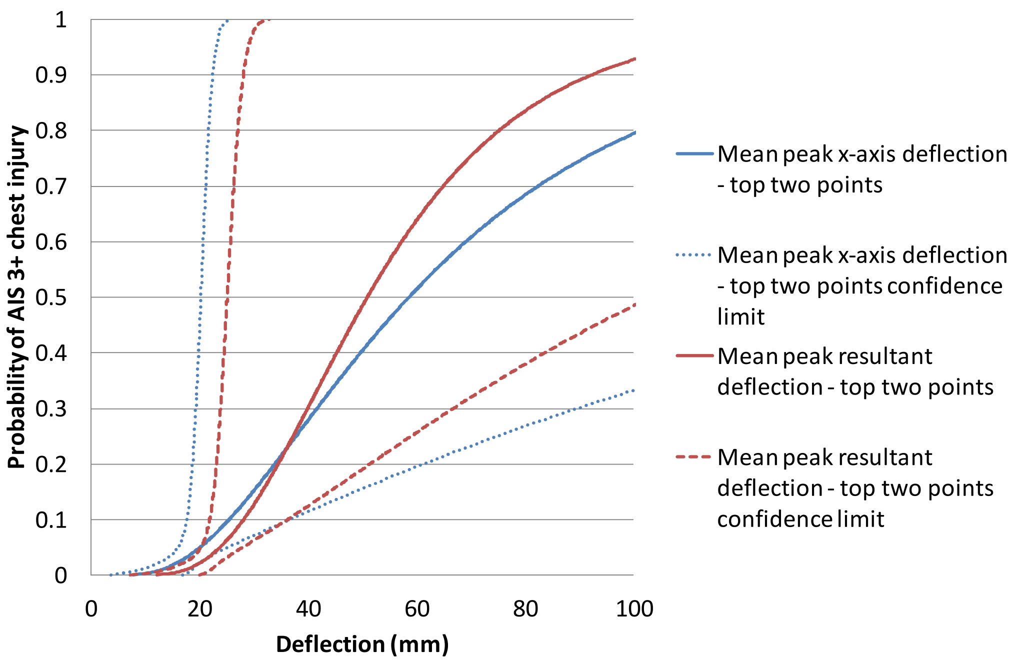

Figure D2. Risk curves showing the probability of an AIS ≥ 3 thorax injury with mean peak x-axis or resultant chest deflection measured at the top two IR-Tracc positions in the THORAX Demonstrator, derived using survival analysis

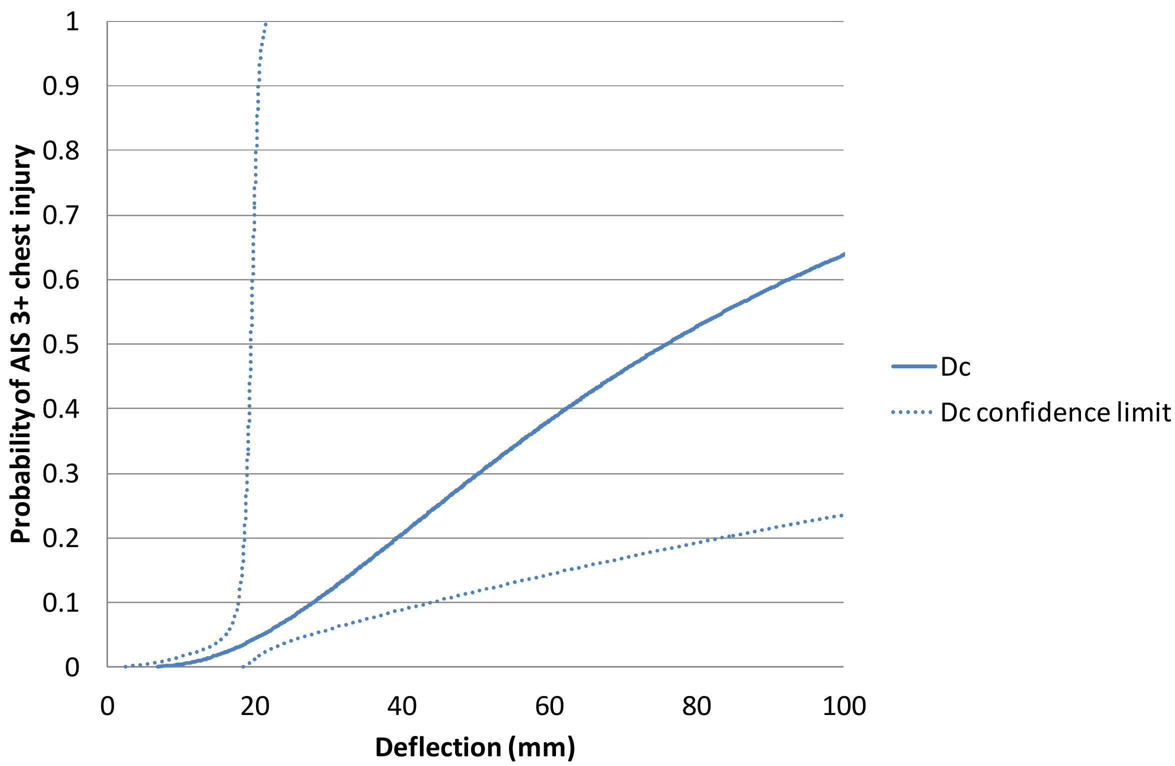

Figure D3. Risk curves showing the probability of an AIS ≥ 3 thorax injury with Dc (the Combined Deflection) chest deflection measure in the THORAX Demonstrator, derived using survival analysis.